INTRINSIC PROPERTIES OF LARVAL DROSOPHILA MOTONEURONS AND THEIR CONTRIBUTION TO MOTONEURON RECRUITMENT AND FIRING BEHAVIOR DURING FICTIVE LOCOMOTION

by

Jennifer Elise Schaefer

A Dissertation Submitted to the Faculty of the

GRADUATE INTERDISCIPLINARY PROGRAM IN PHYSIOLOGICAL SCIENCES

In Partial Fulfillment of the Requirements
For the Degree of

DOCTOR OF PHILOSOPHY

In the Graduate College

THE UNIVERSITY OF ARIZONA

2010

THE UNIVERSITY OF ARIZONA

GRADUATE COLLEGE

As members of the Dissertation Committee, we certify that we have read the dissertation prepared by Jennifer Elise Schaefer

entitled Intrinsic properties of larval Drosophila motoneurons and their contribution to motoneuron recruitment and firing behavior during fictive locomotion

and recommend that it be accepted as fulfilling the dissertation requirement for the Degree of Doctor of Philosophy

_____ Date: 04/22/10
Richard B. Levine, PhD

_____ Date: 04/22/10
Carsten Duch, PhD

_____ Date: 04/22/10
Ralph Fregosi, PhD

_____ Date: 04/22/10
Andrew Fuglevand, PhD

_____ Date: 04/22/10
Lucinda Rankin, PhD

Final approval and acceptance of this dissertation is contingent upon the candidate's submission of the final copies of the dissertation to the Graduate College.

I hereby certify that I have read this dissertation prepared under my direction and recommend that it be accepted as fulfilling the dissertation requirement.

_____ Date: 04/22/10
Dissertation Director: Richard B. Levine, PhD

STATEMENT BY AUTHOR

This dissertation has been submitted in partial fulfillment of requirements for an advanced degree at the University of Arizona and is deposited in the University Library to be made available to borrowers under rules of the Library.

Brief quotations from this dissertation are allowable without special permission, provided that accurate acknowledgment of source is made. Requests for permission for extended quotation from or reproduction of this manuscript in whole or in part may be granted by the head of the major department or the Dean of the Graduate College when in his or her judgment the proposed use of the material is in the interests of scholarship. In all other instances, however, permission must be obtained from the author.

SIGNED: Jennifer E. Schaefer

ACKNOWLEDGEMENTS

I have been privileged to learn from excellent mentors and colleagues during my time in the Physiological Sciences Graduate Program. First and foremost is my advisor, Dr. Levine, whose endless patience, scientific expertise, insight, guidance and support have not only taught me about science and how to be a scientist but have also modeled professionalism and instilled confidence. I am eternally grateful for his excellent mentoring and support.

My dissertation committee members, Carsten Duch, Ralph Fregosi, Andrew Fuglevand, and Cindy Rankin, have been instrumental in my development as a scientist. I would like to thank them for sharing their expertise and for their encouragement. Additionally, Levine lab members including Cortnie Hartwig, Kim Lance, Rene Luedeman, Earlphia Sells, Subashini Srinivasan, and Jason Worrell have been not only excellent colleagues but also excellent friends. Earlphia Sells, Subashini Srinivasan, and Jason Worrell have been especially important for my scientific development and enjoyment of graduate school. Motor control journal club members including Fiona Bailey, Erika Eggers, Ralph Fregosi, Andrew Fuglevand, Rick Levine, Jason Pilarski, Ann Revill, Subhashini Srinivasan, Doug Stuart, Hilary Wakefield, and Jason Worrell have provided innumerable insights and thought-provoking discussions that have enriched and framed my scientific development.

Thank you to the Physiological Sciences faculty for the excellent courses, guidance, feedback, and encouragement. I am also eternally grateful to Holly Lopez for her endless assistance.

I have tried to develop not only as a scientist but also as a teacher throughout my graduate career. Cindy Rankin has provided me with instrumental encouragement, instruction, feedback, and opportunity in the teaching world. I would also like to thank those involved in the BioME Graduate Fellowship Program, especially Kathleen Walker and Rebecca Sampson, for part they have played in my development as a teacher. Finally, thank you to the participants of the Science Educators Happy Hour for their discussions, advice, and camaraderie.

Finally, I would like to thank my family and friends. Thank you to my parents for instilling in me a love of learning and for always providing me with support and love. Thank you to my brother, Adam, and sister, Maggie, for their friendship, love, and encouragement. Thank you to the Schaefer's, Shade's, and Rapstad's for their support. To my friends and classmates: Vera, Renata, Jada, Amber-Dawn, Al, Heather, Maggie, Edward, Erin, Zelieann, Danika, Chrisy, Katie, Nellie, Erika, Jenny, Wieke, Karl, Nick, Joe, and the Gusto ladies. You have kept me sane and enriched my life during graduate school. And finally, thank you to my husband, Scott, for supporting me, believing in me, encouraging me, and teaching me how to reach for my dreams.

TABLE OF CONTENTS

TABLE OF CONTENTS - Continued

LIST OF FIGURES

LIST OF TABLES

ABSTRACT

Locomotion is controlled in large part by neural circuits (CPGs) that generate rhythmic stereotyped outputs in the absence of descending or sensory inputs. The output of a neural circuit is determined by the configuration of the circuit, synapse properties, and the intrinsic properties of component neurons. In order to understand how a neural circuit functions component neurons, their connections, and their intrinsic properties must be characterized. Motoneurons are a useful cell in which to begin investigation of CPG function because they are accessible and provide a measure of the cumulative activity of the circuit. *Drosophila* is a potentially useful model system for the study of motoneuron intrinsic properties, their contribution to locomotion, and of locomotor CPGs because the genetic and molecular techniques available in *Drosophila* are surpassed in no other organism and because the *Drosophila* nervous system is small in comparison to vertebrate nervous systems. Further, whole-cell *in situ* patch clamp recordings from adult and larval motoneurons in relatively intact preparations are possible.

Therefore, the first goal of this work was to investigate whether the firing behavior and recruitment of identified *Drosophila* 1b and 1s motoneurons is analogous to the recruitment of high-threshold, phasic and low-threshold, tonic motoneurons in other organisms. The second goal was to determine whether active conductances influence motoneuron recruitment in response to synaptic input. The final aim was to investigate how these factors influence CPG output to muscles.

Findings from current clamp studies indicate that1b motoneurons are more easily recruited than 1s motoneurons, in agreement with the hypothesis that 1b motoneurons are analogous to low-threshold motoneurons described in other organisms. Further, orderly recruitment of *Drosophila* 1b motoneurons before 1s motoneurons is not a result of passive properties. Instead, the Shal channel that encodes a large portion of I_A in motoneuron somatodendritic regions is a critical determinant of delay-to-spike in larval *Drosophila* motoneurons. These findings are behaviorally-relevant because the same recruitment order is seen in simultaneous recordings from motoneuron pairs recruited by synaptic input.

CHAPTER 1. INTRODUCTION

Directed movement is required for the survival of most animals. Even simple animals must escape from predators, find food, and obtain shelter. Controlled and directed movements are generated through the response of individual or groups of muscles to nervous system instructions that determine the timing, coordination, and force of muscle contractions. The nervous system's task of generating and forwarding commands to single or thousands of muscle fibers, depending on the organism and the movement task, is termed "motor control".

Neural circuits are the functional building blocks utilized by nervous systems to control functions such as emotion, cognition, autonomic functions, and motor control and are composed of component neurons that make specific connections with each other via synapses. The configuration of the circuit, the synaptic connections, and the intrinsic properties of the neurons all determine the final output of a neural circuit. In order to understand how a neural circuit functions, then, the component neurons and their connections and intrinsic properties must be characterized.

We were interested in how intrinsic properties of component neurons contribute to the generation of motor commands by neural circuits. Specifically, we were interested in the last order neurons, the motoneurons, whose activity represents the cumulative output of the neural circuit to muscles. The intrinsic properties of the motoneurons themselves have been increasingly shown to contribute to the output of neural circuits. Therefore, we

utilized *Drosophila* as a model organism in which to characterize the intrinsic properties of motoneurons in order to investigate their contribution to motor behaviors.

1.1 Investigating neural circuit control of movement

Characterization of neural circuits is a daunting task due to the vast numbers of neurons and synapses that may compose a single circuit, but great progress has been made in the dissection of the circuits controlling movement in a variety of organisms. Dissection of neural circuits is more complicated in vertebrates than invertebrates because of the relatively larger size of vertebrate nervous systems and because vertebrate neural circuits employ groups of similar neurons as the basic functional unit while invertebrate circuits employ individual neurons as the functional unit.

The problem of dissecting neural circuits is further complicated by the realization that neural circuits at different levels of the nervous system can participate in a single motor task. For example, neural circuits involved in the control of mammalian movement reside in the motor cortex, cerebellum, brainstem, and spinal cord. Conversely, individual circuits can be reconfigured for different movements and behavioral states. In this case, synaptic connections between neurons are physically maintained while synaptic strengths and ionic conductances are modified by neuromodulators to achieve functional rearrangement of the circuit (Dickinson 2006; Marder and Bucher 2001). Clearly, motor control is a complex task for neural circuits in both vertebrates and invertebrates.

The complexity of the motor control task requires that researchers simplify the problem in order to understand how the nervous system coordinates and controls movement. The relatively small size of circuits in invertebrates permits consistent identification and characterization of component neurons. All of the 302 neurons in the *C. elegans* nervous system are known and their morphology, location, and synaptic partners are described, allowing characterization of the neural circuits responsible for different behaviors. Specifically, sets of interneurons controlling locomotion have been identified (Tsalik and Hobert 2003). Other well-described neural circuits include the crustacean stomatogastric ganglion (STG) which is composed of largely interconnected motoneurons and controls the stomach. The morphology, location, connections, neurotransmitter type, and synaptic partners of each of the approximately 30 component neurons have been identified and much is known about the effects of neuromodulators on individual components of the STG circuitry (Marder and Bucher 2007). The location, morphology, and physiology of the component neurons of neural circuits controlling a variety of leech behaviors such as heartbeat, swimming, and bending have also been well-described (Kristan et al. 2005). Therefore, dissection of invertebrate neural circuits provides a more feasible alternative to dissection of mammalian circuits and many of the principles that were first described in invertebrates also apply to mammalian neural circuits.

1.2 Central pattern generators

Most of the previously-mentioned neural circuits, not coincidentally, are circuits that control stereotyped, repetitive movements. Study of such movement facilitates

quantification of behavioral phenotypes that result from modification of discrete circuit elements. Stereotyped, rhythmic movements that can be produced in the absence of continued descending or afferent input are generated by neural circuits called central pattern generators (CPGs). The study of CPG production of rhythmic movement has contributed core principles to our understanding of neural circuits. Principles that have emerged from studies of invertebrate CPGs include the understanding that motor circuitry can function without sensory feedback, although sensory feedback refines the movement command. Also, neural circuits are often widely-distributed and interneuron sharing between neuronal circuits due to neuromodulatory influences allows task-dependent reconfiguration of circuits. Finally, studies of invertebrate CPGs have taught us that common cellular characteristics, including ionic currents and synaptic properties, contribute to neural circuit function across organisms (Comer and Robertson 2001; Pearson 1993). The role of sensory input, neuromodulation, and the flexibility of CPG circuits are the focus of the following discussion.

1.2.1 Central pattern generators: role of sensory input

Innumerable studies in deafferented preparations, beginning with the work of Sherrington, demonstrated that sensory input is not necessary for CPG output. Rather, sensory input to CPGs initiates, stabilizes, and coordinates CPG output, in addition to correcting CPG activity in response to environmental stimuli. For example, lamprey swim CPG activity was initiated by afferent input to the brainstem that evoked plateau potentials in reticulospinal neurons to initiate swimming (Di Prisco et al. 2000). In the

lobster STG, activation of different sensory inputs that worked through the same projection neurons produced different gastric mill rhythms (Blitz et al. 2004). Stabilization of cycle frequency in the locust flight CPG was provided by afferent input from a proprioceptive sense organ in the wing (Ausborn et al. 2007). Experimental observations and modeling studies indicated that the phase lag between segments in the leech swimming and crawling and lamprey swimming CPGs was decreased by afferent input (Wallen and Williams 1984; Yu et al. 1999; Eisenhart et al. 2000; Cang and Friesen 2002; reviewed in Friesen and Cang 2001). Sensory input serves a similar sculpting function for mammalian CPGs, where it coordinated output to different muscles in the cat hindlimb during walking (reviewed in Hultborn and Nielsen 2007). The effects of afferent input are mediated through a variety of mechanisms, including presynaptic inhibition, differential activation of interneurons, and alteration of membrane properties in circuit neurons (Rossignol et al. 2006).

1.2.2 Central pattern generators: neuromodulation of CPGs

Neuromodulation is important for the generation of different motor patterns and behaviors by CPG circuits. Direct synaptic effects of neuromodulators have been demonstrated in a variety of invertebrates and vertebrates. In the *Aplysia* feeding CPG, co-release of two neuropeptides potentiated acetylcholine-mediated EPSPs onto downstream neurons (Koh et al. 2003). In the *Tritonia* mollusk escape CPG, 5-HT enhanced EPSPs at an identified synapse (Katz and Frost 1995). The crustacean STG has been an especially useful model for investigations of neuromodulator effects on neural

circuits because the component cells and synapses are well-known. Release of the peptide proctolin from an STG projection neuron caused synaptic depression in other projection neurons leading to inhibition of the gastric mill rhythm (Briggman and Kristan 2008). In vertebrates, 5-HT prevented synaptic release from interneurons in the lamprey swim CPG while dopamine inhibited the 5-HT effect and reduced EPSP amplitude via a presynaptic effect (Svensson et al. 2001; Svensson et al. 2003).

Neuromodulators also have non-synaptic effects on ionic conductances that generally work through phosphorylation or G-protein-mediated mechanisms. Neuromodulation of intrinsic conductances in vertebrate motoneurons is discussed in *Chapter 1: Active motor neurons*. Invertebrate studies have demonstrated a variety of neuromodulator effects on ionic currents. Dopamine, octopamine (an invertebrate counterpart to noradrenaline), and 5-HT depolarized the activation voltage of I_h and increased its activation rate in the lobster pyloric network (Peck et al. 2006). 5-HT also depolarized the membrane potential, triggered bursting, and enhanced post-inhibitory rebound in motoneurons of the gastropod mollusk feeding CPG (Straub and Benjamin 2001). These motoneurons are electrotonically coupled to CPG interneurons and therefore alteration of motoneuron intrinsic properties influenced the function of the CPG.

Neuromodulator effects on synaptic properties and ionic conductances can occur simultaneously, complicating interpretation of neuromodulator actions. For example, dopamine had dual effects on identified synapses in the lobster pyloric CPG where it

increased synaptic inhibition, reduced synaptic depression and reduced electrical coupling, which would be expected to decrease neuronal communication. Instead, the circuit was relatively unaffected because of a dopamine-induced enhancement of post-inhibitory rebound in downstream neurons (Johnson et al. 2005). Clearly, neuromodulators play a complex and important role in controlling and modifying motor output, and invertebrate model systems can provide valuable insight into the mechanisms of neuromodulator action (Dickinson 2006).

1.2.3 Central pattern generators: flexibility of CPGs

A further complication to understanding neural circuits, and specifically CPGs, is the finding that not only can circuit components be reconfigured via neuromodulation to produce different outputs, but the reverse is also true. A variety of circuit parameters and configurations can produce the same outputs. Computational modeling of the pyloric CPG first showed that a remarkable variety of intrinsic properties and synaptic strengths within a network could produce indistinguishable outputs (Prinz et al. 2004). Further evidence that stereotyped output could be produced by varying circuit parameters was provided in a comparison of four ion channel, I_A, I_h, I_{KCa}, and I_K, expression levels in three motoneurons of the crab STG pyloric circuit. Currents in cells from different animals that displayed similar CPG outputs varied two- to four-fold in all of the motoneurons, although each identified motoneuron maintained a recognizable pattern of channel expression (Schulz et al. 2006). Marder and Goaillard suggest that such variability in neural circuits provides robustness and flexibility (Marder and Goaillard

2006). Further circuit flexibility is provided by the often widely-distributed nature of CPGs. For example, zebrafish escape circuitry that initiates turning and swimming includes a large population, rather than a discrete subset, of descending interneurons (Gahtan et al. 2002). Widely-distributed CPG circuitry may provide redundancy that is important for survival in the event of injury or damage. In fact, it appears that recovery of locomotor function after spinal cord injury can rely on the compensation of undamaged circuit components for damaged components through reconfiguration of the circuit and/or incorporation of new neurons into the circuit (Marder and Bucher 2001; Pearson 2001).

Although model systems such as the crustacean STG and the leech swim CPG have provided great insight into the function of neural circuits and CPGs, the impacts of intrinsic properties, synaptic communication, and neuromodulation on circuit output are poorly understood in most systems. It is often difficult to reliably identify and access CPG cells and even more difficult to record from them in a behaving animal. Further, specific targeting of mutations for manipulations of the CPG is impossible in all but a few organisms for which advanced genetic and molecular tools are available. Finally, the complexity of most CPG circuits dictates that intrinsic properties of large numbers of cells need to be investigated in order to comprehend the intricacies of each circuit. Therefore an invertebrate model system that uses a CPG to produce rhythmic and stereotyped movements and for which advanced genetic tools are available could provide valuable insights into the control of movement by neural circuits and how the intrinsic

properties of neurons contribute to circuit output. The *Drosophila* larva is just such an organism.

1.3 Drosophila as a model system

Drosophila is a potentially useful model system for the study of motoneuron intrinsic properties, their contribution to locomotion, and of locomotor CPGs for a variety of reasons. The genetic and molecular techniques available in *Drosophila* are surpassed in no other organism. The *Drosophila* nervous system is small compared to vertebrate nervous systems and locomotor behavior is simple and stereotyped in the case of the crawling larva, eclosing pupa, and flying adult, making these behaviors amenable to quantification. Further, whole-cell *in situ* patch clamp recordings from adult and larval motoneurons are possible, providing a more intact preparation in which to study intrinsic properties than the slice preparations required for recording from many vertebrate motoneurons.

1.3.1 Drosophila as a model system: GAL4-UAS system

Foremost among the genetic tools available in *Drosophila* is the GAL4-UAS system (Brand and Perrimon 1993). In this system, taken from yeast, the sequence for a transcriptional activator protein called GAL4 is inserted into the *Drosophila* genome downstream of a promoter of interest. When transcription of the promoter is activated by endogenous transcription factors, GAL4 protein is produced. GAL4 protein specifically binds to the “upstream activating sequence” (UAS site) inserted into the *Drosophila*

genome upstream of the sequence for a protein of interest. GAL4 binding to the UAS site then activates transcription of the protein of interest. Commonly used proteins of interest in the motor control field are reporter proteins such as GFP, modified ion channels, and even sequences for RNA interference (RNAi) molecules that recognize and destroy mRNA encoding ion channels or other proteins. The GAL4-UAS system, then, imparts spatial control of protein expression according to the promoter behind which the GAL4 sequence is inserted.

Advances in the GAL4-UAS system impart increased spatial specificity of protein expression via introduction of an additional enhancer trap element coding for GAL80 protein (Suster et al. 2004). GAL80 is a transcriptional repressor protein that, when present, binds the UAS site and prevents GAL4 activation of transcription. The GAL80 sequence inserted downstream of a second promoter prohibits GAL4 action in subsets of cells expressing the second promoter. For example, insertion of the GAL4 sequence downstream of a promoter called C380 confers specific expression in larval motoneurons and in cholinergic interneurons (Budnik et al. 1996). Interneuronal expression of the protein of interest can be prevented by insertion of the GAL80 sequence downstream of the promoter for acetylcholinesterase to prevent cholinergic interneuron expression of the protein of interest while preserving expression in motoneurons (Kitamoto 2002).

It is possible that long-term alteration of protein levels may cause homeostatic compensation. This is especially true for ion channel proteins that alter neuronal

excitability. Temporal control that limits the possibility of compensation can be obtained through insertion of a temperature-sensitive GAL80 sequence anywhere in the genome. In this case, the GAL80 protein prevents GAL4 activity until a temperature shift from 25°C to 32°C causes an inactivating conformational change in the GAL80 protein and permits GAL4 activation of transcription (McGuire et al. 2003). Temperature-sensitive expression of GAL80 allows researchers to both diminish the likelihood of misleading results due to homeostatic compensatory mechanisms and to pursue investigations into the mechanisms of homeostatic compensation.

1.3.2 Drosophila as a model system: RNAi technique

As mentioned previously and is discussed in greater detail in *Chapter 3*, RNAi has recently been added to the *Drosophila* genetic toolbox. RNAi technique utilizes a transgene for a double-stranded hairpin RNA (dsRNA) (Fire et al. 1998). This dsRNA is transcribed and then processed into small interfering RNA's (siRNA) that unite with a variety of proteins to form an RNA-induced silencing complex (RISC). The RISC complex recognizes, binds to, and causes degradation of mRNA's with complementary sequences to the siRNA (reviewed in Hannon 2002), resulting in knockdown of a protein of interest. Long utilized in cell culture and *C. elegans*, RNAi is an exceptionally powerful tool in *Drosophila* because its expression is cell-autonomous, in contrast to other organisms in which expression of RNAi in one cell causes organism-wide effects (Van Roessel et al. 2002). Therefore, RNAi sequences expressed in *Drosophila* using the GAL4-UAS system confer tissue-specific knockdown of a gene of interest. The RNAi

strategy is especially appealing because a library of *Drosophila* RNAi stocks targeting approximately 90% of the putative protein coding genes in *Drosophila* is available (Dietzl et al. 2007).

1.3.3 Drosophila as a model system: nervous system size

Beyond its genetic and molecular advantages, *Drosophila* is an advantageous model for studies of neuronal intrinsic properties and CPG function because the relatively small size of the nervous system facilitates identification of the motoneurons and interneurons that compose neural circuits. Estimates of the number of neurons in the human nervous system are in the billions. In contrast, the *Drosophila* nervous system contains approximately 100,000 neurons. Therefore, it is feasible to label neurons with marker proteins using the GAL4-UAS system and achieve consistent identification of individual neurons from animal to animal. Additionally, identification of CPG component neurons is potentially more feasible because CPGs in organisms with small nervous systems generally utilize individual neurons as building blocks whereas larger nervous systems utilize groups of neurons as circuit components.

1.4 Drosophila crawling

Drosophila larval body wall muscles are bilaterally and segmentally-repeated. Approximately 30 muscles in longitudinal, transverse, and oblique orientations are found in each abdominal hemisegment while the exact number of muscles varies in thoracic segments where the arrangement is slightly modified (Fig. 11). Motoneuron cell bodies

are located in the ventral ganglion and axons travel through segmental nerves to the muscles (Fig. 10). Thirty-one motoneurons and 43 sensory neurons have been identified per hemisegment (Landgraf et al. 1997; Bodmer and Jan 1987; Brewster and Bodmer 1995). The target muscle of each motoneuron has been relatively well-described in the embryo and larva, but the developmental origins of some larval motoneurons remains unclear, as addressed in *Chapter 3: Discussion* (Landgraf et al. 1997; Hoang and Chiba 2001).

Drosophila embryonic and larval crawling is a relatively simple behavior that involves peristaltic waves of muscle contraction proceeding from posterior to anterior for forward crawling and anterior to posterior for backward crawling. During each wave of forward crawling, the head of the animal is initially propelled forward by hydrostatic pressure generated by contraction of posterior segments (Berrigan and Pepin 1995). In the embryo, the anterior-most segments then remain on the crawling substrate while the peristaltic wave progresses through the animal (Crisp et al. 2008). Therefore, the role the anterior-most segments in crawling is unique, allowing the head to act as a fulcrum as the posterior portion of the animal moves forward.

Sensory feedback fine-tunes *Drosophila* crawling behavior, similar to its role in other organisms. The isolated CNS is capable of generating a fictive crawling pattern measured in extracellular nerve recordings and *Drosophila* embryonic CPG circuits develop the capacity to produce rhythmic peristaltic waves in the absence of sensory

input, but sensory input is required for development of normally patterned locomotion (Fox et al. 2006; Suster and Bate 2002). Multidendritic sensory neurons residing in the body wall act as proprioceptors that provide input to the CPG to facilitate propagation of the peristaltic wave and increase the speed of crawling (Hughes and Thomas 2007).
As described for other CPGs, the larval *Drosophila* crawling CPG requires appropriate neuromodulator activity in order to generate normal crawling behavior. Tyramine and octopamine, invertebrate counterparts to the adrenergic system, had opposing effects on crawling behavior such that a correct ratio of the two chemicals was important for normal crawling (Saraswati et al. 2004). Serotonin and dopamine are also important neuromodulators of the crawling CPG as inhibition of serotonergic and dopaminergic neurons caused aberrant circular crawling patterns rather than directed forward crawling (Suster et al. 2003).

Important questions about the crawling behavior in *Drosophila* larvae remain. The composition of the crawling CPG is unknown. Further, basic questions about the crawling pattern remain unanswered. It is unknown whether muscles within a segment contract simultaneously or with more precise patterning. Some evidence exists to indicate that there may be offsets in muscle contraction within a hemisegment, although it has not been well-described. Recordings of EJC's from dorsal and ventral neuromuscular junctions were offset such that activity in a ventral muscle occurred prior to activity in a lateral or a dorsal muscle (Fox et al. 2006). Examination of video of the crawling behavior also indicates that there may be an offset in dorsal and ventral muscle

contractions within a segment (Hughes and Thomas 2007). This offset may be different in thoracic and abdominal segments to facilitate specialized abdominal and thoracic roles during crawling. Additionally, intracellular muscle recordings during fictive crawling indicated that dorsal muscles usually contract before ventral muscles although the reverse relationship is occasionally observed (E. McKiernan and C. Duch, unpublished observation).

Although the neural circuits that control crawling are unknown, principles from segmental CPGs controlling other wave-like behaviors may provide insight into the expected structure and function of the *Drosophila* crawling CPG. Leech and lamprey studies of segmental coordination of swimming and crawling indicate that each segment (or few segments) contains a microcircuit that produces the motor pattern for that segment, and segments differ in cycle period and robustness of motor pattern (Hocker et al. 2000; Puhl and Mesce 2008). The coordination of intersegmental phase lags occurs via ascending and descending projections (Marder and Bucher 2001; Hill et al. 2003). Intersegmental coupling occurs between neighboring and distant segments but varies in strength between different segments to generate appropriate swimming patterns (Williams 1992; McClellan and Hagevik 1999). In leech crawling, intersegmental coordination is stabilized by descending neuromodulatory influences (Puhl and Mesce 2010). Leech and lamprey swim with dorsal-ventral and left-right alternating waves, respectively, not peristaltic waves. Nonetheless, intersegmental coupling of segmental oscillators is a principle that likely applies to the larval *Drosophila* crawling CPG.

It is also possible that the local segmental CPG circuits in *Drosophila* are similar to those in the well-studied leech swim CPG. The leech segmental microcircuit is composed of four bilaterally- and segmentally-repeated pairs of interneurons. The interneurons within a hemisegment are interconnected via mostly inhibitory synapses and bilateral hemisegments exhibit strong electrical and chemical coupling (Friesen et al. 1978). Therefore, the *Drosophila* crawling CPG may utilize inhibitory connections between interneurons within a hemisegment, although excitatory connections within and between hemisegments are not ruled-out. Indeed, immunohistochemistry indicates that inhibitory and excitatory interneuron populations are present in the ventral ganglion, although it is unknown whether or how they participate in the crawling CPG.

Drosophila has potential strengths as a model system in which to investigate principles of neural circuits and the contribution of intrinsic and synaptic properties to circuit output. Much work remains, though. Component neurons of the crawling CPG and their synaptic connections must be identified in order to elucidate circuit structure. Intrinsic properties of component neurons must be investigated in order to understand how circuit output is generated. A wide variety of molecular and genetic tools available in *Drosophila* can then be applied to the motor circuitry to gain further insight into the generation of motor output. Therefore, a useful place in which to begin investigations of the control of movement by neural circuits is the motoneuron itself. The motoneuron is

an accessible cell whose activity is readily quantifiable in the periphery and is an identified CPG component neuron that provides a direct measure of CPG output.

1.5 Size principle

Studies in mammalian motoneurons have historically interpreted motoneuron excitability and recruitment according to the size principle first proposed by Henneman. This explanation utilizes cable properties to describe the mechanism underlying the recruitment of motoneurons. Small motoneurons appear to have high specific membrane resistivity compared to large motoneurons (reviewed in Powers and Binder 2001). This observation, combined with the small size of the cells, predicts that small motoneurons will have a higher input resistance than large motoneurons and will require less current to reach firing threshold, or have a lower "rheobase" current. Studies have also shown that the synaptic input to small and large motoneurons in the same pool is roughly equivalent (Mendell and Henneman 1971; Henneman and Mendell 1981). Therefore, a given set of synaptic inputs will bring a small motoneuron to firing threshold before a large motoneuron and small motoneurons will be recruited before large motoneurons in an orderly manner.

Motoneuron size and axon diameter are correlated (Burke et al. 1982). Small motoneurons have smaller diameter axons that can produce fewer axon branches and innervate fewer muscle fibers than large motoneurons. Therefore, mammalian low-threshold motor units are comprised of small, readily-recruited motoneurons that

innervate a small number of muscle fibers and generate low levels of force (Burke et al. 1973; Henneman and Mendell 1981; Enoka 1995). High-threshold motor units consist of slowly recruited, large motoneurons that innervate a large number of muscle fibers and generate high levels of force.

Other organisms display an analogous division of motoneurons into “phasic” and “tonic” types. High-threshold, phasic motoneurons in the crayfish abdomen project to large, powerful muscle fibers and are silent except when recruited for escape activity. Low-threshold, tonic motoneurons project to thin muscle fibers and exhibit spontaneous activity that is useful for maintaining normal locomotor and postural functions (Atwood 2008; Kennedy and Takeda 1965a; Kennedy and Takeda 1965b). Insect motoneurons innervating the hind leg of the locust and the ventrolateral abdominal muscles of the blowfly larva also display a division into tonic and phasic types (Hoyle and Burrows 1973; Hardie 1976). Motoneurons in the crayfish leg are recruited in an orderly manner according to size of the cell body and input resistance, largely in agreement with the size principle (Hill and Cattaert 2008).

1.5.1 Size principle in Drosophila

Drosophila larval glutamatergic motoneurons are of two types that are hypothesized to be analogous to high-threshold and low-threshold motoneurons based largely on the similarity of larval neuromuscular junction morphology and physiology to previously-described neuromuscular junctions in other organisms. Crustacean low-threshold, tonic

motoneurons form large synaptic terminals that initially release small amounts of neurotransmitter in response to stimulation but then undergo facilitation, while high-threshold, phasic motoneurons form small terminals that initially produce large EJP's that undergo depression (Lnenicka et al. 1986). *Drosophila* type 1b ("big") neurons that project to a single muscle may be analogous to crustacean tonic motoneurons because they have "big" synaptic terminals and produce small EJP's that undergo facilitation in response to repetitive stimuli. Type 1s ("small") neurons project to groups of muscles, have "small" synaptic terminals, and produce larger EJP's that undergo depression in response to repetitive stimuli (Atwood et al. 1993; Kurdyak et al. 1994; Lnenicka and Keshishian 2000). The morphology and physiology of 1b and 1s neuromuscular junctions confer the potential for orderly recruitment of *Drosophila* muscles in a manner similar to the orderly recruitment of vertebrate and crustacean muscle fibers.

Differences exist between *Drosophila* and vertebrate muscles and neuromuscular junctions that must be considered in the interpretation of motoneuron recruitment. Insect neuromuscular junctions are unlike vertebrate neuromuscular junctions in that they exhibit graded synaptic transmission. Additionally, *Drosophila* muscles are a single muscle fiber, which implies that recruitment of a single *Drosophila* muscle is equivalent to recruitment of a vertebrate muscle fiber. Finally, vertebrate muscle fibers are strictly innervated by a single axon and *Drosophila* muscles can be multiply innervated, but *Drosophila* muscles are comparable to vertebrate muscle fibers in that an individual *Drosophila* muscle is innervated by only a single 1b or 1s axon (Hoang and Chiba 2001).

The graded nature of synaptic transmission and the muscle morphology in the *Drosophila* larva, while not identical to that in vertebrates, supports the gradual development of force through orderly recruitment of *Drosophila* motoneurons. Graded output from a single 1b and a single 1s motoneuron onto a single muscle implies that the smaller EJP produced by 1b terminals will produce a relatively smaller amount of force in the target muscle compared to the large EJP produced by type 1s terminals. Therefore, orderly recruitment of 1b motoneurons before 1s motoneurons would initially generate small increments of force. Recruitment of 1s motoneurons would then increase force production not only due to greater activation of individual muscles by large EJP's but also because 1s motoneurons innervate and recruit multiple muscles. It remains to be seen whether 1b motoneurons are recruited before 1s motoneurons during crawling and, if they are, whether the size principle underlies such a recruitment pattern. Additionally, the ion channels and intrinsic properties of *Drosophila* motoneurons remain relatively undescribed and the role of these properties in motor output is unknown.

1.6 Active motor neurons

Evidence that motoneurons are more than follower cells has accumulated over time, dating almost to the introduction of the size principle. Dendritic K^+ and Ca^{++} currents appear to impart most vertebrate motoneuron active properties, and the functional relevance of modulation of synaptic input to motoneurons by motoneuron active properties remains a topic of great interest.

Notably, Schwindt and Crill described a persistent inward current (PIC) in motoneurons that, once activated, amplifies synaptic inputs and causes motoneurons to exhibit bistable behavior (Schwindt and Crill 1980; Schwindt and Crill 1977). The PIC has since dominated studies of active properties in vertebrate motoneurons. The PIC is carried by slowly activating, non-inactivating L-type Ca^{++} channels and fast activating, non-inactivating Na^{+} channels. Activation of the PIC depends on a combination of 5-HT and depolarization and has the largest effect in small, easily-recruited motoneurons (Hounsgaard et al. 1988; Lee and Heckman 1998). Once activated, the PIC allows the cell to continue firing in the absence of continued input until a hyperpolarizing conductance is introduced to return the cell to a subthreshold state. It appears that the PIC is a mostly dendritic phenomenon and modeling predicts localization of L-type Ca^{++} channels near synaptic sites, although the exact distribution of the channels carrying the PIC remains unclear (Lee and Heckman 2000; Simon et al. 2003; Elbasiouny et al. 2005; Zhang et al. 2006).

Further progress was made in understanding the active properties of motoneurons with the discovery by Harris-Warrick and colleagues of a hyperpolarization-activated inward current (I_h) in neonatal rat motoneurons (reviewed in Kiehn et al. 2000). I_h maintains a more depolarized resting potential, aiding cells in their return to firing threshold and possibly imparting motoneurons with some degree of intrinsic rhythmicity. These findings are supported by immunolabeling of ventral horn motoneurons by the antibody to that HCN1 channels that have been proposed to carry I_h in the rat spinal cord (Milligan

et al. 2006). Inward-rectifying K^+ currents (K_{ir}) similarly maintain a depolarized resting potential and neonatal rat spinal motoneurons were shown to also express I_{Kir} (Kjaerulff and Kiehn 2001).

Dendritic K^+ currents have been well-studied in brain neurons, such as CA1 pyramidal cells of the hippocampus, and knowledge of K^+ currents in motoneurons is relatively sparse but accumulating. In addition to the previously discussed I_{Kir}, Ca^{++}-activated, delayed-rectifier, M-type and pH-sensitive K^+ conductances have been shown to modulate excitability in motoneurons, sometimes through their interaction with other active conductances. Small conductance, Ca^{++}-activated , slowly-inactivating K^+-currents (SK) in many neuron types return the membrane to rest following activation of voltage-gated Ca^{++} channels. In adult rat spinal motoneurons, I_{SK} was shown to be activated by, and contribute to the termination of, the PIC (Li and Bennett 2007). Immunohistochemical studies also demonstrated the presence of the delayed-rectifier Kv2.1 channel at synapses in the cell body and dendrites of rat spinal motoneurons (Muennich and Fyffe 2004). This finding indicates that delayed-rectifier channels may modulate synaptic inputs to motoneurons. The slowly-activating, non-inactivating voltage-gated M-current activates near the resting potential and was shown to decrease firing frequency and increase adaptation of firing frequency in adult turtle spinal motoneurons (Alaburda et al. 2002). I_M is so named because it is reduced by acetylcholine acting on muscarinic receptors and, indeed, reduction of I_M by muscarine was found in this study. These findings, combined with visualization of muscarinic

receptors in rat spinal motoneuron dendrites (Hellstrom et al. 2003), indicate a role for I_M in synaptic modulation.

Considering that the most distinguishing characteristic of neurons is their dendritic morphology, further study of the distribution of ion channels within motoneuron dendrites will be important for understanding motoneuron behavior and motor output. Studies in a variety of other neuron types indicate that the precise localization of ion channels within dendritic arbors varies according to neuron identity and may have profound effects on integration of synaptic inputs and neuronal firing behavior. For example, cortical pyramidal cell A-type channels cluster at GABAergic postsynaptic specializations (Burkhalter et al. 2006). Kv4 (Shal) channels carrying I_A increase in density in a proximal to distal gradient in CA1 pyramidal cell dendrites in the hippocampus, regulating action potential back-propagation and reducing distal EPSP amplitudes (Hoffman et al. 1997). CA1 cells also exhibit a proximal to distal increase in the density of HCN channels that carry I_h while periglomerular olfactory bulb cells exhibit a uniform density of HCN channels and HCN expression is excluded from hippocampal basket cell somatodendritic regions but found in the axon terminals (Lorincz et al. 2002; Holderith et al. 2003; Notomi and Shigemoto 2004). Numerous other observations of dendritic ion channel distributions and effects on neuronal behavior are well-described in (Nusser 2009).

Another motoneuron property that could enhance the contribution of active currents to motor output is the possible gap junctional coupling of motoneurons. Studies in neonatal rat preparations indicate that activity within a motoneuron may influence other neighboring motoneurons via gap junctions (Sharifullina et al. 2005). Gap junctional coupling in neonatal motoneurons imparts an oscillatory pattern of activity that enhances motoneuron firing responses. It is not clear that this phenomenon is present in adult preparations under normal conditions and could therefore be primarily a developmental phenomenon rather than a functional strategy (Chang and Balice-Gordon 2000). Gap junctional coupling is enhanced, though, in adult preparations in which the motor pool has suffered damage, indicating that motoneurons may be able to modify their coupling according to systemic conditions and needs (Chang et al. 2000).

Neuromodulator effects on motor output are mediated partly through modulation of interneuron and motoneuron intrinsic properties. One of the most-studied examples is the activation of motoneuron PICs by 5-HT. This activation is thought to amplify synaptic input and initiate bistable behavior, especially in small motoneurons, causing the motoneuron to fire continuously in the absence of prolonged drive from the CPG. Additionally, 5-HT increased excitability of motoneurons in the neonatal rat via I_h enhancement (Kjaerulff and Kiehn 2001; Takahashi and Berger 1990). 5-HT also increased turtle motoneuron excitability by decreasing a TASK-like (pH-sensitive) K^+ conductance (Perrier et al. 2003). Descending noradrenergic pathways have also been shown to initiate locomotion. Noradrenaline decreased motoneuron voltage threshold for

firing and increased rat lumbar motoneuron excitability through inhibition of K_{ir} (Fedirchuk and Dai 2004; Tartas et al. 2010). In contrast, the noradrenergic system hyperpolarized hypoglossal motoneurons through inhibition of I_h (Parkis and Berger 1997).

1.7 Electrophysiology in Drosophila

In order to utilize *Drosophila* for studies of motor circuitry and the contribution of motoneurons to motor output, electrophysiological studies of motoneurons and CPG interneurons will be required. Electrophysiological studies of the larval *Drosophila* neuromuscular junction have long been utilized for studies of synaptic release, but electrophysiological studies in the central nervous system have been limited by the small size of the organism. It is encouraging, though, that physiological studies increasingly complement existing knowledge of the *Drosophila* nervous system. Extracellular recordings from segmental nerves have provided valuable quantification of the segmental activation patterns in a variety of other organisms including leech swimming and crawling, lamprey swimming, cat walking, and turtle swimming. Therefore, it is no surprise that extracellular nerve recordings have been utilized to quantify fictive crawling in the filleted *Drosophila* larval preparation. Forward crawling, which occurs via an anteriorly-progressing peristaltic wave, has an approximately 15 sec cycle period in abdominal segments and increasing cycle offsets in increasingly distant segments (Fox et al. 2006). Extracellular recordings have further been used to quantify neuromodulator

effects on CPG output, such as the previously-discussed finding that the ratio of octopamine to tyramine is important for normal crawling behavior.

Intracellular recordings from cultured *Drosophila* neurons are a well-established method by which to investigate the contributions of ion channels to cellular behavior and to identify ion channel modulators. Cultures of primary dissociated embryonic neurons have been utilized to characterize a variety of neuronal properties including Na^+ currents, acetylcholine-activated currents, and K^+ currents (Wu et al. 1983; O'Dowd and Aldrich 1988; Albert and Lingle 1993; Wu and Ganetzky 1984). The "giant" neuron culture system in which cultured cells are grown from cell division-arrested neuroblasts produces large neurons with correspondingly large neurites that facilitate physiological recordings and investigation of ionic currents (Wu et al. 1990). This system was used to identify Na^+, Ca^{++}, voltage-gated K^+, Ca^{++}-activated K^+, Na^+-activated K^+, and persistent Na^+ channels in *Drosophila* neurons (Saito and Wu 1991). Further work in the "giant" neuron culture system showed that Shaker, an A-type K^+ channel, narrows spike shape and increases firing rate while Shab, a slowly-inactivating voltage-gated channel, is important for repolarization and repetitive firing behavior (Peng and Wu 2007a). Primary cultures of *Drosophila* larval motoneurons, larval brain neurons, and pupal neurons have since been developed (Hartwig et al. 2008; Kraft et al. 2006; Sicaeros et al. 2007). Unfortunately, the nature of cultured cells is such that neuronal characteristics and behavior can be modified by culture conditions. Therefore, it is difficult to know

which aspects of cultured cell identity are relevant *in vivo* and how those aspects of cellular identity function in a behaving animal.

In recent years, intracellular recordings from larval *Drosophila* motoneurons have become feasible. The dense glial covering and the small size of these cells had previously made such recordings technically implausible. Rohrbough and Broadie first described an *in situ* patch clamp technique in which the glial sheath covering the motoneurons was enzymatically-degraded in order to access unidentified larval motoneurons and measure their intrinsic properties (Rohrbough and Broadie 2002). Further progress was made when the same technique was used to dye-fill and record from identified motoneurons in order to unambiguously correlate abdominal motoneuron morphology and target with firing behavior (Choi et al. 2004).

Advances have since made patch clamp recordings from adult brain interneurons possible, even in a behaving animal. The first study utilizing whole-cell recordings in the adult brain investigated the response to and integration of olfactory stimuli (Wilson et al. 2004). Whole-cell recordings were then utilized to examine synaptic integration and construct an electrotonic model of the extensively-studied projection neurons of the antennal lobe (Gouwens and Wilson 2009). Excitingly, recordings from identified visual interneurons in a behaving animal recently determined that the gain of cellular responses was increased during flight, indicating that neuronal state was altered according to behavioral state (Maimon et al. 2010).

1.8 Drosophila larval motor neuron intrinsic properties

Valuable information regarding CPG control of *Drosophila* crawling may be gained from *in situ* patch clamp recordings of larval *Drosophila* motoneurons. Whole-cell recordings are attractive for the insight they may provide into the intrinsic properties of motoneurons, but also because synaptic input to motoneurons represents the complete output of CPG interneuronal circuitry. Therefore, CPG output may be monitored through measurement of synaptic currents in motoneurons.

Initial studies of unidentified abdominal motoneurons examined synaptic input and found that acetylcholine application elicited large excitatory responses and bursting in motoneurons while both GABA and glycine elicited inhibitory synaptic potentials (Rohrbough and Broadie 2002). Subsequently, whole-cell patch clamp combined with dye filling of abdominal motoneurons provided the first records of intrinsic properties of identified larval motoneurons and described diversity in firing behavior and K^+ channel kinetics among identified motoneurons (Choi et al. 2004). Specifically, correlation of cell body morphology and location with muscle target(s) and neuromuscular junction morphology indicated that the 1s motoneuron MNISN-1s exhibited longer delay-to-spike compared to four 1b motoneurons. A possible explanation for this observation was provided by voltage clamp studies indicating that I_A inactivation kinetics differed between MNISN-1s and the 1b motoneuron MN6/7-1b. Finally, a third study in the thoracic 1b motoneuron MN1-1b and thoracic MNISN-1s found that I_{Ca} was carried predominantly by an L-type channel and contributed to motoneuron firing behavior by

increasing the interspike interval and decreasing firing frequency through its effects on AHP magnitude, likely due to activation of I_{KCa} (Worrell and Levine 2008).

Many questions regarding larval *Drosophila* motoneuron firing behavior and intrinsic properties remain. It is unknown whether and to what degree diversity of intrinsic properties and firing behavior exists among larval motoneurons, motoneuron subtypes, and segmental homologues. Further, it is unknown whether motoneuron intrinsic properties are behaviorally-relevant or important for modulation of synaptic input. Finally, apart from Ca^{++} channels, it is unknown what types of ion channels are expressed by larval motoneurons and whether they confer active properties that influence motoneuron recruitment by the CPG during crawling. K^+ channels are an ideal place to begin investigation of the latter question due to their impressive diversity and the multitude of effects K^+ channels have been shown to have on neuronal firing behaviors.

1.9 Potassium channels

K^+ channels are critically important to the function of many cell types, including neurons. Pancreatic β-cells rely on K^+ channels to maintain resting membrane potential for coupling of insulin release to circulating glucose levels (reviewed in Koster et al. 2005). K^+ channels are associated with increased proliferation in tumor cells (reviewed in Wang 2004). Appropriate rhythm generation and electrical conduction in the heart require K^+ channel function. A variety of K^+ channel types are required to maintain vascular tone

and other smooth muscle functions (reviewed in Ko et al. 2008). Finally, it has long been known that K^+ channels are critical to the firing behavior of neurons. In neurons, K^+ channels return the membrane potential to baseline after an action potential, maintain the resting membrane potential, regulate bursting frequency, and more.

K^+ channels are the most diverse of the ion channels. In humans, voltage-gated K^+ channels are encoded by 40 genes from 12 subfamilies whose members may heteromultimerize with each other to create further channel diversity (reviewed in Wulff et al. 2009). In addition to traditional voltage-gated K^+ channels, ATP-sensitive, Ca^{++}-activated, Na^+-activated, inward-rectifying, g protein-coupled, and pH-sensitive K^+ channels exist. This diversity makes understanding the contribution of K^+ channels to organismal physiology challenging. Initial studies of K^+ channels measured net outward currents without differentiating channel identity. It is now possible, using pharmacological and molecular techniques, to dissect the contribution of individual channel types, subtypes, and accessory subunits to cellular function.

1.9.1 Potassium channels in Drosophila

The *Drosophila* genome contains four known voltage-gated K^+ channel genes and two Ca^{++}-activated K^+ channel genes. *shaker* and *shal* encode transient, inactivating, A-type K^+ channels. *shaker* belongs to the Kv1 subfamily of K^+ channels and *shal* to the Kv4 subfamily. *shaw* and *shab* encode delayed rectifier channels and belong to the Kv3 and Kv2 subfamilies, respectively (Butler et al. 1989). Shaw channels appear to be non-

inactivating while Shab channels are very slowly inactivating (Singh and Singh 1999). *slowpoke* (*slo*), codes for a large-conductance voltage- and Ca^{++}-activated K^+ channel (Elkins et al. 1986). A small-conductance, voltage- and Ca^{++}-activated K^+ channel gene (*sk*) is also present (Nolazco et al. 2001). Additionally, *ether-a-go-go* (*eag*) encodes a K^+ channel with as yet undefined properties and function in neurons (Warmke et al. 1991) and evidence of a slowly-activating non-inactivating M-type-like current has been demonstrated (S. Srinivasan, unpublished observation).

The *Drosophila* voltage-gated A-type channel Shaker is expressed throughout the nervous system and in muscle, as evidenced in immunological and physiological studies (Salkoff and Wyman 1983; Rogero et al. 1997). Alternate transcripts of the channel are differentially expressed in distinct brain regions (Schwarz et al. 1990). The functional role of Shaker has been well-studied in *Drosophila* muscle and neuronal cell culture. It narrows action potentials and increases firing rates in cultured cells and carries the majority of I_A in muscle (Peng and Wu 2007a; Haugland and Wu 1990). Shaker also controls the basal level of synaptic release at the larval neuromuscular junction (Ueda and Wu 2006). The second *Drosophila* A-type channel, Shal, is the predominant carrier of I_A in developing embryonic motoneurons (Baines and Bate 1998). Shal inactivation kinetics are regulated by an accessory protein that imparts functional variety to the channel (Diao et al. 2009). Although the relative distribution of Shaker and Shal in *Drosophila* larval motoneurons is unknown, Shal was shown to contribute the majority of the somatic I_A in larval *Drosophila* mushroom body neurons while Shaker made a significant contribution

to somatic I_A in only a small portion of cells (Gasque et al. 2005). An identified adult *Drosophila* flight motoneuron displays both Shaker and Shal-mediated currents in whole-cell patch clamp recordings from the cell body but exhibits Shaker localization in axons (Ryglewski and Duch 2009). Shaker localizes to axon terminals and Shal to somatodendritic regions in rat central neurons and the functional relevance of Shal dendritic localization has been extensively demonstrated in studies of dendritic active properties (see *Chapter 1: Active motoneurons*) (Sheng et al. 1992). Therefore, it may be predicted that Shal carries the majority of I_A in the somatodendritic regions of larval motoneurons while Shaker is enriched at axon terminals and in muscle.

Drosophila delayed-rectifier K^+ channels are less well-studied than their A-type counterparts. Shab and Shaw currents have been found in larval muscle (Hegde et al. 1999). The slowly-inactivating Shab encoded a major portion of I_K in cultured neurons and myotubes (Tsunoda and Salkoff 1995). In neurons, Shab reduced light-induced depolarization in *Drosophila* photoreceptor cells and was important for sustained neurotransmitter release during repetitive neuromuscular junction stimulation (Ueda and Wu 2006; Vahasoyrinki et al. 2006). Shab was also required for sustained firing in cultured neurons (Peng and Wu 2007b). The non-inactivating Shaw channel was found in the somatodendritic and axonal regions of *Drosophila* embryonic peptidergic neurons and motoneurons, where it maintained a hyperpolarized resting potential and low firing rate (Hodge et al. 2005). In contrast, Shaw mutations had little effect on muscle physiology. Shaw was also found in the presynaptic terminal of peptidergic

neuromuscular junctions and was required for rhythmic output of central clock neurons controlling the circadian cycle (Martinez-Padron and Ferrus 1997; Hodge and Stanewsky 2008).

Ca^{++}-activated K^+ channels (K_{Ca}) in the vertebrate nervous system include two families, BK and SK. BK is a large-conductance voltage- and Ca^{++}-sensitive channel while SK is a small conductance channel that is voltage insensitive. BK channels are coded by a single gene, *slowpoke,* with diversity generated through alternate splicing and through heteromeric assembly with the three identified β subunits (Adelman et al. 1992). Three SK genes have been identified that appear to undergo a great deal of alternate splicing (Kohler et al. 1996; Shmukler et al. 2001). BK channels are important for action potential repolarization and SK channels limit firing frequency (Faber and Sah 2003). *Drosophila* K_{Ca} channels are also encoded by *slowpoke* and *sk* and are expressed in a variety of tissues including nervous, muscle, tracheal, and midgut. Expression patterns are based upon the five tissue-specific promoters of *slo* (Becker et al. 1995; Brenner et al. 1996; Bohm et al. 2000). Further tissue-specific expression arises from alternate splicing and tissue-specific variants exhibit distinct biophysical properties (Brenner et al. 2000; Yu et al. 2006). As in vertebrate neurons, studies in *Drosophila* muscle showed that Slo channels were important for post-action potential repolarization (Atkinson et al. 1998).

It becomes clear that even in *Drosophila*, where relatively few K^+ channel genes are expressed, enough variety exists to make dissection of the functional contributions of K^+

channels to neuronal behavior and circuit output challenging. Further, the localization of ion channels within somatodendritic regions of larval motoneurons is unknown. As discussed in *Chapter 1: Active motoneurons*, localization of any of the K^+ channels to the dendrites could have an important effect in synaptic integration and cellular behavior. Encouragingly, the accessibility of larval motoneurons for patch clamp recording and the wealth of genetic tools available in *Drosophila* make the larval *Drosophila* motoneuron a powerful model for studies of the contribution of intrinsic properties, including ion channels, to motoneuron behavior.

1.10 Summary and statement of aims

The control of movement by neural circuits is a critically important function of any nervous system. It is also a complicated task due to the requirement that most motor behaviors be robust but also flexible for responses to the environment and behavioral state. Therefore CPG circuits are often composed of an intimidating number of different neurons and neuronal populations and undergo task-dependent reconfiguration. Dissection of the control of movement by neural circuits is therefore a difficult task for researchers and is aided by utilization of smaller invertebrate nervous systems in which individual circuit neurons and their connections can be identified. The larval *Drosophila* crawling CPG is a potentially useful model for studies of CPG control of movement due to the advanced genetic and molecular tools available in *Drosophila*.

Drosophila larval motoneurons are a useful place to begin investigations of the CPG control of crawling because the interneuronal components of the crawling CPG are unidentified and because increasing evidence exists that motoneurons provide active modulation of CPG output. Such active modulation is difficult to study in vertebrate systems where individual motoneurons cannot be identified and targeted from animal to animal and where reduced slice preparations are generally required for electrophysiological studies. Further, genetic perturbations of motoneuron and circuit properties are substantially more available and feasible in *Drosophila* than in most vertebrate systems. Finally, *Drosophila* glutatmatergic motoneurons are hypothesized to be divided into two types that are analogous to high-threshold and low-threshold motoneurons described in vertebrates and other organisms. Therefore, the effects of active properties on identified *Drosophila* motoneuron recruitment can be investigated using powerful genetic tools.

Therefore, the goal of this work is to investigate whether the firing behavior and recruitment of identified *Drosophila* 1b and 1s motoneurons is analogous to the recruitment of high-threshold and low-threshold motoneurons in other organisms, whether active conductances influence the motoneuron response to synaptic input, and how these factors influence CPG output to muscles. Therefore, three major aims are addressed. First, determine whether four identified thoracic motoneurons in the *Drosophila* larva generate unique firing behaviors and whether the firing behaviors of 1b and 1s motoneurons are analogous to the firing behaviors high-threshold and low-

threshold motoneurons in other organisms. Second, determine whether passive properties or active currents underlie the firing behavior and recruitment of identified motoneurons. Finally, determine whether the firing behaviors of identified motoneurons are relevant to crawling behavior and whether motoneuron intrinsic properties actively contribute to CPG motor output.

CHAPTER 2: ROLE OF INTRINSIC PROPERTIES IN DROSOPHILA MOTONEURON RECRUITMENT DURING FICTIVE CRAWLING

* this work has been submitted and is in review at the Journal of Neurophysiology as

Schaefer, J.E., Worrell, J.W., and Levine, R.B. Role of intrinsic properties in Drosophila motoneuron recruitment during fictive crawling.

2.1 Introduction

Motoneurons must integrate diverse inputs from sensory networks, central pattern generators, and higher order brain centers into coherent output in order to generate coordinated movements. In most organisms the motoneurons conserve a division into high-threshold and low-threshold types that are responsible for generating powerful and precise movements, respectively. Mammalian low-threshold motor units are comprised of small, readily-recruited motoneurons that innervate a small number of muscle fibers and generate low forces (Burke et al. 1973; Henneman and Mendell 1981; Enoka 1995). High-threshold motor units consist of slowly recruited, large motoneurons that innervate a large number of muscle fibers and generate high levels of force. Other organisms display an analogous division. High-threshold, phasic motoneurons in the crayfish abdomen project to large, powerful muscle fibers and are silent except when recruited for escape activity. Low-threshold, tonic motoneurons project to thin muscle fibers and exhibit spontaneous activity that are useful for maintaining normal locomotor and postural functions, similar to mammalian low-threshold motor units (Atwood 2008). Insect motoneurons innervating the hind leg of the locust and the ventrolateral abdominal muscles of the blowfly larva also display a division into high-threshold and low-threshold types (Hoyle and Burrows 1973; Hardie 1976).

Drosophila melanogaster larval glutamatergic motoneurons are of two types that may be analogous to high-threshold and low-threshold neurons. The divergence in *Drosophila* motoneurons has been well-studied at the neuromuscular junction. Type 1b (“big”)

neurons project to a single muscle and have “bigger” synaptic terminals. Type 1s (“small”) neurons project to groups of muscles and have “smaller” synaptic terminals (Lnenicka et al. 1986; Kurdyak et al. 1994; Lnenicka and Keshishian 2000). Therefore, 1b neurons may be analogous to low-threshold motoneurons and 1s neurons analogous to high-threshold motoneurons.

This positions the *Drosophila* larval locomotor system as a potentially powerful model in which to investigate the recruitment pattern of motoneurons, the importance of intrinsic properties to recruitment, and the behavioral relevance of recruitment order. Genetic tools allow consistent identification and manipulation of the intrinsic properties of neuronal populations and individual motoneurons. Further, the larval *Drosophila* central nervous system generates a peristaltic crawling movement in segmentally-repeated muscles (Fox et al. 2006), a relatively simple movement compared to the left/right and extensor/flexor alternation generated by the mammalian locomotor central pattern generator.

It is now possible to investigate the role of intrinsic properties in *Drosophila* motoneuron recruitment using *in situ* patch clamp recordings (Rohrbough and Broadie 2002; Choi et al. 2004; Worrell and Levine 2008). Previous studies have examined motoneurons referred to as MN1-1b (also known as aCC), MNISN-1s (RP2) and RP3 (MN6/7-1b). We use the terminology set forth by Hoang and Chiba for all neurons except RP3 (see *Chapter 2: Methods* for explanation of RP3 terminology) (Hoang and Chiba 2001). In previous patch clamp studies, MN1-1b and RP3 exhibited a lower current threshold for

spiking and a higher spike frequency than MNISN-1s (Choi et al. 2004; Worrell and Levine 2008). The intrinsic properties of 1b and 1s motoneurons studied to-date appear to correlate with neuromuscular junction physiology, yet it is unknown whether these properties are characteristic of neuron type (1b/1s) or simply the individual neuron (MN1-1b; MNISN-1s; RP3) because descriptions of 1s intrinsic properties are based upon a single motoneuron. Importantly, it is also unknown whether differences in intrinsic properties of *Drosophila* motoneurons are behaviorally-relevant. Therefore, we set out to compare 1b and 1s motoneurons projecting to dorsal muscles (MN1-1b and MNISN-1s) and ventral muscles (RP3 and MNSNb/d-1s) using whole-cell current clamp protocol and whole-cell recordings of synaptically-evoked firing behavior during fictive locomotion.

Recordings were made from thoracic motoneurons because a recent study indicated differences in thoracic and abdominal locomotor patterns (Dixit et al. 2008). Therefore, it is possible that the intrinsic properties of thoracic motoneurons are specialized to facilitate a specialized role of thoracic muscles. This possibility remains untested as the majority of whole-cell recordings have been performed on abdominal motoneurons (Rohrbough and Broadie 2002; Choi et al. 2004).

We find that resting membrane potential, voltage threshold, and delay-to-spike differ between 1b and 1s motoneurons. The longer delay-to-spike in 1s motoneurons is not due to passive properties of the cells, but is likely a result of active currents. The Shal A-type

K^+ current (I_A) is the primary determinant of delay-to-spike and recruitment patterns. Functional differences between 1b and 1s motoneurons are behaviorally-relevant, as a longer delay-to-spike is seen in MNISN-1s compared to MN1-1b when dual recordings of synaptically-evoked activity during bouts of fictive locomotion are compared. Additionally, based on comparisons of drive potentials recorded simultaneously from the cells, it appears that MN1-1b and MNISN-1s share a large portion of their synaptic input.

2.2 Methods

2.2.1 Drosophila stocks

Whole-cell current clamp recordings were obtained *in situ* from late 3rd instar *Drosophila* larval motoneurons in ventral ganglion thoracic segments 2 and 3. The GAL4-UAS system was used to drive expression of GFP in identified motoneurons. Lines used included: heterozygous dHb9-GAL4 (Broihier and Skeath 2002) to label RP3 (thoracic MN6/7-1b homologue, see below) [w;UAS-cd8-GFP;dHb9-GAL4], homozygous RRA-GAL4 (Fujioka et al. 2003) to label MN1-1b and MNISN-1s [w;UAS-cd8-GFP;RRA-GAL4], heterozygous vGLUT-GAL4 to label MNSNb/d-1s [w;UAS-cd8-GFP;vGLUT-GAL4], homozygous OK371-GAL4 (Mahr and Aberle 2006) to label MN1-1b, MNISN-1s, and RP3 [w;OK371-GAL4;UAS-cd8-GFP], and homozygous w;RN2-GAL4,UAS-mcd8-GFP;act<cd2<GAL4,UAS-flp for *shal* knockdowns. Vienna Stock Center #103363 (ShalRNAi) was used for *shal* knockdown experiments. vGLUT-GAL4 was a generous gift from the laboratory of S. Birman. The UAS-cd8-GFP source was Bloomington Stock Center #5137. For some recordings, Alexa 568 and/or rhodamine-dextran were included in the intracellular solution to confirm motoneuron identity based on neurite morphology and axon trajectories.

Motoneurons names are designated according to peripheral targets (1b) and host nerve (1s) (Hoang and Chiba 2001) with the exception of the motoneuron referred to as RP3. "RP3" is the embryonic name of this motoneuron (Landgraf et al. 1997). In the larval abdomen, RP3 forms the 1b neuromuscular junction shared by muscles 6 and 7.

Therefore, the abdominal motoneuron is called MN6/7-1b. The muscle target of the thoracic motoneuron, however, is a previously undescribed ventral muscle (personal communication from L. Feng, M. Landgraf). Therefore, we use the embryonic terminology RP3 for lack of a described and named muscle target.

To examine the possibility that differences in genetic background contributed to the differences that were observed in the functional properties among motoneurons, recordings were obtained from MN1-1b and MNISN-1s using OK371-GAL4 to drive GFP expression. The firing behavior and passive properties of these cells were not different from recordings made from cells labeled with GFP using the RRA-GAL4 driver line (data not shown). The parental line w;RN2-GAL4,UAS-mcd8-GFP;act<cd2<GAL4,UAS-flp served as the control line for the RNAi knockdown experiments.

2.2.2 Preparation

Dissection and desheathing of the preparation were performed in Ca^{++}-A solution (118 mM NaCl, 2 mM NaOH, 2 mM KCl, 4 mM $MgCl_2$, 1.8mM $CaCl_2$, 25 mM sucrose, 5 mM trehalose, 5 mM HEPES; approx. 295 mOsm; pH 7.1) (J Jan and Jan 1976). Osmolarity of all solutions was verified with a 5520 VAPRO osmometer (Wescor). Recordings obtained during fictive locomotion utilized a modified Ca^{++}-A solution containing 3.3mM $CaCl_2$ and 2.5mM $MgCl_2$. Protease 14 added to Ca^{++}- A-solution (2mg/ml) was applied to the ventral ganglion to degrade the glial sheath through a

micropipette with the tip broken to a diameter of approximately 10µm. Alternating positive and negative pressure was administered to apply protease and remove debris.

2.2.3 Electrophysiology

Thin-walled borosilicate electrodes were pulled on a PP-83 (Narishigie) to a resistance of 4-7 MΩ and fire-polished using an MF-35 microforge (Narishigie). Electrodes were filled with intracellular solution containing: 120mM potassium gluconate, 10mM HEPES, 1.1mM EGTA, 2mM $MgCl_2$, 0.1mM $CaCl_2$, and 20mM KCl (pH: 7.2; approx. 290mOsm). An Axoclamp 1B amplifier (Axon Instruments) with Clampex 10.1 software (Axon Instruments) was used for single-cell recordings. A Multiclamp 700B amplifier (Axon Instruments) was used for dual-cell recordings. Motoneurons with resting membrane potentials that were more depolarized than -40mV or with seals less than 1GΩ were not used. After verification of a GΩ seal, whole-cell configuration was achieved. In voltage clamp mode, a 40mV hyperpolarizing voltage command was administered and the resulting current measurement was used to calculate input resistance. For current clamp experiments, resting membrane potentials were brought to -60mV through bias current injection into the cell body unless otherwise noted. Current injections were provided in intervals of 10 pA, from -10 pA to 80 pA, lasting 400msec. Mean series resistances were: 13.95 ± 0.30 mΩ (MN1-1b), 15.38 ± 0.22 mΩ (RP3), 14.20 ± 0.39 mΩ (MNISN-1s), and 14.18 ± 0.54 mΩ (MNSNb/d-1s).

1μM tetrodotoxin (TTX, Sigma-Aldrich) was added to Ca^{++}-free A solution (modified Ca^{++}-A solution containing 0mM $CaCl_2$) to isolate voltage-dependent K^+ currents for voltage clamp recording. A holding potential of -80mV was used for voltage clamp studies. The linear leakage current was subtracted from all records. Current amplitude was normalized to whole-cell capacitance and reported as current density in I/V plots. Whole-cell capacitance was calculated from the charging transient following a 40mV hyperpolarizing voltage command. I_A was isolated by subtracting the currents evoked by a series of voltage clamp commands made from a holding potential of -40mV from those obtained from a holding potential of -80mV (see *Chapter 2: Results*).

The large degree of similarity in the EPSPs and firing responses of cells in dual recordings could have reflected electrical coupling of the cells and/or cross-talk between electrodes. However, current injected into one cell produced no response in the other cell (data not shown) and vice versa, ruling out the possibility of electrical coupling or reciprocal synaptic connections. Current injection into the bath also produced no response in the recording from the other electrode, ruling out the possibility of cross-talk between electrodes (data not shown).

2.2.4 Statistical Analysis

Statistical analyses were performed using a standard t-test with Excel software (Microsoft) except for measurement of delay-to-spike with and without a depolarizing

prepulse (Fig. 4b), where a paired t-test was used. Standard error values are reported. Significance was assumed when $p \leq 0.05$.

2.3 Results

We were able to target and perform *in situ* whole-cell patch clamp recordings from GFP-labeled MN1-1b, MNISN-1s, RP3, and MNSNb/d-1s in the second and third thoracic segments of the larval ventral ganglion. Whereas MN1-1b and MNISN-1s innervate muscles in the dorsal body wall, the others innervate ventral targets. Examination of the cellular responses to current injection indicated that all motoneurons exhibited spike shapes comparable to those described in previous studies (Fig. 1) (Rohrbough and Broadie 2002; Choi et al. 2004; Worrell and Levine 2008). Large spikes were separated by noticeable after-hyperpolarization with no evidence of accommodation or adaptation during 400msec current injections. Measurement parameters included resting membrane potential, voltage threshold for spiking, current threshold for spiking (rheobase current), delay-to-spike, firing frequency, and passive membrane properties.

The resting membrane potential of 1s motoneurons was significantly more hyperpolarized than 1b motoneurons (Table 1) and the voltage threshold more depolarized. Voltage thresholds were: -23.81 ± 0.80 for MN1-1b; -24.04 ± 1.03 for RP3; -15.68 ± 0.92 for MNISN-1s; -21.03 ± 1.12 for MNSNb/d-1s (Fig. 2a). MNISN-1s was significantly different from all other neurons while MNSNb/d-1s displayed a trend toward difference from RP3 ($p=0.059$) and MN1-1b ($p=0.057$).

Neither current threshold nor firing frequency distinguished 1b from 1s motoneurons. Thoracic 1b and 1s neurons did not group according to firing frequency, but rather MN1-

1b fired at a significantly higher frequency than all other neurons at current injections ≥40pA (Fig. 2b). These data, combined with the observation that MN1-1b had a lower current threshold than all other cells (Fig. 2c), indicate that MN1-1b is the most excitable of the four cells.

MNISN-1s exhibited a significantly longer delay-to-spike for a given current injection than 1b motoneurons at current injection levels between 60 and 110pA. MNSNb/d-1s exhibited a significantly longer delay-to-spike than MN1-1b at 60, 80, and 90pA injections and a longer delay than RP3 at 60, 70, 90, and 110pA injections (Fig. 1, 3). Additionally, the delay-to-spike relationship for MN1-1b had a significantly more shallow slope than that of the 1s motoneurons (MN1-1b: -2.54msec/pA vs. MNISN-1s: -4.65msec/pA and MNSNb/d-1s: -5.38msec/pA), likely a result of having an already short delay-to-spike at low current injections that excludes substantial shortening at higher injections. The longer delay-to-spike in 1s motoneurons suggests that 1s motoneurons may be recruited after 1b motoneurons during normal behavior (see below).

Although they were more easily recruited by current injection, 1b motoneurons had a significantly lower input resistance than 1s motoneurons (Table 1). Additionally, 1b motoneurons did not achieve more depolarized membrane potentials per current injection than 1s motoneurons (Fig. 2d). There was no consistent pattern of difference between 1b and 1s whole-cell capacitance, an indicator of cell size (Table 1). Therefore, passive properties cannot explain the longer delay-to-spike in 1s neurons.

To determine whether thoracic motoneurons display similar firing properties to previously-studied abdominal motoneurons, current clamp protocols were administered to MN1-1b (n=6) and MNISN-1s (n=3) in abdominal segments 1-3. These cells exhibited the same relationships in firing behavior as thoracic MN1-1b and MNISN-1s (data not shown). Interestingly, the input resistance of abdominal MN1-1b (1028.74±127.95) was significantly higher than that of thoracic MN1-1b (665.99±29.88), while its capacitance was significantly lower (abdominal MN1-1b: 24.363 ± 2.72; thoracic MN1-1b: 32.210 ± 2.01). Therefore, abdominal MN1-1b uses a different strategy to achieve the same firing behavior as thoracic MN1-1b (see *Chapter 2: Discussion*).

2.3.1 Role of A-type current in firing properties

Active conductances may play an important role in the recruitment pattern of *Drosophila* motoneurons. Specifically, an inactivating K^+ current, $I_{A,}$ has been proposed to be important for regulating the delay-to-spike (Choi et al. 2004). To examine this hypothesis, depolarizing prepulses of +20pA or +40pA lasting 1 sec., which are known to inactivate I_A (Salkoff and Wyman 1983), were administered prior to a current injection protocol (Fig. 4a). The delay-to-spike was decreased in all motoneurons, with the most dramatic reduction seen in 1s motoneurons (Fig. 4b). These results are consistent with the hypothesis that I_A is responsible for at least a portion of the delay-to-spike and that it plays a relatively larger role in the firing behavior of 1s neurons.

Drosophila A-type currents are encoded by two genes, *shaker* and *shal* (Tsunoda and Salkoff 1995). Therefore, RNA interference (RNAi) or mutations resulting in reduced function of one or both genes should result in a decreased delay-to-spike. *shal* was targeted for this study because *shaker* mutants were previously found to have no effect on delay-to-spike in abdominal motoneurons (Choi et al. 2004). A *shal* RNAi construct was therefore expressed in MN1-1b and MNISN-1s using a recombination-induced "flipout" strategy in which GAL4 activation in selected motoneurons is controlled by the actin promoter throughout embryonic and larval development (Hartwig et al. 2008). The parental line w;RN2-GAL4,UAS-mcd8-GFP;act<cd2<GAL4,UAS-flp served as the control line in these experiments. In motoneurons expressing the RNAi construct there was a decreased delay-to-spike in MN1-1b and MNISN-1s without a significant change in firing frequency compared to controls (Fig. 5a,b).

Voltage clamp measurements of I_A in MN1-1b and MNISN-1s were performed to verify the effect of ShalRNAi knockdown on the A-type current (Fig. 6a,b). I_A was isolated by subtracting the record obtained at a -40mV holding potential from the record obtained at a -80mV holding potential and measuring the resulting peak transient outward current. Control MN1-1b and MNISN-1s did not differ significantly in I_A or sustained outward current densities (see *Chapter 2: Discussion*). I_A density was decreased in ShalRNAi-expressing MN1-1b and MNISN-1s compared to controls (Fig. 6a,b). Sustained current density was not significantly different in ShalRNAi compared to control cells (Fig. 6b).

2.3.2 Responses of motor neurons to synaptic drive.

Whole-cell patch clamp recordings were obtained from semi-intact preparations undergoing fictive locomotion to determine whether the differences observed between 1b and 1s motoneurons in current clamp experiments are behaviorally-relevant. Extended periods of rhythmic activity were frequently observed in whole-cell records from freshly-dissected preparations. This activity correlated with visible rhythmic peristaltic contractions of the intact body wall muscles. The cycle period of these rhythmic bouts segregated into three groups: short cycle periods of < 2 seconds (consistent with twitches, rejected from analysis), medium cycle periods between 5-12 seconds (consistent with backward fictive locomotion), and long cycle periods > 15 seconds (consistent with forward fictive locomotion) (Fox et al. 2006). Simultaneous recordings from MN1-1b on the right and left sides of abdominal segment 1 during fictive crawling indicate that the cells fire bursts of action potentials in response to rhythmic synaptic input (Fig. 7 top). When the cells were held at similar membrane potentials, they displayed similarly-shaped drive potentials and fired nearly coincident action potentials (Fig. 7 bottom). Right and left pairs of MNISN-1s also displayed simultaneous depolarizations, although not every cycle of synaptic input elicited bursts of action potentials. If one MNISN-1s did not fire action potentials, neither did its contralateral homologue. Depolarizing one of the cells via bias current injection caused it to fire more action potentials per burst than its paired homologue.

Simultaneous recordings were also obtained from MN1-1b and MNISN-1s projecting to the same body wall hemisegment (Fig. 8a). The underlying drive potentials displayed similar time courses and amplitudes, however MN1-1b fired earlier than MNISN-1s and fired more action potentials per burst than MNISN-1s (Fig. 8b). In many recordings, the drive potentials of MNISN-1s and MN1-1b followed the same time course and elicited firing in MN-1b but not MNISN-1s (data not shown). When a current step protocol was administered to both cells during the interburst interval, MN1-1b required less current injection to initiate spiking and MNISN-1s displayed its characteristic delay to first spike. Therefore, the cells embedded in a functioning network display similar firing properties as when driven by current injection.

The synaptic drive to MN1-1b and MNISN-1s during fictive locomotion was examined in simultaneous recordings from cells that were hyperpolarized to prevent activation of voltage-dependent channels. Under these conditions, the drive potentials of MN1-1b and MNISN-1s were nearly identical (Fig. 9b). In some recordings the rhythmic synaptic drive did not evoke action potentials, but took the form of individual EPSPs that occurred nearly one-for-one in MN1-1b and MNISN-1s (Fig. 9c) indicating a common source of synaptic drive.

2.4 Discussion

We find that resting membrane potential and voltage threshold distinguish 1b and 1s motoneurons and provide evidence that *shal* is the gene encoding the A-type K^+ channel that is largely responsible for the characteristic delay-to-spike. When MN1-1b and MNISN-1s were recorded simultaneously during fictive locomotion, MNISN-1s displayed its characteristically longer delay-to-spike, though the time course and amplitude of the drive potentials were similar. MNISN-1s often failed to fire action potentials in response to the shared synaptic drive. Therefore, it appears that the increased delay-to-spike and higher voltage threshold in 1s motoneurons play a functional role in the recruitment of motoneurons during locomotion.

1b motoneurons exhibit a more hyperpolarized voltage threshold than 1s motoneurons. Type 1b neurons also have a shorter delay-to-spike following current injection. These characteristics, together with the more depolarized resting potential of 1b motoneurons, lead to the prediction that 1b motoneurons are more easily recruited than 1s motoneurons. When these findings are considered with existing data from the neuromuscular junction indicating that synaptic release is easier to initiate in 1b motoneurons (Lnenicka and Keshishian 2000), *Drosophila* 1b motoneurons appear to be functionally analogous to tonic motoneurons and 1s motoneurons functionally analogous to phasic motoneurons.

It is of interest that although 1b and 1s motoneurons displayed significant differences in voltage threshold, there was also variation between the dorsally- and ventrally-projecting

1s motoneurons. The voltage threshold for firing of MNISN-1s was significantly higher than that of MNSNb/d-1s. Such a difference in threshold may cause MNISN-1s to fire after MNSNb/d-1s during crawling, resulting in an offset in dorsal and ventral muscle group recruitment. Focal patch recordings of synaptic currents at the neuromuscular junction (Fox et al. 2006), and extracellular nerve recordings from dorsally- and ventrally-projecting nerves (E. McKiernan and C. Duch, personal communication) indicate an offset in dorsal and ventral muscle/nerve activation during fictive locomotion, supporting this idea. Simultaneous intracellular recordings from MNISN-1s and MNSNb/d-1s during fictive locomotion could resolve this question.

The resting membrane potential of 1b motoneurons was significantly depolarized compared to 1s motoneurons. It is likely that the more depolarized resting state of 1b motoneurons facilitates firing by reducing the drive necessary to initiate spiking. This may contribute to the more reliable recruitment of MN1-1b than MNISN-1s during bouts of fictive locomotion. Indeed, depolarizing bias current during fictive locomotion increased the reliability of MNISN-1s recruitment.

Motoneurons targeting dorsal and ventral body wall regions were chosen because there appears to be an offset in ventral muscle contraction and firing of ventrally-projecting motoneurons compared to their dorsal counterparts (supplementary video from Fox et al. 2006; Hughes and Thomas 2007). It is either the case that the crawling CPG provides offset input to dorsally- and ventrally-projecting motoneurons or that the intrinsic

properties of dorsally- and ventrally-projecting motoneurons impart distinct delays to recruitment. Our studies revealed few differences in the firing properties of dorsally- and ventrally-projecting motoneurons. Differences observed were the increased excitability of MN1-1b compared to RP3 and the hyperpolarized voltage threshold of MNSNb/d-1s compared to MNISN-1s (see *Chapter 2: Discussion*). These differences are in accordance with passive properties of the cells (Table 1) and indicate that passive properties work in concert with active properties, such as I_A, to determine the final output of the cell.

In mammals, ordered motoneuron recruitment is explained by the size principal (Henneman and Mendell 1981). According to the size principal, the longer delay-to-spike in 1s motoneurons should be a consequence of a lower input resistance. However, 1s motoneurons have a significantly higher input resistance than 1b motoneurons. Additionally, rheobase current (current injection to spike) was not a parameter that distinguished 1b from 1s motoneurons in this study. If the size principal were guiding recruitment, a higher rheobase would be expected in 1s motoneurons. Therefore, larval *Drosophila* motoneurons must utilize a strategy other than the size principal to generate ordered recruitment. Interestingly *Drosophila* motoneurons of the same identity may also utilize different strategies to generate appropriate recruitment and firing behavior, as abdominal MN1-1b exhibits firing behavior like that of thoracic MN1-1b but has a significantly higher input resistance and lower whole-cell capacitance. Future studies to compare active currents in thoracic and abdominal MN1-1b may be useful to understand

how the higher input resistance in abdominal MN1-1b fails to alter firing behavior compared to thoracic MN1-1b.

2.4.1 Role of A-type current in firing properties.

Active properties of motoneurons, specifically A-type K^+ currents, appear to determine motoneuron recruitment order in *Drosophila* larvae. Two A-type channels are present in *Drosophila*: Shaker and Shal. Genetically-targeted expression of ShalRNAi in MN1-1b and MNISN-1s significantly reduced delay-to-spike. Voltage clamp recordings indicate that I_A is decreased in MN1-1b and MNISN-1s cells expressing ShalRNAi. The decreased A-type current correlates with the shorter delay-to-spike observed in these cells. Therefore, the *shal*-encoded A-type current is the primary determinant of the timing of larval motoneuron recruitment.

However, differences between 1b and 1s motoneuron delay-to-spike cannot be explained by differences in A-current density as measurements of A-current density were equal in MN1-1b and MNISN-1s. Importantly, our results agree with those described by (Choi et al. 2004) indicating that when an inactivating prepulse protocol was administered prior to a -40mV test pulse, I_A in MN1-1b exhibited greater inactivation than in MNISN-1s at voltages $\geq$ -60mV (data not shown). Therefore, the voltage-dependence of I_A inactivation is different in MN1-1b and MNISN-1s such that a greater portion of I_A undergoes closed-state inactivation near rest in MN1-1b. The more depolarized resting potential of MN1-1b would also tend to encourage I_A inactivation. The delay-to-spike is likely shorter in

1b motoneurons because I_A undergoes greater inactivation at low levels of depolarization in 1b than in type 1s motoneurons. It cannot be concluded, though, that this result applies to all 1b and 1s motoneurons as recordings were not performed in MNSNb/d-1s and RP3.

2.4.2 Responses of motor neurons to synaptic drive.

We obtained recordings of MN1-1b and MNISN-1s firing behavior during fictive crawling in order to interpret the behavioral relevance of the firing responses of these cells to current injection. Dual patch clamp recordings were performed from pairs of MN1-1b, MNISN-1s and MN1-1b/MNISN-1s motoneurons during fictive locomotion to determine the relative timing and amplitude of the synaptic drive to MN1-1b and MNISN-1s as well as their firing patterns in response to this drive. Recordings from contralateral pairs of MN1-1b or MNISN-1s motoneurons displayed nearly one-to-one firing patterns as well as synaptic drive potentials with nearly identical time courses and amplitudes. While MN1-1b fired bursts of action potentials during each bout of rhythmic drive, MNISN-1s often did not. When the cells were hyperpolarized to block activation of voltage-dependent channels, drive potentials were similar in amplitude, duration, and timing between cells. This suggests a higher voltage threshold for recruitment of MNISN-1s than MN1-1b in response to behaviorally-relevant synaptic input. Further, dual recordings from MN1-1b and MNISN-1s indicated that, when MNISN-1s did fire a burst of action potentials, it displayed its characteristic delay-to-spike relative to MN1-1b, supporting the role of an A-type K^+ current carried by Shal in patterning recruitment.

Overall, it appears that the A-type current carried by Shal channels is very important in determining the delay-to-spike in larval *Drosophila* motoneurons. The delay-to-spike, then, imparts a recruitment order to 1b and 1s motoneurons that would support an initial development of low force in single muscles driven by 1b motoneurons followed by the recruitment of high-threshold 1s motoneurons that drive the contraction of groups of muscles that can generate greater amounts of force. This does not exclude a contribution of other aspects of motoneuron identity and intrinsic properties to motoneuron behavior. Rather, it is likely that motoneuron type (1b/1s) is a facet of individual motoneuron identity (MNISN-1s/MNSNb/d-1s) and that both contribute to the final output of a motoneuron. The finding that transcription factor expression pattern, a determinant of individual motoneuron identity, modifies motoneuron electrical properties (Pym et al. 2006) supports the idea that motoneuron type is an aspect of individual motoneuron identity. This indicates that specific firing behaviors and electrical properties are shared among a type of motoneurons while other parameters are unique to individual motoneuron based on their genetic identities.

2.5 Acknowledgements

Thank you to the S. Birman laboratory for sharing the vGLUT-GAL4 line.

Support for this study came from NIH grant NS28495 to RBL, NIH fellowship T32 GM008400 to JS, and NSF fellowship 0638744 to JS.

The current address of JW is the UCLA Department of Neurobiology.

Table 1. Properties of identified motor neurons.
1s and 1b motoneurons are significantly different in resting membrane potential, input resistance, and capacitance.

	resting membrane potential (mV)	input resistance (mΩ)	capacitance (pF)
MN1-1b (n=16)	-46.6 ± 1.3	666.0 ± 29.9	32.2 ± 2.0
RP3 (n=21)	-47.1 ± 1.0	496.0 ± 17.8*	14.4 ± 0.8*
MNISN-1s (n=16)	-50.6 ± 1.0*,**	1051.7 ± 57.9*,**	24.9 ± 1.1*,**
MNSNb/d-1s (n=12)	-51.4 ± 0.9*,**	1090.8 ± 83.9*,**	22.9 ± 0.9*,**

*indicates significant difference with MN1-1b, ** indicates significant difference with RP3

Figure 1. Current clamp recordings of motoneuron spiking behavior.
1b motoneurons are blue, 1s motoneurons are red. Current injections in 20pA intervals beginning at -20pA are shown. **A.** MN1-1b **B.** RP3 **C.** MNISN-1s **D.** MNSNb/d-1s

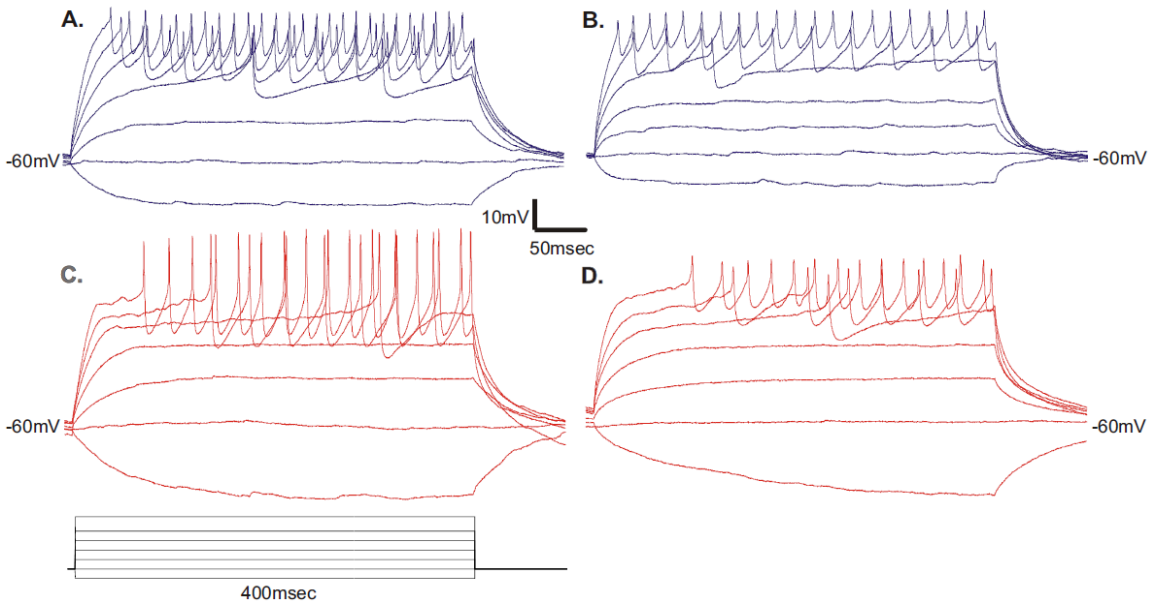

Figure 2. Voltage threshold and delay-to-spike distinguish 1b vs. 1s motor neuron firing behavior.
A. 1b motoneurons have a more hyperpolarized spike threshold than 1s motoneurons. MNISN-1s (n=16) is significantly different from all other motoneurons while MNSNb/d-1s (n=12) shows a trend toward difference with MN1-1b (n=16, p=0.059) and RP3 (n=21, p=0.066) **B.** MN1-1b has a higher firing frequency than all other neurons for current injections ≥40 pA. **C.** Current threshold does not distinguish 1b and 1s neurons. MN1-1b has a significantly lower current threshold than all other motoneurons. **D.** Current injections produce significantly less depolarization in RP3 than other motoneurons at some current levels but there are no systematic differences among the type 1b and 1s motor neurons.

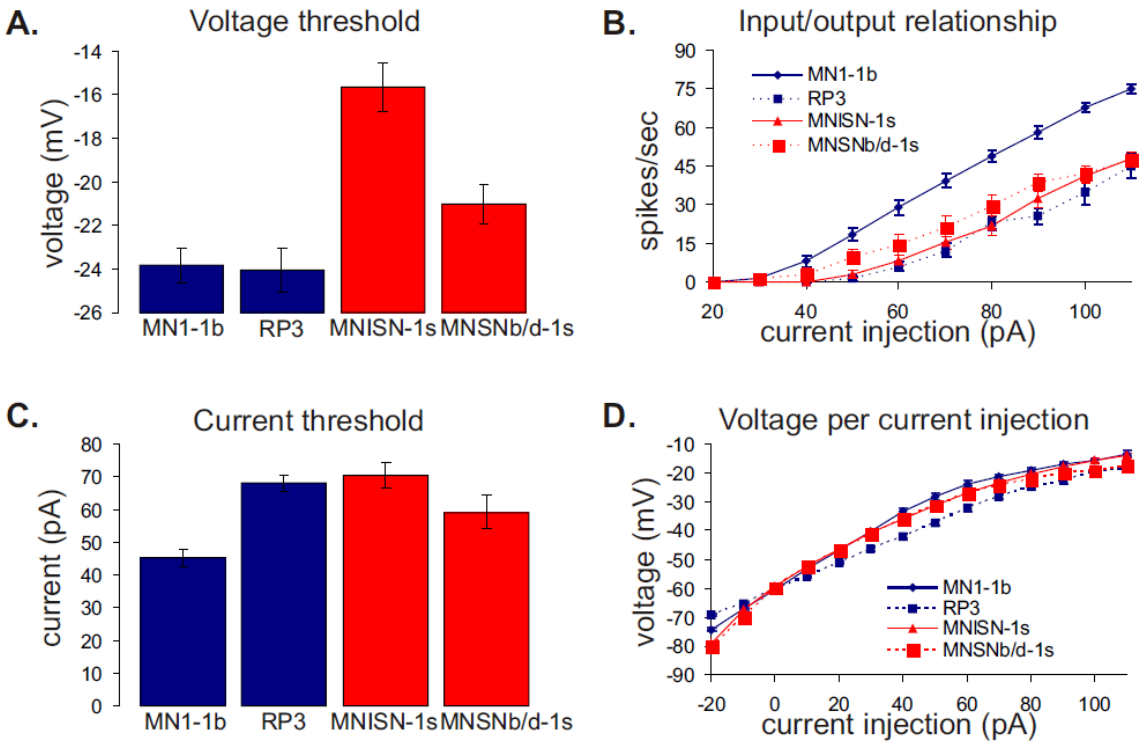

Figure 3. Delay-to-spike is longer in 1s motor neurons.
A. Mean delay-to-spike per current injection level. MNISN-1s (n=16) is significantly different from MN1-1b (n=16) and RP3 (n=21) between 50 pA and 110 pA. MNSNb/d-1s (n=12) is significantly different from MN1-1b at 60, 80, and 90 pA, and from RP3 at 60, 70, 90, and 110 pA. **B.** Grey curves are individual neurons, bold curves indicate average values. Note that the left portion of 1s average delay curves appear artificially low and variable because many individual neurons do not spike at low current injection levels.

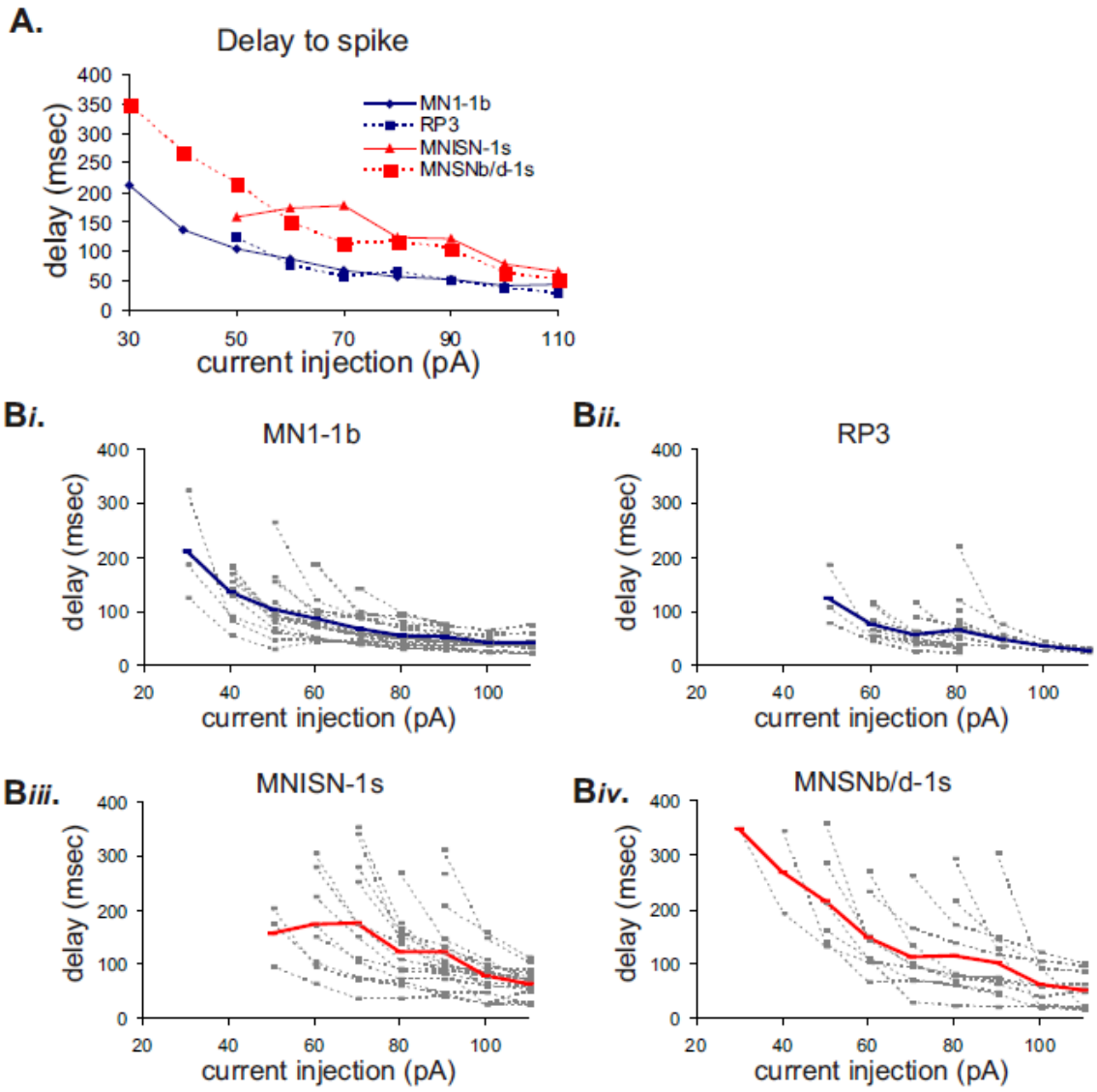

Figure 4. Active properties of motor neurons contribute to delay-to-spike. Delay-to-spike is significantly decreased when a 1 sec. prepulse is provided prior to current clamp protocol. **A.** MNISN-1s firing response with no prepulse (top) and with a +40pA prepulse (bottom). **B.** Delay-to-spike for 80pA current step. Black bars are delay after no prepulse. Decrease in delay-to-spike after +20pA prepulse (grey bars) is significant for MN1-1b (n=11) and MNSNb/d-1s (n=11), decrease in delay after +40pA prepulse (white bars) is significant for MNISN-1s (n=12) and MNSNb/d-1s. RP3 (n=13) decreases were not significant.

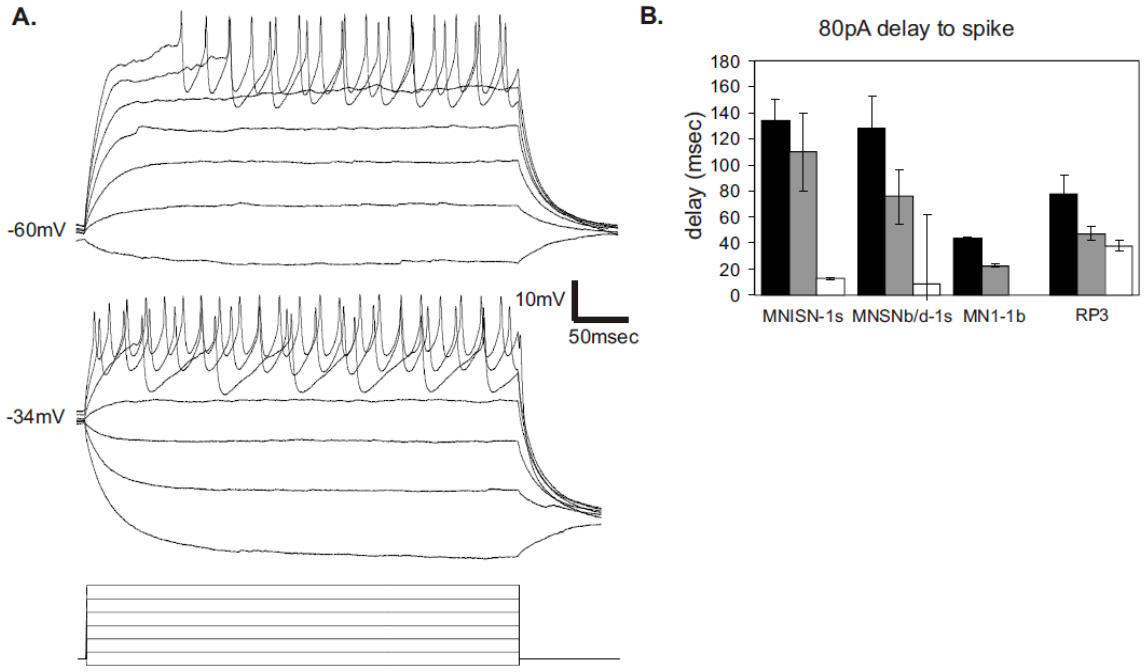

Figure 5. ShalRNAi expression decreases delay-to-spike and increases firing frequency.

ShalRNAi expression in MN1-1b and MNISN-1s significantly modified firing behavior. **A.** Current clamp recordings from control and ShalRNAi-expressing cells. Obvious decreases in delay-to-spike are observed in MN1-1b and MNISN-1s. **B.** ShalRNAi decreased delay-to-spike in MN1-1b ShalRNAi (n=3) and MNISN-1s ShalRNAi(n=5) compared to control MN1-1b (n=6) and MNISN-1s (n=5), respectively. Significant decreases for MN1-1b were observed at current injection levels ≥ 80pA. Significant differences for MNISN-1s were observed at 70, 100, and 110pA current injection levels. Firing frequency was not significantly changed in MN1-1b or MNISN-1s ShalRNAi-expressing cells.

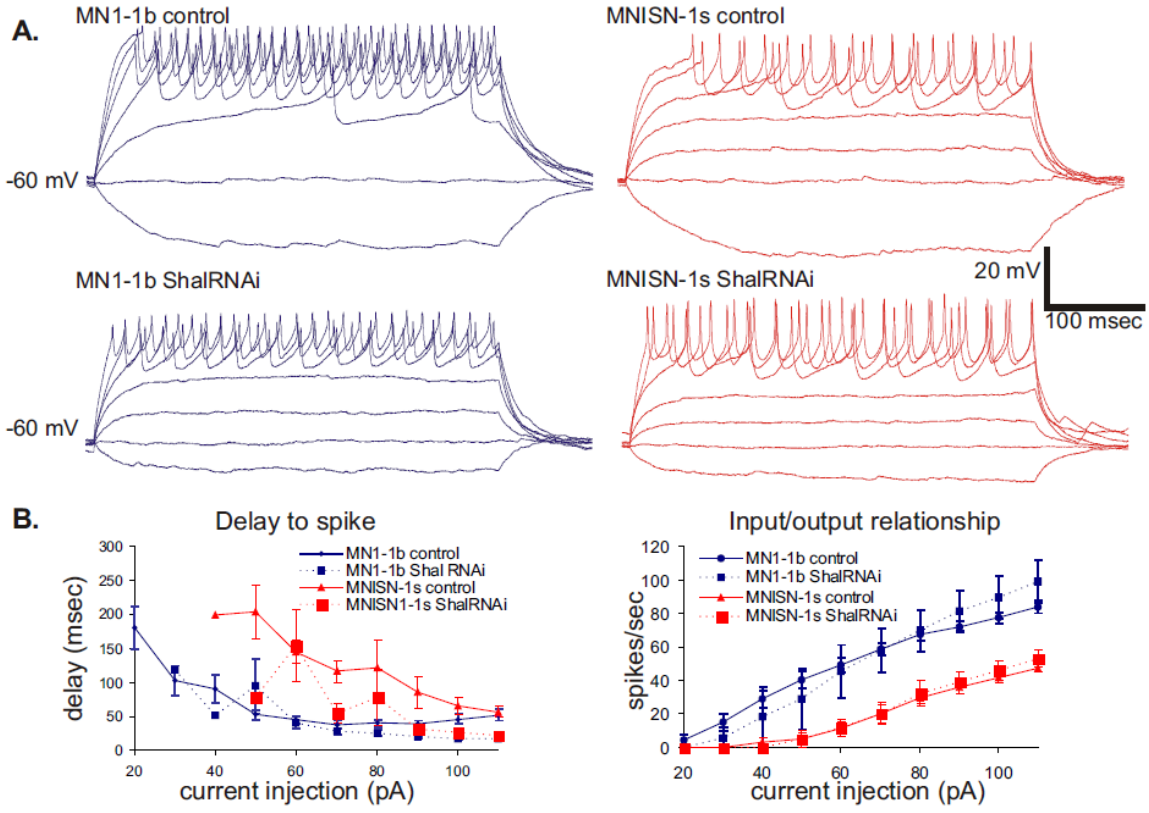

Figure 6. ShalRNAi expression decreases I_A.
A. Voltage clamp recordings of K^+ currents from control and ShalRNAi-expressing MN1-1b and MNISN-1s. Voltage steps of 20mV starting at -120mV from a holding potential of -80mV are shown. The transient peak outward current is absent from ShalRNAi cells. **B.** Voltage clamp record obtained from a holding potential of -40mV was subtracted from voltage clamp record obtained from a -80mV holding potential in order to isolate I_A. Representative subtracted records are shown for a MNISN-1s control cell (left) and a MNISN-1s ShalRNAi cell (right). **C.** V/I plot of I_A density and sustained outward current density in control MN1-1b (n=5), ShalRNAi MN1-1b (n=3) MNISN-1s (n=5) and ShalRNAi MNISN-1s (n=4). Significant decreases in MNISN-1s I_A density were observed at -80, 20, 40, and 60mV steps. No differences in sustained current density were observed.

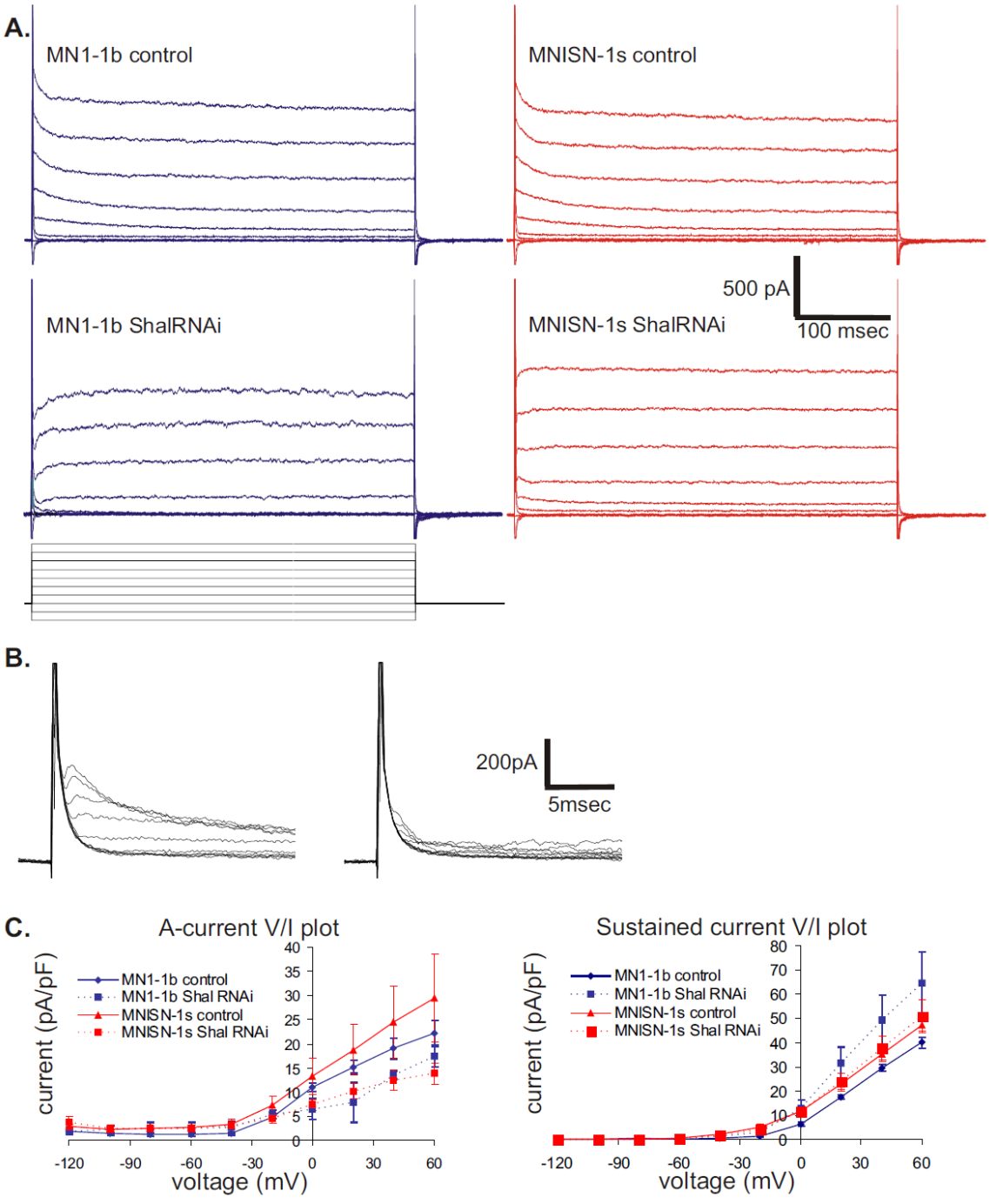
A.
MN1-1b control
MNISN-1s control
500 pA
100 msec
MN1-1b ShalRNAi
MNISN-1s ShalRNAi
B.
200pA
5msec
C.
A-current V/I plot
current (pA/pF)
MN1-1b control
MN1-1b Shal RNAi
MNISN-1s control
MNISN-1s Shal RNAi
voltage (mV)
Sustained current V/I plot
current (pA/pF)
MN1-1b control
MN1-1b Shal RNAi
MNISN-1s control
MNISN-1s Shal RNAi
voltage (mV)

Figure 7. Dual recordings from MN1-1b right and left homologues.
Dual whole-cell patch clamp recordings from contralateral MN1-1b homologues in the first abdominal segment of the ventral ganglion during fictive locomotion. Cells receive coincident excitation and fire nearly simultaneously.

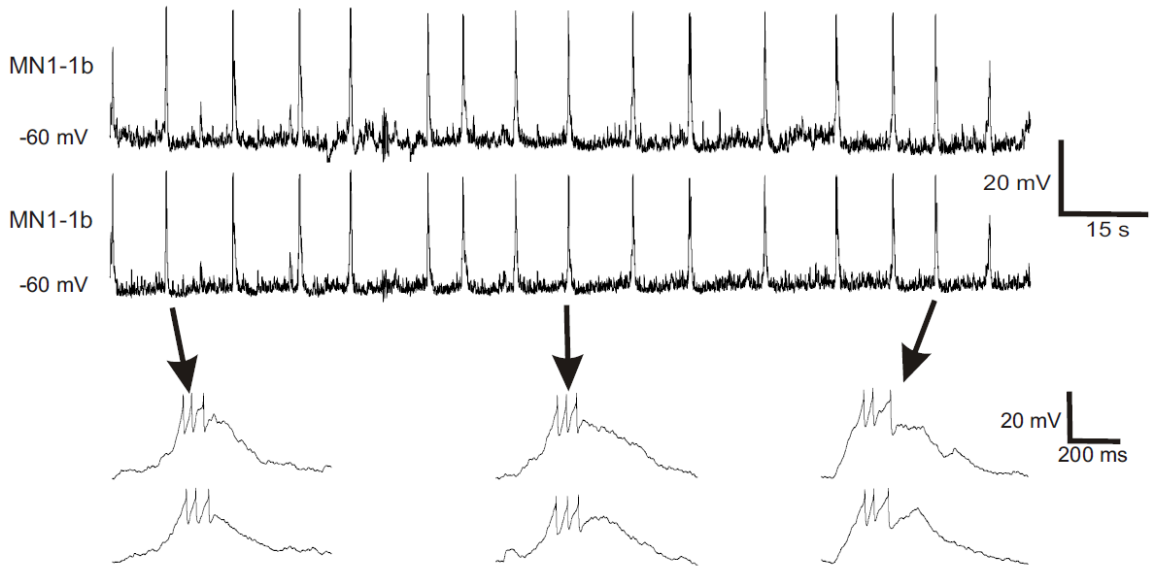

Figure 8. Dual recordings from MN1-1b and MNISN-1s projecting to same body wall hemisegment.

A. Dual whole-cell patch clamp recordings from MNISN-1s (red) and MN1-1b (blue) display coincident rhythmic drive during fictive locomotion. **B.** MNISN-1s fires later than MN1-1b in response to synaptic input during fictive locomotion. **C.** Current clamp recordings from pair of cells shown in A. Current injections of -20, 10, 50, 110, and 130, 150pA are shown.

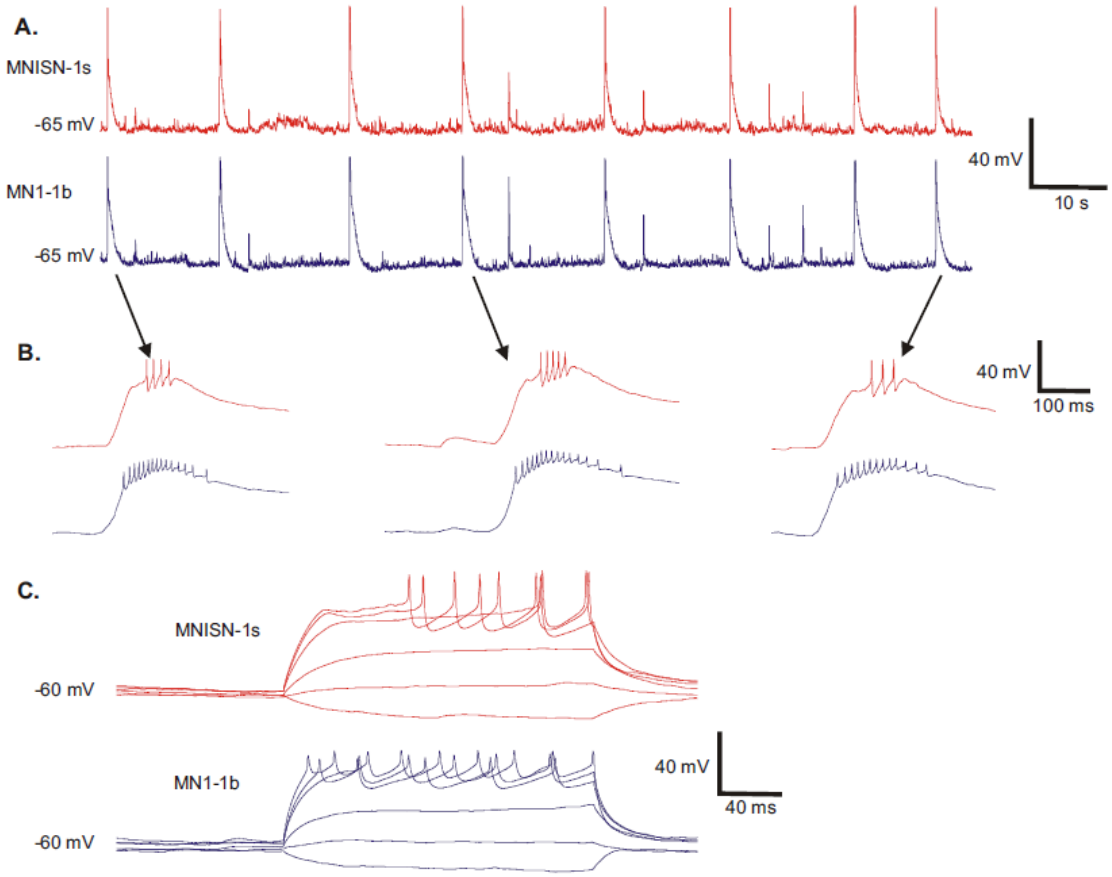

Figure 9. MN1-1b and MNISN-1s receive common synaptic input.
A. Dual patch clamp recording from MNISN-1s (red, top) and MN1-1b (blue, bottom) during fictive locomotion display nearly identical drive potentials. **B.** Overlay of simultaneous bursts generated in MNISN-1s and MN1-1b highlighting similar drive potential amplitude and shape when resting at -60mV (left) and when brought to -80mV to block spiking (right). **C.** In some recordings, it was possible to discriminate one-for-one EPSPs that did not elicit action potentials in MNISN-1s and MN1-1b.

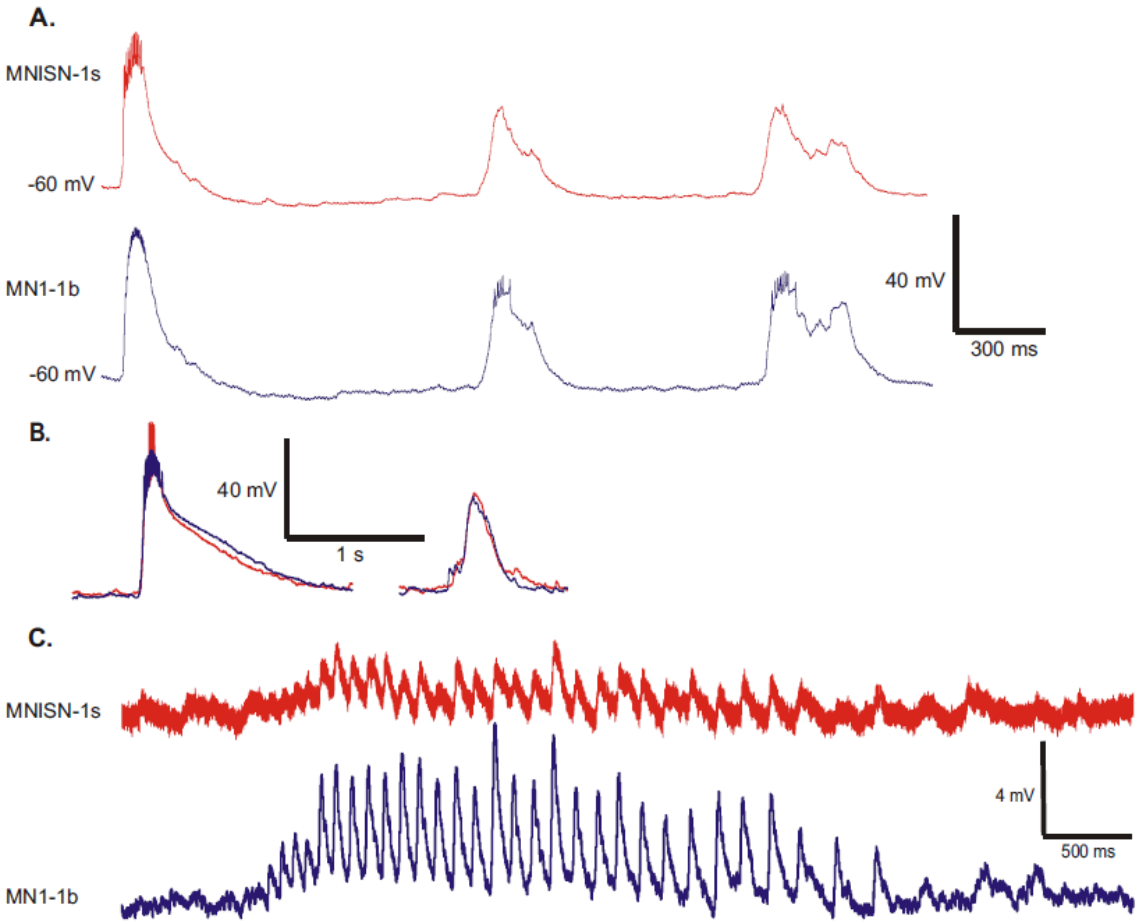

CHAPTER 3: MOTONEURON IDENTITIES AND INTERACTIONS WITH CENTRAL PATTERN GENERATING CIRCUITRY

3.1 Introduction

Although the previous study addressed the importance of motoneuron intrinsic properties for behaviorally-relevant recruitment, additional questions remain. This chapter will address three questions for which my research provided information that will be useful for future studies.

First, motoneuron names, morphology, and targets are distinct between the well-studied embryo and the larva and in different body segments. Therefore, clarification of larval thoracic motoneuron morphologies and muscle targets will assist researchers in the field to reduce ambiguity in the identification of larval and embryonic motoneurons and of abdominal and thoracic homologues. Therefore, the first aim was to determine whether larval thoracic motoneuron identity, morphology, and muscle targets could be correlated with embryonic and abdominal homologues.

Second, it is important to consider the input that presynaptic circuitry provides to larval motoneurons if we wish to understand how motoneurons contribute to behavior. This requires analysis of the synaptic drive received by the motoneurons. The second aim, therefore, was to investigate whether synaptic inputs to all four motoneurons could be observed in electrophysiological recordings and whether intrinsic properties of dorsal vs. ventral and thoracic vs. abdominal motoneurons specialize their output responses to synaptic input for crawling behavior.

Finally, we were interested to understand the different roles of the two I_A carriers, Shaker and Shal, and how RNAi technique could be utilized to examine their contributions to motoneuron behavior. Thus, we sought to understand what considerations must be taken into account when using RNAi strategy and how Shal and Shaker may fulfill different roles in a cell.

3.1.1 Developmental origins of motor circuitry

Neuronal identity and motor circuits in the mammalian spinal cord are determined by developmental origins and a transcription factor code that is uniquely expressed in different neuronal subpopulations. A similar transcription factor code seems to function in designating *Drosophila* motoneuron identity. The following will first address the transcriptional code in vertebrates, and specifically its function in the development of ventral spinal cord circuitry that controls movement. The function of transcription factor codes in the development of *Drosophila* motoneurons and its similarities to vertebrate development will then be discussed.

A gradient of Sonic hedgehog (Shh) protein in the neural tube, decreasing in concentration from ventral to dorsal, generates different interneuron classes depending upon the Shh concentration to which the cells are exposed (Marti et al. 1995; Roelink et al. 1995; reviewed in Jessell 2000). Briefly, five Shh-repressed (class I) and two Shh-induced (class II) homeodomain proteins are differentially expressed according to Shh

concentration. The classes undergo cross-repressive interactions, resulting in five progenitor domains in the neural tube that produce five classes of neurons: four main classes of spinal cord interneurons, in addition to motoneurons (Briscoe et al. 2000). Each class of neuron can be identified by unique expression of identified transcription factors and unique positioning and projections in the spinal cord.

Starting dorsally, the V0 class of interneurons is formed from the most dorsal progenitor domain and expresses the Evx1/2 transcription factor. V1 interneurons express the Engrailed1 (En1) transcription factor, V2 interneurons express Chx10, motoneurons express Islet1/2 (Isl1/2), and V3 interneurons formed from the most ventral progenitor domain express the Sim1 transcription factor (reviewed in Goulding and Pfaff 2005). Each class of neuron then produces various subclasses that also express distinct transcription factors and have unique projection patterns and functions. For example, the V1 class produces Renshaw cells, 1a inhibitory interneurons, and other unidentified subclasses, have ipsilateral projections, and have been shown to be important for locomotor cycle speed (Gosgnach et al. 2006). Researchers can begin to dissect organizational principles of neural circuits and CPGs through identification of interneuron types in the spinal cord based on the unique transcription factors expressed by classes and subclasses of neurons. Complications can arise, though, because transcription factor expression is not necessarily exclusive to neuronal subclasses. For example, the transcription factor Hb9 is expressed in interneurons with rhythmogenic capabilities but also specifies motoneuron identity (Arber et al. 1999; Wilson et al. 2005).

Therefore, it should not be assumed that shared transcription factor expression defines a wholly shared identity and function for groups of neurons.

3.1.2 Developmental origins of Drosophila motor neurons

Many of the transcription factors that have been shown to be important in spinal cord differentiation and development were first identified in *Drosophila*. Additionally, some of the transcription factors shown to be differentially expressed by classes and subclasses of vertebrate interneurons are homologous to transcription factors whose cross-repressive interactions determine neuronal identity in *Drosophila*.

In vertebrates, the Dbx transcription factor is expressed in progenitors that produce both the V0 and V1 subclasses of interneurons and Evx defines the V0 class of interneurons. In *Drosophila*, the Dbx homologue has cross-repressive interactions with the Evx homologue, Even-skipped (Eve), and the Hb9 transcription factor that is expressed in vertebrate rhythmogenic interneurons and motoneurons such that Dbx expression causes the interneuronal identity of short, local axon projections (Lacin et al. 2009). Eve and Hb9, although not expressed solely in *Drosophila* motoneurons, together specify the motoneuronal identity of a long axon projecting to body wall muscles when expressed in combination with other unknown transcription factors. The body wall muscles of larval *Drosophila* seen in figure 11 can be divided into dorsal, lateral, and ventral groups that are innervated by distinct groups of 1b and 1s motoneurons. The decision of whether a motoneuron axon will project dorsally, ventrally, or laterally is made during embryonic

development according to the combinatorial expression of transcription factors. Eve specifies the dorsally-projecting axons observed in MN1-1b and MNISN-1s while Hb9 and Islet, which is expressed in motoneurons in vertebrates, specify a ventrally-projecting axon, as in RP3 (Thor and Thomas 1997; Landgraf et al. 1999; Odden et al. 2002). Cross-repressive interactions of Eve and Hb9 maintain a separation of dorsally- and ventrally-projecting axons (Broihier and Skeath 2002).

Interestingly, transcription factors may also control the electrical development of *Drosophila* neurons. Overexpression of Eve in Eve-expressing motoneurons caused a decrease in the Slo K_{Ca} channel and in a nicotinic acetylcholine receptor subunit (Pym et al. 2006). RT-PCR confirmed that Eve transcriptionally represses these genes, indicating that the electrical properties of motoneurons are a piece of their identity that is partly specified by genetic programs.

Therefore., differentially-expressed transcription factor promoters and the GAL4-UAS system can be used to drive expression of reporter proteins, such as GFP, in identified subsets of motoneurons in order to characterize the morphology and targets of motoneurons and to investigate the intrinsic properties of identified motoneurons

3.1.3 Synaptic input to motor neurons

The larval *Drosophila* ventral ganglion is arranged in segmentally-repeated and bilaterally-mirrored hemisegments. The approximately 33 motoneurons in each

hemisegment project to approximately 31 segmentally-repeated body wall muscles. Descending and ascending projections and dendritic arbors are primarily found in a region of neuropil that runs longitudinally through the ganglion near the middle of each hemisegment. Commissural projections connect the left and right halves of each segment. The motoneurons targeted for this study are part of a cluster of 5-6 motoneurons with cell bodies located on the dorsal surface of the ganglion near the midline. These motoneurons have contralaterally- or ipsilaterally-projecting axons that exit the ganglion in segmental nerves that branch near the body wall to form smaller nerves. These nerves, the intersegmental nerve, segmental nerve a, segmental nerve c, and segmental nerve b/d, target different body wall regions. The peripheral nerves carry afferent sensory axons in addition to motor axons.

Direct inputs to motoneurons are likely provided by segmental CPG circuits but the identity of the presynaptic interneurons remains unknown. Measurements of synaptic currents in motoneurons via whole-cell patch clamp indicated that unidentified motoneurons receive cholinergic, GABAergic, and glycinergic inputs (Rohrbough and Broadie 2002). Input to motoneurons outside of those provided by CPG circuitry may include descending projection neurons from the brain lobes that provide a link between sensory and motor centers of the *Drosophila* central nervous system. It is likely that these projection neurons would provide input to CPG interneurons but it is possible that they provide direct input to the motoneurons as well. Sensory afferents may also provide direct synaptic input to motoneurons. The dorsal longitudinal stretch receptors that span

the dorsal length of each body wall segment have been shown to encode important motor feedback in a variety of insects and to provide direct input to motoneurons in the tobacco hornworm, *Manduca sexta* (Tamarkin and Levine 1996; Schrader and Merritt 2007). Input from multidendritic sensory afferents located across the body wall modulates CPG activity to facilitate crawling speed (Hughes and Thomas 2007). This input is likely provided to interneuronal circuitry but may also be provided directly to motoneurons. See *Chapter 1: Drosophila crawling* for further discussion of the crawling behavior. Widespread direct sensory inputs to motoneurons are unlikely if the *Drosophila* crawling CPG circuitry is structured similarly to that of the swimming leech in which sensory feedback modulates motor output through polysynaptic pathways (Cang et al. 2001). Additionally, any inputs to the motoneurons may be altered by neuromodulators.

Identification of synaptic partners is time-consuming and labor-intensive, generally requiring visualization of pre- and postsynaptic machinery through electron microscopy or reconstruction of immunolabeled neurons in order to measure distance between apposed membranes. The benefit of such studies is that multiple discrete synapses per neuron can be visualized. The transsynaptic tracer pseudorabies virus has been utilized in vertebrate systems to identify presynaptic partners of injected neurons without electron microscopy or reconstructions. Unfortunately, no such known transsynaptic tracer effectively functions in the *Drosophila* system. Electrophysiological measurements of synaptic currents and postsynaptic potentials also allow identification of synaptic inputs, although electrophysiological identification of presysnaptic partners requires directed

activation and/or removal of candidate presysnaptic neurons. This strategy is also time-consuming as single or populations of presynaptic candidates must be individually studied. Further, electrophysiological measurement of synaptic inputs is best achieved through labor intensive whole-cell recordings.

Increasingly, alternate techniques for circuit analysis are being developed that greatly facilitate identification of synaptic connections and may prove useful in *Drosophila* studies. For example, Ca^{++}- and voltage-imaging techniques are increasingly employed in mammals and zebrafish to identify rhythmically-active interneuron populations that are likely to be part of pattern generating circuits. Synaptic contacts could then be identified using the GAL4-UAS system and the related LexA/LexAop system for GFP reconstitution across synaptic partners (GRASP). GRASP utilizes split GFP molecules expressed in different neuronal subsets that are able to form fluorescent GFP only when the membranes of the neuronal subsets meet (Gordon and Scott 2009).

3.1.4 Role of motor neurons in crawling

Intrinsic properties of the motoneurons may modulate synaptic input from the CPG prior to giving a command to the muscle. In *Drosophila* crawling, there are a variety of potential contributions that motoneurons could make to the motor pattern. As described in *Chapter 1: Drosophila crawling*, thoracic segments have a specialized "anchoring" role during crawling and differences in the pattern of thoracic and abdominal muscle contraction may facilitate this role. If the thoracic muscle contraction pattern is

specialized, either the crawling CPG provides unique output to thoracic segments, thoracic motoneurons have unique intrinsic properties that modulate common CPG output, or thoracic neuromuscular junctions and/or muscles have unique functional properties. The third possibility is unlikely because *Drosophila* larval muscles and neuromuscular junctions have been extensively studied and exhibit no obvious differences in the thorax and abdomen. It is possible that thoracic motoneurons prolong firing throughout the peristaltic wave in order to prolong thoracic muscle contraction and create a stable fulcrum for the rest of the body. Prolonged firing in vertebrate motoneurons has been shown to result from PIC activation (see *Chapter 1: Active motor neurons*). If thoracic motoneuron PICs are more easily engaged than abdominal motoneuron PICs, contraction of thoracic muscles would be prolonged. It is also possible that thoracic motoneuron firing is facilitated by a greater intrinsic excitability of thoracic motoneurons compared to abdominal motoneurons. If thoracic motoneurons have a more hyperpolarized voltage threshold or a higher input resistance, they would fire more in response to a given input than less excitable motoneurons in the abdomen.

Another potential specialization of motoneurons for crawling relates to the possible temporal offset between dorsal and ventral muscle contraction within a segment (see *Chapter 1: Drosophila crawling*). If there is an offset between dorsal and ventral muscle contraction, it may be due to an offset in CPG output, motoneuron intrinsic properties, or differences in neuromuscular junction and muscle properties. If dorsally- and ventrally-projecting motoneurons impart distinct offsets in muscle contraction, distinct voltage

thresholds, current thresholds, or delays-to-spike could underlie such an offset and could be distinguished in whole-cell recordings.

3.1.5 Utilization of RNAi

Differentially-expressed transcription factors and the GAL4-UAS system are useful for experimental alteration of intrinsic properties. Countless studies have utilized this system to express non-native proteins and overexpress native protein in specific tissues. Knockdown of protein function has also been achieved through expression of dominant negative protein constructs. The recent addition of RNAi to the *Drosophila* toolbox dramatically broadens experimental possibilities. Although the principles behind the GAL4-UAS and RNAi strategies are straightforward, inherent complexities of the technique can make utilization more complex than is immediately obvious. Therefore, it is worthwhile to consider possible complications of the RNAi strategy.

The effectiveness of UAS-RNAi strategy in reducing protein levels depends on the efficacy of the RNAi construct and its interaction with endogenous transcripts of the cell. Additionally, the strength of the GAL4 promoter used to drive RNAi expression determines the magnitude of siRNA production and subsequent protein reduction. The strength with which a given promoter is activated varies by cell and developmental stage. Further, promoter strength may be regulated by environmentally-inducible factors. Therefore, each of these factors may need to be considered in order to obtain optimal RNAi effectiveness under the control of a strongly-expressed GAL4 promoter.

The RNAi strategy relies on the cell's RNA degradation machinery to effectively destroy endogenous mRNA complementary to the RNAi sequence. RNAi technique expresses a transgene for dsRNA that is processed into siRNA's. siRNA's unite with the RISC complex that binds to and causes degradation of mRNA's with complementary sequences (Fire et al. 1998; Hannon 2002), resulting in knockdown of the protein of interest. The RNAse enzyme Dicer is responsible for initiating the process by cutting the dsRNA into the siRNA (Lee et al. 2004). Therefore, RISC complexes and Dicer must be capable of expanding their ongoing roles in the cell to implement the additional burden of exogenous RNAi demands. Therefore, the RNAi technique may be more effective if Dicer or RISC proteins are overexpressed using the GAL4-UAS system to supplement the endogenous RNA degradation machinery.

3.1.6. Role of I_A

I_A has been shown to have a variety of functions in different cell types, including modulation of firing frequency, delay to spike, interspike interval, and action potential shape. Two channels carry I_A in *Drosophila*: Shaker (Kv1) and Shal (Kv4). It is possible that differences in channel structure and physiology impart specialized roles for Shaker and Shal in the control of motoneuron firing behavior.

As described in *Chapter 1: Active motor neurons* and *Chapter 1: Potassium channels in Drosophila*, Shaker has been shown to localize to axonal and presynaptic regions and Shal to somatodendritic regions in many cell types. This is likely the case in *Drosophila*

motoneurons as Shal antibody staining is observed in the larval central neuropil and within the proximal portion of the motor nerve as it exits the ventral ganglion (Bergquist et al. 2010). Shaker antibodies are currently unavailable in *Drosophila* but Shaker is known to be expressed at the presynaptic terminal of the neuromuscular junction in Drosophila larvae (Ganetzky and Wu 1982). Differences in the amino acid sequences of Kv1 and Kv4 channels have been shown to determine the distinct distribution of these channels to axonal vs. dendritic compartments of the cell.

Differences in Shaker and Shal amino acid sequences could also impart distinct functional roles for the channels. Specifically, Shal channels are unique in that they seem to prefer a closed-state inactivation while Shaker channels display the more traditional N-type inactivation. The N-type inactivation of Shaker channels depends on a region of positively charged amino acids in the cytoplasmic N-terminus of the channel that undergo electrostatic interaction that induces movement of this region to block the open pore. The number of positively charged residues found in this N-terminus region is dramatically reduced in Shal channels and little evidence of N-type inactivation in Shal channels exists Jerng et al. 2004). Instead, it may be that an interaction between the Shal S6 region (which serves as the activation gate) and the loop between S4 (the voltage sensor) and S5 confers a closed-state inactivation preference for Shal (Jerng et al. 2004). The closed state inactivation begins to take effect in many cells near the resting potential and increases as the cell depolarizes. Subunit composition and interactions with accessory proteins such as K^+ channel interacting proteins (KChIPs) and have been shown to affect

the inactivation properties of Shal channels (Gebauer et al. 2004). In *Drosophila* motoneurons, it appears that Shal is the predominant carrier of the A current in somatodendritic regions and Shal inactivation properties can be modified by the SKIP accessory protein (Diao et al. 2009). Shal predominance in somatodendritic regions may imbue motoneurons with increased potential for variability in delay-to-spike. While Shaker channels must transiently open prior to inactivation, and thereby reduce motoneuron excitability in a stereotypical manner, Shal channels can be inactivated without opening and their degree of inactivation can vary depending on membrane potential and accessory subunits. Some motoneurons may therefore have a reduced Shal current due to closed-state inactivation prior to receiving excitation. Indeed, this appears to be the case in 1b motoneurons due to their depolarized resting potential and hyperpolarized voltage-dependence of inactivation (Table 1; Choi et al. 2004).

We were interested in addressing three major aims. First, are larval thoracic motoneuron morphology and muscle targets similar to abdominal and embryonic homologues? Second, do intrinsic properties of dorsal vs. ventral and thoracic vs. abdominal motoneurons specialize them to contribute to crawling in response to synaptic input? Finally, what considerations must be accounted for when using RNAi strategy to dissect the specific contribution of Shal to motoneuron firing behavior? We find that care should be taken in motoneuron identification because aspects of motoneuron morphology and muscle targets differ between thoracic and abdominal segments. Whole-cell patch clamp recordings are useful for visualization of rhythmic synaptic inputs from the crawling CPG

to all four motoneurons and modulation of CPG output by motoneurons is primarily dependent upon type (1b/1s) rather than dorso/ventral and abdomino/thoracic differences in motoneuron intrinsic properties. Finally, RNAi is a powerful tool for investigation of motoneuron active properties but must be utilized with care. The RNAi experiments suggest that Shal is responsible for delay-to-spike but not firing frequency and that firing frequency is either independent of I_A or dependent on Shaker channels outside of the reach of our space clamp.

3.2 Methods

3.2.1 Drosophila stocks

The GAL4-UAS system was used to drive expression of GFP and ShalRNAi in identified motoneurons. Lines used included: heterozygous dHb9-GAL4 (Broihier and Skeath 2002) to drive expression in RP3 (thoracic MN6/7-1b homologue, see below) [w;UAS-cd8-GFP;dHb9-GAL4], homozygous RRA-GAL4 (Fujioka et al. 2003) to drive expression in MN1-1b and MNISN-1s [w;UAS-cd8-GFP;RRA-GAL4], heterozygous vGLUT-GAL4 to drive expression in MNSNb/d-1s [w;UAS-cd8-GFP;vGLUT-GAL4], homozygous OK371-GAL4 (Mahr and Aberle 2006) to drive expression in MN1-1b, MNISN-1s, and RP3 [w;OK371-GAL4;UAS-cd8-GFP], and homozygous w;RN2-GAL4,UAS-mcd8-GFP;act<cd2<GAL4,UAS-flp (Hartwig et al. 2008) and w^-;UAS::mRFP;RN2::FLP,Tub<FRT<GAL4,UAS::mRFP, hereafter abbreviated "RN2-FLP" (source: M. Bate) for *shal* knockdowns. Vienna Stock Center #103363 (ShalRNAi) was used for *shal* knockdown experiments. vGLUT-GAL4 was a generous gift from the laboratory of S. Birman. The UAS-cd8-GFP source was Bloomington Stock Center #5137. Images were obtained on a Zeiss LSM510 confocal microscope.

3.2.2 Electrophysiology

Dissection and desheathing of the preparation were performed in Ca^{++}-A solution (described in *Chapter 2: Methods*) (Jan and Jan 1976). Osmolarity of all solutions was verified with a 5520 VAPRO osmometer (Wescor). Protease 14 added to Ca^{++}- A-solution (2mg/ml) was applied to the ventral ganglion to degrade the glial sheath through

a micropipette with the tip broken to a diameter of approximately 10µm. Alternating positive and negative pressure was administered to apply protease and remove debris. Thin-walled borosilicate electrodes were pulled on a PP-83 (Narishigie) to a resistance of 4-7 MΩ and fire-polished using an MF-35 microforge (Narishigie). Electrodes were filled with intracellular solution (described in *Chapter 2: Methods).* An Axoclamp 1B amplifier (Axon Instruments) with Clampex 10.1 software (Axon Instruments) was used for whole-cell recordings. Motoneurons with resting membrane potentials that were more depolarized than -40mV or with seals less than 1GΩ were not used. After verification of a GΩ seal, whole-cell configuration was achieved. In voltage clamp mode, a 40mV hyperpolarizing voltage command was administered and the resulting current measurement was used to calculate input resistance. For current clamp experiments, resting membrane potentials were brought to -60mV through bias current injection into the cell body unless otherwise noted. Current injections were provided in intervals of 10 pA, from -10 pA to 80 pA, lasting 400msec.

1µM tetrodotoxin (TTX, Sigma-Aldrich) was added to Ca^{++}-free A solution (modified Ca^{++}-A solution containing 0mM $CaCl_2$) to isolate voltage-dependent K^+ currents for voltage clamp recording. A holding potential of -80mV was used for voltage clamp studies. The linear leakage current was subtracted from all records. Current amplitude was normalized to whole-cell capacitance and reported as current density in I/V plots. Whole-cell capacitance was calculated from the charging transient following a 40mV hyperpolarizing voltage command.

3.2.3 Statistical Analysis

Statistical analyses were performed using a standard t-test with Excel software (Microsoft). Standard error values are reported. Significance was assumed when $p \leq 0.05$.

3.3 Results

3.3.1 Visualization of identified motor neurons

The GAL4-UAS system was utilized to drive expression of GFP under the control of different identified GAL4 driver lines in hopes that reliable targeting of individual thoracic motoneurons for patch clamp recording could be achieved. Previous studies characterized expression patterns of various GAL4 driver lines via confocal microscopy and it was our hope that GFP expression would be sufficiently strong and reliable to resolve cell bodies on a fluorescent microscope for *in situ* recording. Inspection of GAL4 driver line expression patterns in the ventral ganglion and thoracic body wall segments indicated that GFP expression in the dorsomedial motoneuron cluster is sufficiently sparse in the driver lines described below to reliably permit resolution of identified cell bodies (Fig. 10). Complications arose from the finding that motoneuron targets and cell body locations varied between thoracic and abdominal segments (see *Chapter 3: Discussion*). Dye fills of rhodamine Dextran introduced via the intracellular solution confirmed cellular identity based on dendritic morphologies and axonal projections (ipsilateral vs. contralateral).

The RRA-GAL4 line utilizes a portion of the *eve* transcription factor promoter, causing expression in the dorsally-projecting 1b motoneuron that targets muscle 1, MN1-1b, and the 1s motoneuron that targets the dorsal muscle group, MNISN-1s (Fig. 11) (Worrell and Levine 2008). Dendritic morphologies of MN1-1b and MNISN-1s observed in dye fills from this study were in agreement with previous reports. The vGLUT-GAL4 line

reliably labels the 1s motoneuron that targets the ventral muscle group, MNSNb/d-1s (unpublished line). 1s synaptic terminals on ventral muscle groups were used as the primary method of identification for MNSNb/d-1s because previous descriptions of MNSNb/d-1s dendritic morphology and axonal projections are contested and limited to the embryo, as addressed in *Chapter 3: Discussion*. The Hb9 transcription factor promoter of the dHb9-GAL4 line drives GFP expression in RP3 (MN6/7-1b in the abdomen, see *Chapter 2: Methods* for explanation of motoneuron name), which targets a previously-undescribed ventral muscle in thoracic segments (personal communication, L.Feng, M. Landgraf). Dye fills indicate that thoracic RP3 displays a contralaterally-projecting axon and a comparatively reduced ipsilateral dendritic arbor (data not shown). Additionally, the contralateral dendritic arbor contains a large neurite that projects anteriorly through the neuropil to the subesophageal ganglion or beyond (confirmed by personal communication with L. Feng, M. Landgraf).

3.3.2 Synaptic input to motor neurons

In fortuitous current clamp recordings, EPSPs were observed. Fortuitous recordings from all four motoneurons in gap free mode also displayed EPSPs, sometimes rhythmic (Fig. 12). As described in *Chapter 2: Results*, verification of EPSP identity was achieved via bias current injection to hyperpolarize the membrane. In all cases, this treatment increased the size of the observed event, consistent with an EPSP identity in which amplitude is increased due to increased driving force for inward current. EPSP size differed from recording to recording when the membrane potential was normalized to -

60mV, likely due to a variety of factors (see *Chapter 3: Discussion*). The rhythmic input provided to the four motoneurons studied here indicates that all are likely to participate in crawling behavior. Further, whole-cell recordings of synaptic input may be an avenue through which synaptic inputs and their modulation by motoneuron active properties can be studied in the future.

3.3.3 Role of motor neurons in crawling

Triangular current ramps starting at 0pA, proceeding to 100pA, and then returning to 0pA over the course of 10 sec. were administered to each of the four cells. No evidence of persistent inward currents (PICs), in the form of prolonged firing on the descending ramp, were observed. Therefore, either PICs do not contribute to *Drosophila* motoneuron modulation of CPG output or the appropriate neuromodulatory environment for PIC activation was not present during *in situ* recordings.

As mentioned in *Chapter 2: Methods*, motoneuron firing frequencies were calculated as number of spikes per 400msec. current injection. This quantification method could impose an artificially low firing frequency measurement on 1s motoneurons due to their longer delay-to-spike. Therefore, instantaneous firing frequency was also calculated as number of spikes per time spiking. The input/output relationships between motoneurons were the same for both calculation methods (Fig. 13).

Few obvious or behaviorally-relevant differences between dorsally- and ventrally-projecting motoneurons were observed. Dorsally-projecting MNISN-1s exhibited a significantly more depolarized voltage threshold for firing than ventrally-projecting MNSNb/d-1s, which may imply that the dorsal muscle group is recruited after the ventral muscle group in thoracic segments.

Abdominal and thoracic MN1-1b and MNISN-1s homologues exhibited nearly identical firing behaviors (Fig. 14). Abdominal MNISN-1s had a significantly higher firing frequency at 90 and 110pA current injection levels but displayed no significant differences in delay-to-spike or threshold compared to thoracic MNISN-1s. Abdominal MN1-1b had a significantly longer delay-to-spike only at the 110pA current injection level and displayed no significant differences in firing frequency or threshold compared to thoracic MN1-1b. Intriguingly, abdominal MN1-1b had a significantly higher input resistance (1028.7 ± 128.0mΩ) and lower whole-cell capacitance (24.4 ± 2.7 pF) compared to thoracic MN1-1b (666.0 ±29.9mΩ and 32.3 ± 2.0pF, respectively).

3.3.4 Utilization of RNAi

A variety of GAL4 driver lines and strategies were utilized to induce ShalRNAi expression in MNISN-1s for investigation of the role of Shal in motoneuron recruitment. Findings indicate that promoter choice is critical for successful employment of the RNAi technique. OK371-GAL4-driven expression of ShalRNAi had no effect on firing behavior or K^+ currents either with or without concurrent Dicer overexpression (Fig. 15).

The RN2-FLP line (w-;UAS::mRFP;RN2::FLP,Tub<FRT<GAL4,UAS::mRFP) was expected to induce strong and long-lasting expression of ShalRNAi due to its utilization of the tubulin promoter (see *Chapter 3: Discussion*). RN2-FLP did, indeed, increase firing frequency and decrease delay-to-spike (Fig. 15). Unfortunately, the RN2-FLP control cells also exhibited altered firing frequency and delay-to-spike compared to RRA-GAL4 and OK371-GAL4 control cells. The alterations in firing behavior may reflect damage to the cells induced by strong expression of the red fluorescent protein (mRFP), as images of these cells revealed abnormal dendritic "blebbing" (unpublished observation). Therefore, voltage clamp studies were not undertaken. In contrast, successful RNAi technique was obtained with the w;RN2-GAL4,UAS-mcd8-GFP;act<cd2<GAL4,UAS-flp driver line described in *Chapter 2*.

3.3.5 Role of I_A

The role of Shal for motoneuron delay-to-spike and recruitment are described in *Chapter 2* (Fig. 5 and 6). A-type currents have also been shown to have an effect on firing frequency in a variety of cell types. Interestingly, expression of ShalRNAi had no effect on firing frequency in MN1-1b or in MNISN-1s (Fig 5). It is possible, however, that Shal is responsible for delay-to-spike in these cells while the primary effect of the A-type current on firing frequency is mediated by Shaker. If Shaker has a role in firing frequency, it would be expected that the prepulse protocol utilized in Fig. 4 would cause an alteration in firing frequency but not in the ShalRNAi experiments. Therefore, firing frequency after 20pA and 40pA prepulses were compared to the firing frequency in the

absence of a depolarizing prepulse in all four motoneurons. No significant differences were observed in firing frequency in any of the motoneurons for any of the prepulse conditions. (Fig. 13).

The A-type current carried by Shal may have a role in the modulation of synaptic input in *Drosophila* motoneurons. 3 out of 5 ShalRNAi-expressing MNISN-1s cells exhibited increased amplitude and, possibly, frequency of EPSPs in whole-cell recordings (Fig. 16). The effect of ShalRNAi on EPSP frequency is unclear because the apparent increase could reflect an unmasking of EPSPs that were previously below the amplitude at which they can be distinguished by whole-cell recordings in the cell body. ShalRNAi expression had no apparent effect on EPSP amplitude or frequency in ShalRNAi-expressing MN1-1b cells (data not shown).

3.4 Discussion

3.4.1 Visualization and developmental origins of identified motor neurons

Reliable visualization of identified motoneurons for patch clamp recording can be achieved through selection of GAL4 driver lines that drive strong GFP expression in limited subsets of motoneurons. Visual identification of motoneurons based on dendritic morphology, cell body location, and axonal projections can be confirmed through introduction of fluorescent dye into the cell via the intracellular solution.

Thoracic and abdominal motoneurons can differ in muscle targets and dendritic morphology, as can larval and embryonic homologues. Therefore, developmental tracking will be necessary to definitively determine embryonic and larval homologues, but predictions of embryonic homologues for each of the four thoracic motoneurons studied can be made based on dendritic morphology and axonal projections.

Our findings regarding thoracic MN1-1b and MNISN-1s are in line with previous descriptions of larval and embryonic abdominal morphology and targets. See figure 11 for image of muscle organization. MN1-1b undergoes little remodeling between the embryonic and third instar larval stages. It exhibits large bipolar dendrites and an ipsilaterally-projecting axon that targets muscle 1 in thoracic and abdominal segments (Sink and Whitington 1991; Landgraf et al. 1997; Schmid et al. 1999; Hoang and Chiba 2001; Choi et al. 2004; Kim et al. 2009). MNISN-1s morphology is also highly conserved in embryonic and larval thoracic and abdominal segments. The MNISN-1s

dendritic arbor is largely ipsilateral although a small contralaterally-projecting neurite leaves the cell body (Landgraf et al. 1997; Choi et al. 2004; Kim et al. 2009). MNISN-1s targets are somewhat modified between embryonic and larval stages. The axon projects ipsilaterally through the intersegmental nerve to innervate dorsal muscles 2 and 18 (according to Sink and Whitington 1991; Landgraf et al. 1997)) or 2, 3, 11, 19, and 20 (according to Schmid et al. 1999) in the embryo and the extends its axonal projections to target larval muscles 1, 2, 3, 4, 9, 10, 19, 20 and possibly 18 (Hoang and Chiba 2001; Choi et al. 2004; Kim et al. 2009).

In contrast to the relatively conserved dorsally-projecting motoneurons, there appears to be a good deal of remodeling and retargeting of ventrally-projecting motoneurons comparing embryo to larva and thorax to abdomen. In the embryo, the contralaterally-projecting axon of the RP3 motoneuron targets the cleft between muscles 6 and 7 and the major dendritic arbor is found in the contralateral neuropil, although an ipsilateral arbor is present (Landgraf et al. 1997; Sink and Whitington 1991). The larval abdominal RP3 exhibits similar dendritic morphology and muscle target (Hoang and Chiba 2001; Choi et al. 2004) although one report states that the ipsilateral dendritic arbor is greatly reduced or absent in abdominal segments (Kim et al. 2009). Our dye fills indicate that the larval thoracic RP3 has unique dendritic morphology, displaying a clear ipsilateral dendritic arbor and large anteriorly-projecting neurite in the contralateral arbor, and targets an undescribed ventral muscle target (confirmed by personal communication with L. Feng and M. Landgraf). It is tempting to predict that the anteriorly-projecting neurite may

serve as a link between brain centers and the motor circuitry, although its role is unstudied. The different muscle targets of thoracic and abdominal RP3 is a consequence of different ventral muscle patterns in abdominal and thoracic body wall segments, seen in figure 11.

MNSNb/d-1s is the most difficult of the identified motoneurons for which to correlate embryonic vs. larval and abdominal vs. thoracic homologues. MNSNb/d-1s morphology has not been well-described in the larva. It is clear that a 1s motoneuron innervates larval ventral abdominal muscles including 6, 7, 12, 13, 14, 15, 16, and 30 (Hoang and Chiba 2001; Choi et al. 2004). The position of the cell body and the central morphology of MNSNb/d-1s have been difficult to determine because this motoneuron is, for unknown reasons, not labeled by other known GAL4 driver lines that label the dorsomedial group of motoneurons. Choi et al. describe fortuitous dye fills of this neuron and Kim et al. use the MARCM genetic technique to GFP label single cells in the larva. Both studies are limited to the abdomen and describe MNSNb/d-1s as having a contralaterally-projecting axon and its major dendritic arbor in the contralateral neuropil. We find that the vGLUT-expressing MNSNb/d-1s targets a group of thoracic ventral muscles of undescribed identity (Fig. 11). A single dye fill of this motoneuron appeared to show an ipsilaterally-projecting axon but further and more successful dye fills are necessary to verify this finding. The likely embryonic precursor of larval MNSNb/d-1s is the RP5 motoneuron because it also exhibits a major contralateral dendritic arbor and a contralaterally-projecting axon that targets muscles 13,14,15, and 16 (Sink and Whitington 1991).

Schmid et al similarly describe RP5 as innervating muscles 6, 7, 12, 13, 15, and 16 (Schmid et al. 1999). Data contradicting this conclusion comes from Landgraf et al, who describe RP5 as innervating only ventral muscle 12 (Landgraf et al. 1997). Hoang and Chiba use the Landgraf description to predict that a second motoneuron innervating muscles 6 and 7 in the embryo, called 6/7b, to be the embryonic precursor of MNSNb/d-1s, rather than RP5. Assuming that Sink and Whittington and Schmid et al. are correct in their identification of RP5 as innervating multiple ventral muscles, RP5 is the logical precursor to MNSNb/d-1s. Therefore, we find that the likely MNSNb/d-1s embryonic homologue is RP5 and that thoracic MNSNb/d-1s may have a different axonal morphology than its abdominal counterpart.

3.4.2 Synaptic input to motor neurons

EPSP's were observed in whole-cell patch clamp recordings from all four motoneurons. The relative shape and amplitude of EPSPs varied from preparation to preparation. A variety of factors likely cause this variation. According to Ohm's law, cellular input resistance has a major effect on the somatic voltage change caused by synaptic currents. The EPSP, therefore, looks larger in cells with higher input resistances. It should be noted that the converse is also true; synaptic input lowers input resistance. It is unlikely that input resistance is the sole determinant of EPSP shape and amplitude in gap free recordings because RP3 has a very low input resistance and can exhibit large EPSPs (Fig. 12). Dendritic diameter and synaptic location will also have a marked effect on EPSP size, as the length constant increases with diameter. Differences in series resistance

between recordings may be another technical source of variation. The series resistance varies from recording to recording, although differences between cells were not significant. Increased series resistance causes a smaller measured voltage change by the electrode. Variation in preparation health, especially in the number of synaptic contacts preserved during the desheathing process, may increase variation in EPSP size and frequency. Finally, small variations in intracellular and extracellular solutions may vary the driving force for synaptic currents. Therefore, voltage clamp studies measuring specific synaptic currents will be useful for studying synaptic integration in *Drosophila* motoneurons.

Measurement of synaptic inputs may also be confounded by cellular morphology. Larval motoneurons have a large primary neurite leaving the cell body. The dendritic arbor then branches from this primary neurite in the neuropil before the primary neurite forms the axon and exits the ventral ganglion to innervate muscle. A subset of neurons also have a secondary dendritic arbor in the opposite neuropil (Fig. 10). The spike initiating zone is likely located at the distal side of the dendritic arbor. Therefore, it is unclear how representative somatic recordings are of inputs seen by the spike initiating zone in the behaving animal. It is clear that synaptic inputs recorded from the cell body are relevant to motoneuron recruitment based on the recordings of relative synaptic input and recruitment of MN1-1b and MNISN-1s (Fig. 8).

3.4.3 Role of motor neurons in crawling

Although apparent differences in the timing of muscle contraction are observed between dorsal and ventral muscle groups within a hemisegment (Fox et al. 2006; video from Hughes and Thomas 2007; and unpublished observation, E. McKiernan and C. Duch), no obvious differences were seen in the intrinsic properties of dorsally- vs. ventrally-projecting 1b or 1s motoneurons (Fig. 1, 2, 3). The behavioral relevance of the hyperpolarized MNSNb/d-1s voltage threshold compared to MNISN-1s could be investigated using simultaneous whole-cell recordings during fictive locomotion to resolve whether there is an offset in motoneuron firing during crawling and if it is due to motoneuron intrinsic properties or to offset CPG outputs. The specialized role of thoracic segments in the crawling behavior also does not appear to be supported by differences in intrinsic properties between thoracic and abdominal motoneuron homologues as the firing responses of abdominal and thoracic motoneurons to current injection are similar (Fig. 14).

Abdominal MN1-1b would be expected to be more excitable and exhibit a lower current threshold (rheobase), higher firing frequency, and shorter delay-to-spike than thoracic MN1-1b based on its higher input resistance and lower capacitance. Instead, abdominal and thoracic MN1-1b homologues generate the same firing behavior in spite of distinct passive properties. This may indicate that abdominal MN1-1b has a larger amplitude or kinetically distinct I_A compared to thoracic MN1-1b. Voltage clamp recordings comparing thoracic and abdominal K^+ currents could resolve this discrepancy.

3.4.4 Utilization of RNAi

Successful RNAi technique requires adequate RISC and Dicer function and a strong GAL4 driver line. GFP expression is a useful indicator of the spatial activity and, to some extent, the temporal activity of a promoter because it can be analyzed visually without intensive techniques such as PCR. GFP expression does not, however, provide precise temporal resolution of promoter strength because GFP is a relatively long-lasting protein. Therefore, a GAL4 line may exhibit strong GFP expression in a specific cell at a given time point due to persistence of the GFP protein even if the promoter activity is weak at that time. In this case, RNAi expression in the same cell at the same time point will be weak because the RNAi molecule is quickly degraded so that RNAi levels more closely track promoter activity. It is likely that this phenomenon caused the RNAi strategy to be ineffective using the conventional GAL4 driver line OK371 (Fig. 15). On the other hand, the RN2-FLP line utilizes RN2, an eve promoter related to RRA that is also selectively expressed in MN1-1b and MNISN-1s, in a strategy wherein recombination places GAL4, and therefore ShalRNAi, expression under the control of the ubiquitous tubulin promoter only in RN2-expressing cells. Although this strategy resulted in a decreased delay-to-spike and increased firing frequency, we also observed significant differences in firing behavior between RN2-FLP control and control cells from conventional driver lines, indicating that mRFP-induced cellular damage may occur. Therefore, voltage clamp studies were not undertaken in RN2-FLP. We saw no benefit of increased Dicer expression in our studies, but endogenous Dicer levels may vary

spatially and temporally and may therefore exogenous Dicer may be beneficial in other RNAi experiments.

The “flip out” strategy used in successful RNAi experiments (Fig. 5 and 6) was effective because it exploits homologous recombination in a subset of cells to drive RNAi and GFP expression by the very strong, ubiquitous actin promoter (Hartwig et al. 2008). This line, w;RN2-GAL4,UAS-mcd8-GFP;act<cd2<GAL4,UAS-flp, utilizes the weak RN2 promoter to drive UAS-flipase at early stages of development. In the random subset of RN2-expressing cells that undergo homologous recombination, flipase removes a transcriptional stop cassette (denoted by “<”) and causes activation of the actin-GAL4 sequence. The actin promoter is strongly activated throughout the life of the animal and therefore transcription of UAS-controlled sequences is strongly activated in the subset of cells throughout development. In these experiments, UAS-GFP and UAS-ShalRNAi transcription was activated by the actin promoter, as well as by the RN2 promoter, producing strong ShalRNAi expression throughout development. Although Shal knockdown appeared to be specific to I_A (Fig. 6), any homeostatic compensation for ShalRNAi reduction of activity levels could be investigated by co-expression of temperature sensitive GAL80 in order to gain temporal control of the RNAi mechanism.

3.4.5 Role of I_A

It was expected that I_A inactivation and/or knockdown through depolarizing prepulse and ShalRNAi expression would affect both firing frequency and delay-to-spike because it

has been shown to modulate these parameters in a variety of other cell types (Chapter *1: Potassium channels*). ShalRNAi was expected to modulate firing frequency was expected because Shaker mutants had previously been shown to have no effect on firing frequency (Choi et al. 2004) Unexpectedly, our experiments showed that ShalRNAi had no effect on firing frequency (Fig 5). Therefore, the possibility that Shaker is the dominant A-type channel responsible for firing frequency was reconsidered. Differential contributions of Shal and Shaker to firing behavior could be investigated through comparison of the firing response after a depolarizing prepulse (which should inactivate both Shal and Shaker) and after ShalRNAi expression (which should knock down only Shal). If Shaker were responsible for firing frequency an increased frequency would be expected after a depolarizing prepulse but not after ShalRNAi expression. No effect on firing frequency was observed in either treatment. It is possible that I_A does not play a role in the firing frequency of these motoneurons. This could be the case if I_A inactivation is not removed due to insufficient amplitude of the afterhyperpolarization between spikes in our recordings. Or, the likely localization of Shaker to the axon (*Chapter 1: Potassium channels*) may indicate that Shaker functions at the spike initiating zone, a location that could be outside of the region that we are able to clamp for our recordings. If this is the case, the depolarizing prepulse would fail to inactivate Shaker channels at the spike initiating zone and have no effect on firing frequency.

The results of *Chapter 2* experiments clearly indicate that Shal is important for delay-to-spike in *Drosophila* motoneurons. It is likely that 1b and 1s motoneuron delays-to-spike

vary due to differences in Shal inactivation properties (Choi et al. 2004), possibly conferred by accessory proteins (Diao et al. 2009). ShalRNAi-expressing MNISN-1s motoneurons also displayed increased amplitude EPSPs compared to control cells (Fig. 16). The absence of this effect in MN1-1b recordings may reflect different roles of Shal in MN1-1b and MNISN-1s or effects of different cellular morphologies on EPSPs. Increased EPSP amplitude recorded at the MNISN-1s cell body may result from a variety of ShalRNAi-induced cellular alterations. It is theoretically possible that the RN2-GAL4 driver line unexpectedly drives ShalRNAi expression in presynaptic cells, causing increased excitability and synaptic release. This is unlikely as no presynaptic GPF expression was observed and there was no effect in MN1-1b, which receives shared input (Fig. 8). This possibility could be investigated through whole-cell recordings from unlabeled MNISN-1s cells in ShalRNAi animals. Unlabeled cells did not undergo homologous recombination and therefore do not express GFP or ShalRNAi. MNISN-1s can be identified in the absence of GFP expression based on cell body location and size and confirmatory dye fills. Contralateral MNISN-1s pairs in the same animal receive largely shared synaptic inputs (Fig. 7). Therefore, ShalRNAi-induced presynaptic alterations would have similar effects on EPSPs in contralateral MNISN-1s pairs regardless of whether the motoneuron is positive for GFP and ShalRNAi or not unless ShalRNAi expression has effects on the development of the dendritic arbor. Electrical activity is important for the development and maintenance of dendritic morphology, likely via Ca^{++}-dependent pathways (reviewed in Parrish et al. 2007). Therefore, an alternate explanation for ShalRNAi effects on EPSP amplitude is that motoneurons

expressing ShalRNAi develop altered dendritic morphology and/or size in response to increased cellular excitability. EPSP amplitude at the cell body could be altered by the change in dendritic morphology. This possibility could be resolved via comparative imaging and reconstruction of ShalRNAi- and GFP-expressing MNISN-1s dendritic arbors and comparison to GFP-expressing MNISN-1s dendritic arbors in the parental line that are devoid of ShalRNAi expression. Such studies are being developed in conjunction with C. Duch.

Finally, increased EPSP amplitudes in ShalRNAi-expressing MNISN-1s may indicate a role for Shal in synaptic integration. I_A distribution has been well-studied in CA1 pyramidal cell dendrites in the hippocampus where Kv4 (*shal*) channel density gradients regulate action potential back-propagation and reduce distal EPSP amplitude (Hoffman et al. 1997). Cortical pyramidal cell A-type channels likely influence synaptic integration by clustering at GABAergic postsynaptic specializations (Burkhalter et al. 2006). It is possible that Shal also plays a role in dendritic integration of synaptic inputs to *Drosophila* motoneurons. This possibility could also be investigated via whole-cell recordings from contralateral labeled and unlabeled MNISN-1s cells in the ShalRNAiline. Whereas ShalRNAi presynaptic effects would be expected to have similar effects on EPSP measurements at the cell body in labeled and unlabeled MNISN-1s, ShalRNAi effects on synaptic integration would be expected only in GFP- and ShalRNAi-expressing MNISN-1s. If such differential effects were seen, investigations of the localization of Shal channels within the dendritic arbor would be important. A UAS-

GFP-tagged Shal construct like that developed by Diao et al. would be useful for such an investigation (Diao et al. 2009).

Figure 10, Expression patterns of GAL4 driver lines.

A. GFP expression driven by the panneuronal elav-GAL4 driver. Box indicates the dorsomedial cluster of motoneuron cell bodies where the four motoneurons studied here are found. Neuropil regions containing motoneuron dendritic arbors indicated with arrows. **B.** RRA-GAL4 driver line expression pattern. MNISN-1s, circled in red, exhibits no obvious contralateral dendritic arbor. aCC, circled in blue, has a noticeable contralateral dendritic arbor. Image by E.Sells. **C.** vGLUT-GAL4 driver line expression pattern. MNSNb/d-1s is circled in red. **D.** dHb9-GAL4 driver line expression pattern. Thoracic RP3 is circled in blue.

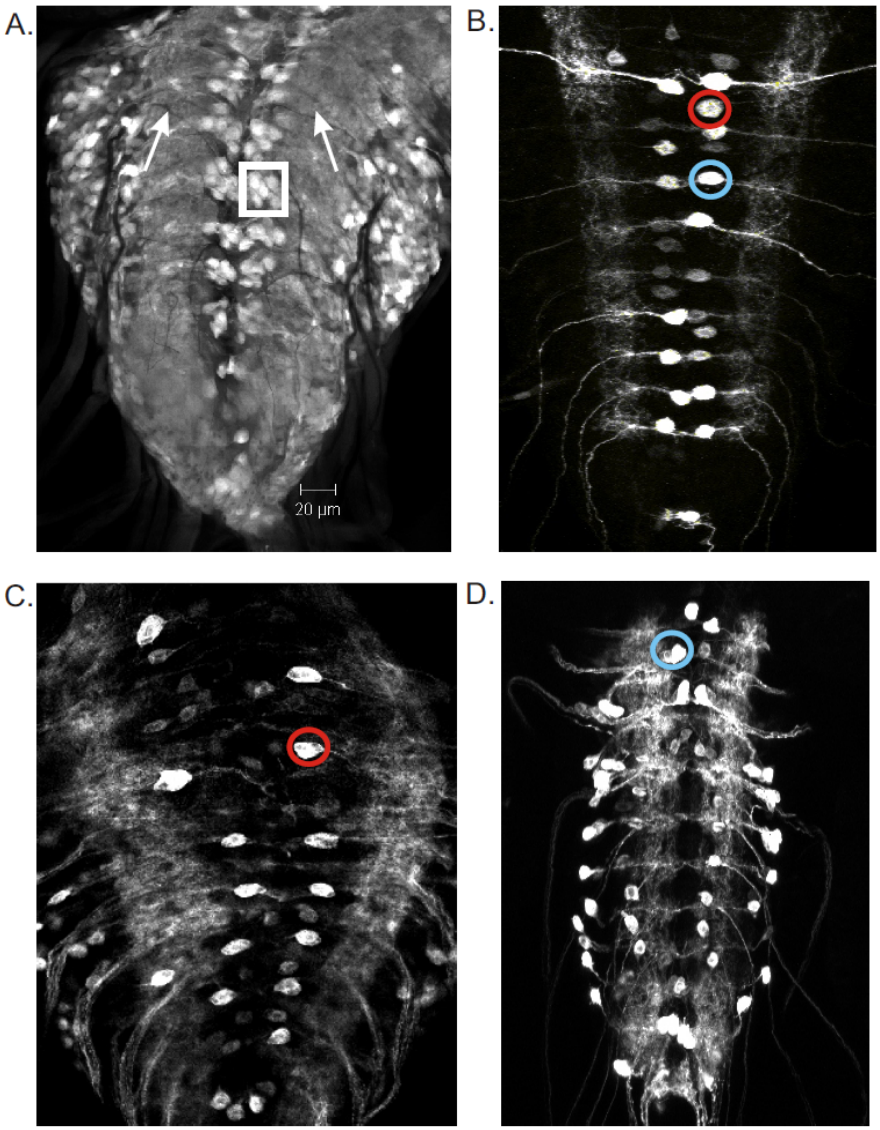

Figure 11. Segmental muscle patterns.
A filleted preparation was treated with the actin-binding rhodamine phalloidin. The ventral midline is marked at right and the dorsal midline at left. Muscles are numbered. Segments are numbered at left. Clear modifications in thoracic segments compared to the well-described abdominal segments are observed (Hartenstein 2006).

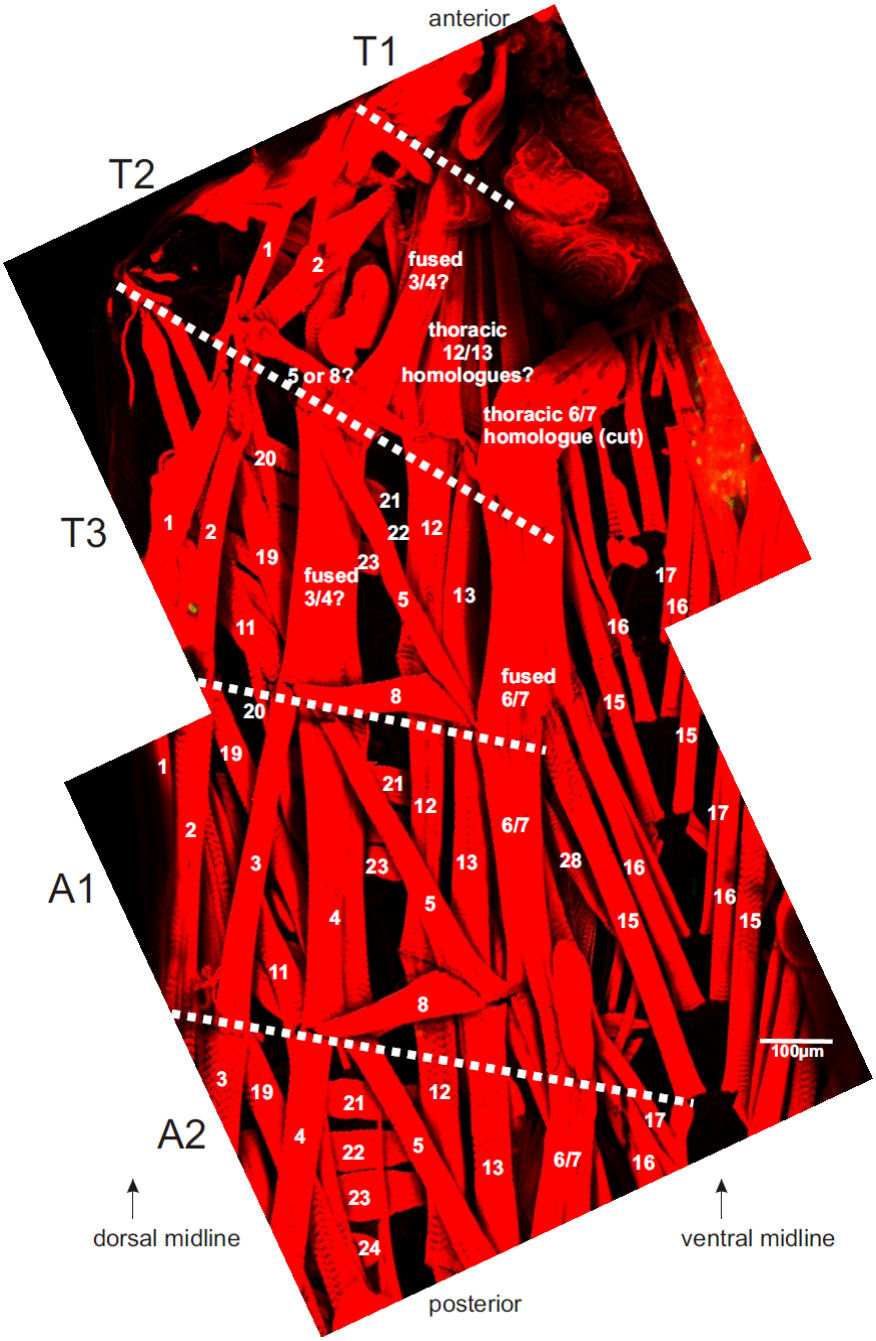

Figure 12. Synaptic input to identified motor neurons.
Bouts of EPSPs are observed in fortuitous recordings from each of the four motoneurons. Regions highlighted by red boxes are enlarged above the extended recording. Large scale bar at bottom right applies to all extended recordings. **A.** MN1-1b **B.** RP3 **C.** MNISN-1s **D.** MNSNb/d-1s

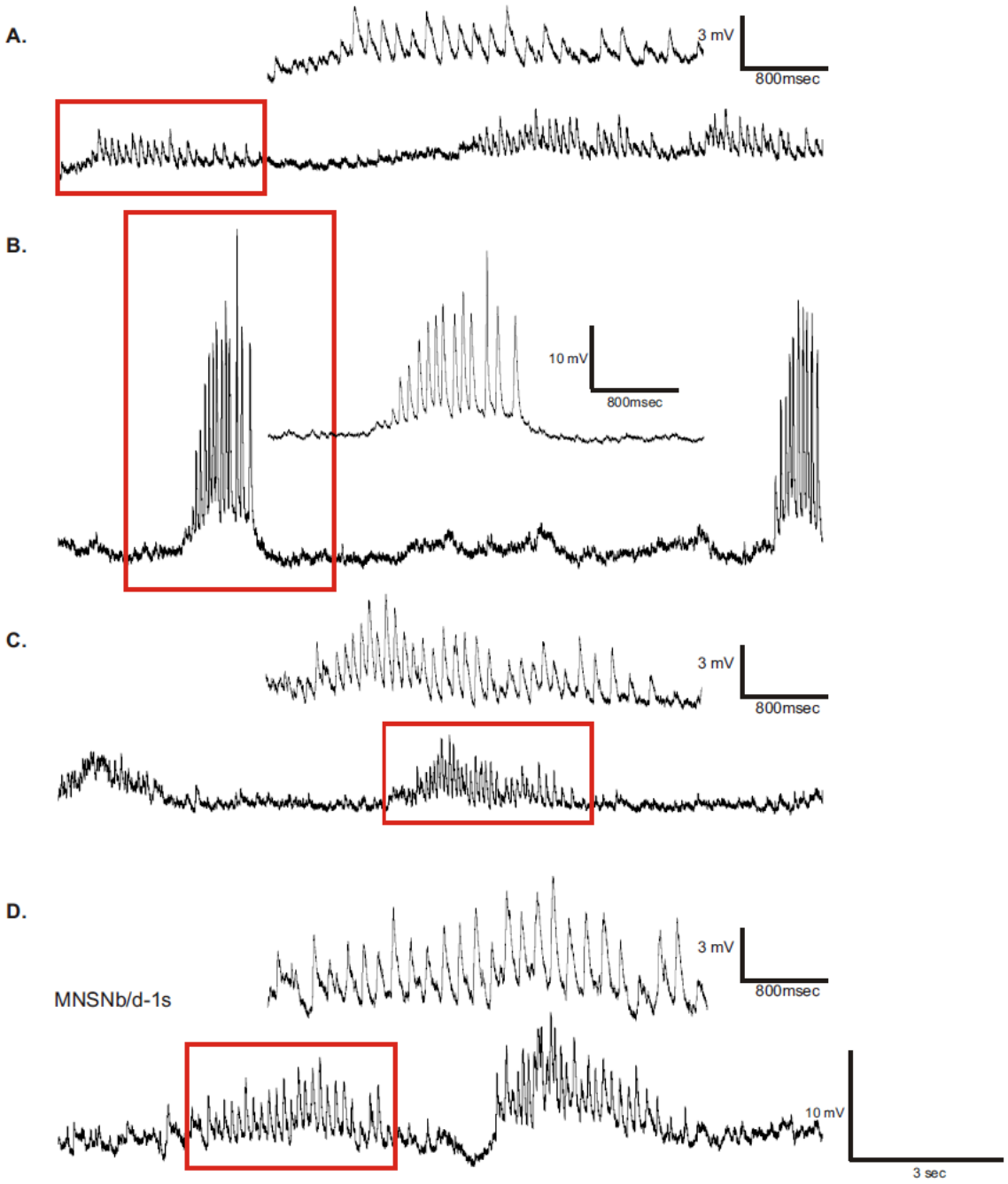

Figure 13. Depolarizing prepulse effect on firing frequnecy.
No differences in input/output relationships for the four identified motoneurons were observed after different magnitudes of depolarizing prepulse.

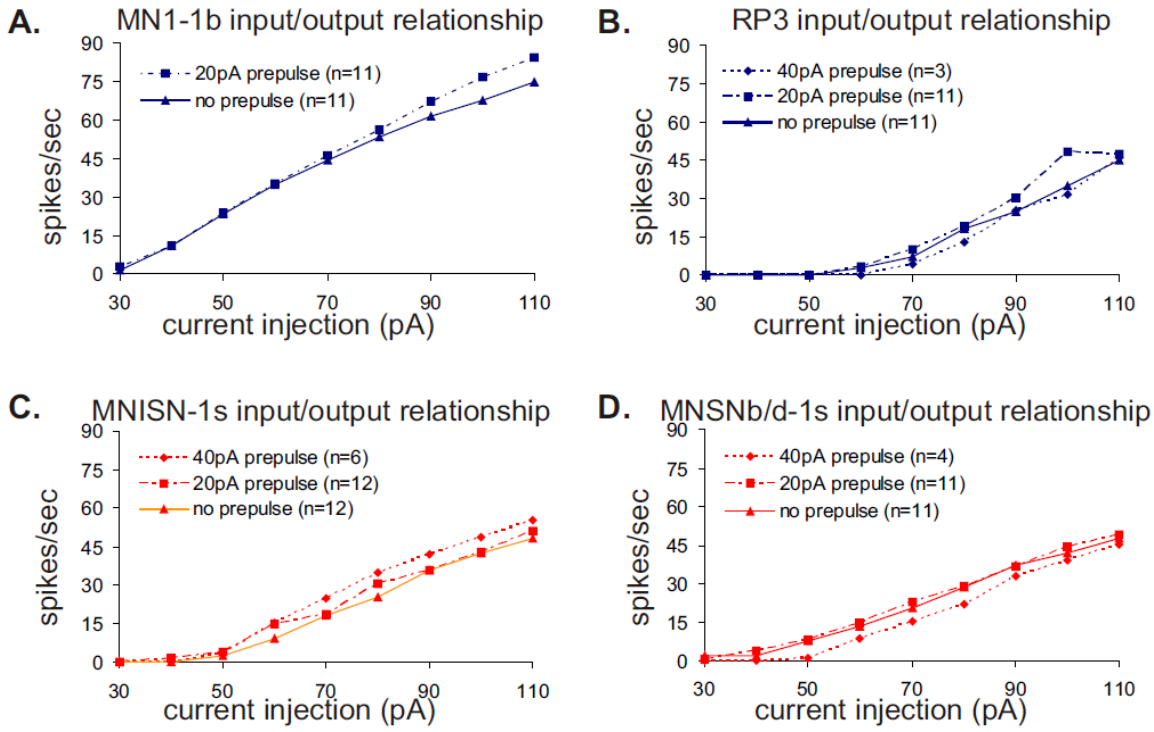

Figure 14. Comparison of abdominal and thoracic motor neuron intrinsic properties.

A. No significant differences in voltage threshold exist between abdominal and thoracic MN1-1b and MNISN-1s homologues. **B.** The input/output relationships of thoracic and abdominal motoneuron MN1-1b counterparts are not significantly different. Significant differences in thoracic (n=19) and abdominal (n=3) MNISN-1s firing frequency were found only at 90 and 110pA current injection levels. **C.** No significant differences in current threshold exist between abdominal and thoracic MN1-1b and MNISN-1s homologues. **D.** The delay-to-spike was not significantly different comparing MNISN-1s thoracic and abdominal homologues. A significantly shorter delay-to-spike in thoracic MN1-1b (n= 17) compared to abdominal MN1-1b (n=6) was seen at the 110pA current injection level.

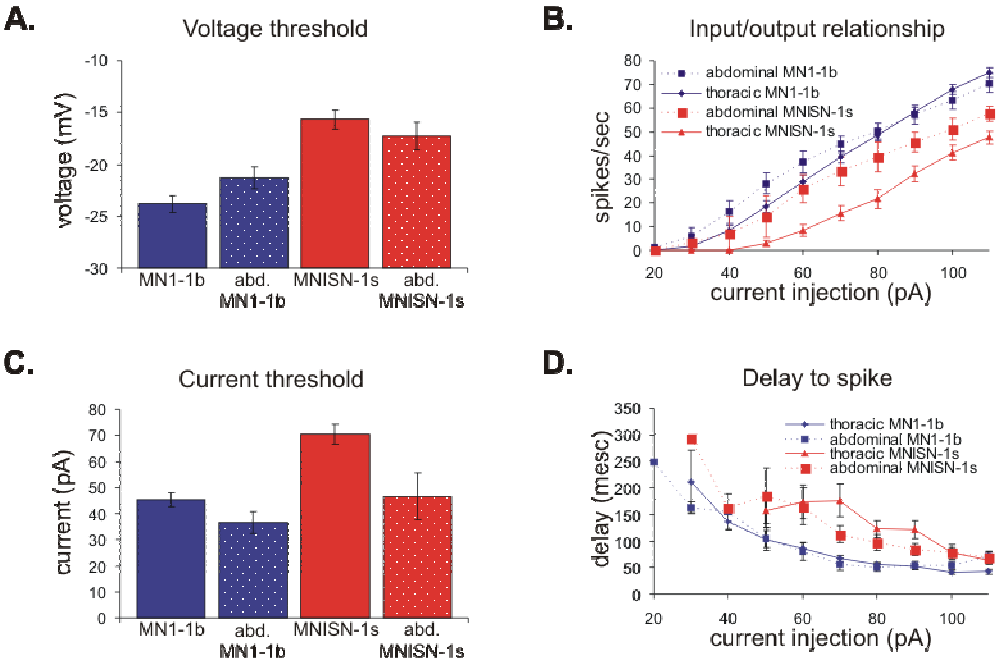

Figure 15. Effectiveness of GAL4 lines for RNAi technique.

All data from MNISN-1s. **A.** ShalRNAi expression under the control of RN2-FLP significantly decreased delay-to-spike at current injections ≥70pA (n=9) compared to control (n=8). ShalRNAi expression under the control of OK371 (n=5) did not significantly alter delay-to-spike compared to control (n= 4) and Dicer expression did not increase ShalRNAi effectiveness (n=3). **B.** ShalRNAi expression under the control of RN2-FLP significantly increased firing frequency at current injection levels between 50 and 90pA compared to control. ShalRNAi expression under the control of OK371 did not significantly alter firing frequency and Dicer expression did not increase ShalRNAi effectiveness. **C.** Peak transient K^+ currents were measured from leak-subtracted recordings without a subtraction protocol. Current density was not significantly altered by ShalRNAi expression under the control of OK371 (n=5) or RRA (n=5) compared to control (n=5 each for OK371 and RRA) and Dicer did not increase ShalRNAi effects (n=5). **D.** Sustained K^+ current density was not significantly altered by ShalRNAi expression under the control of OK371 or RN2-FLP and Dicer did not increase ShalRNAi effectiveness.

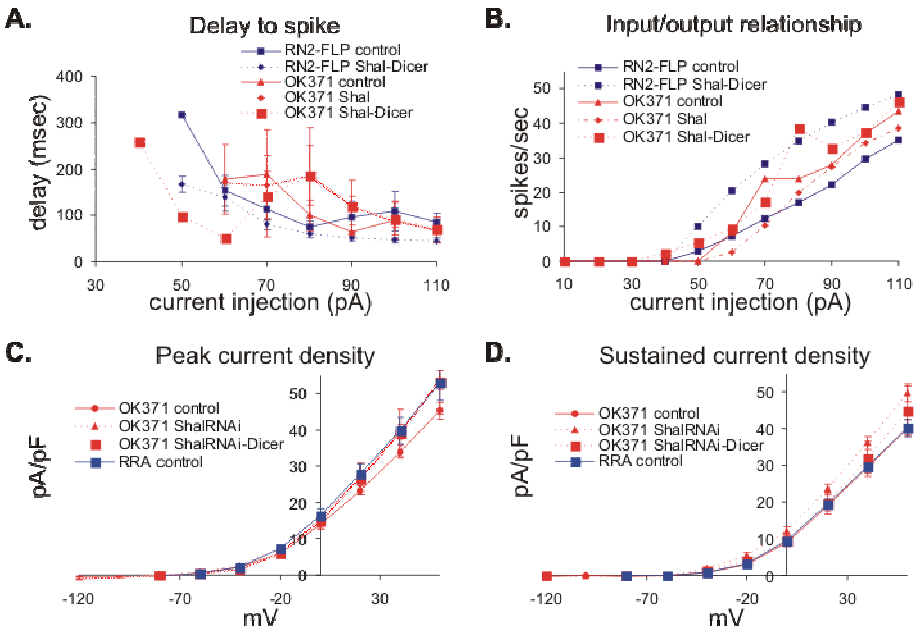

Figure 16. ShalRNAi modification of synaptic input.
Three out of five MNISN-1s motoneurons expressing ShalRNAi exhibited increased EPSP amplitudes. **A.** Prolonged recordings from a control and a ShalRNAi MNISN-1s. Cells were normalized to a -60mV resting potential via bias current injection. **B.** Enlarged view of regions highlighted in red boxes, control is to the left and ShalRNAi is to the right.

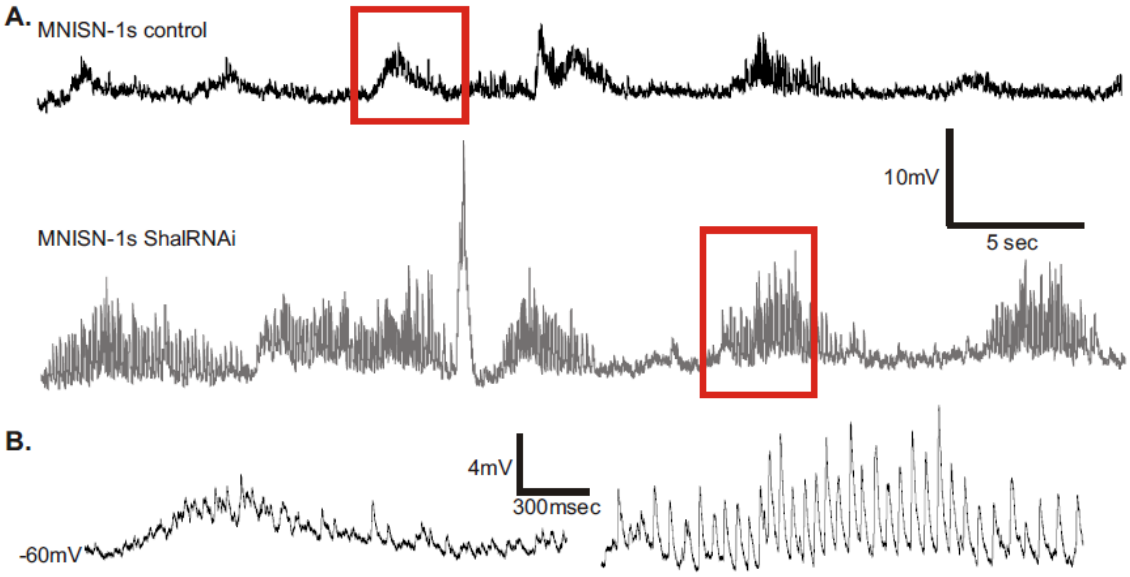

CHAPTER 4: CONCLUSIONS

4.1 Summary of results

The main goals of this work were to investigate whether the firing behavior and recruitment of identified *Drosophila* 1b and 1s motoneurons are analogous to the recruitment of low-threshold and high-threshold motoneurons in other organisms, whether active conductances influence the motoneuron response to synaptic input, and how motoneuron intrinsic properties participate in the crawling behavior. Therefore, three aims were addressed. First, we set out to determine whether four identified thoracic motoneurons in the *Drosophila* larva generate unique firing behaviors and whether the firing behaviors of these 1b and 1s motoneurons are analogous to the firing behaviors of low-threshold and high-threshold motoneurons in other organisms. The second aim was to determine whether passive properties or active currents are responsible for the firing behavior and recruitment of identified motoneurons. Finally, we wanted to determine whether the firing behaviors of identified motoneurons are relevant to crawling behavior and whether motoneuron intrinsic properties actively contribute to CPG motor output.

The first aim was to examine identified motoneuron firing behavior and determine whether 1s and 1b motoneurons are analogous to high-threshold and low-threshold motoneurons, respectively. Therefore, GAL4-UAS induced expression of GFP in identified motoneurons was used to visually target the motoneurons for whole-cell current clamp recordings (Fig. 10). MN1-1b and RP3 were chosen as representative 1b motoneurons and MNISN-1s and MNSNb/d-1s as representative 1s motoneurons. We find that 1b motoneurons have significantly more hyperpolarized voltage thresholds and

significantly shorter delays-to-spike than 1s motoneurons (Fig. 2 and 3). Together, these findings indicate that1b motoneurons are more easily recruited than 1s motoneurons, in agreement with the hypothesis that 1b motoneurons are analogous to low-threshold motoneurons. 1b and 1s motoneurons were not distinguishable based on firing frequency as MN1-1b exhibited a higher firing frequency than all other motoneurons (Fig. 2 and 13).

The second aim was to determine whether passive properties or active currents are responsible for the firing behavior and recruitment of identified motoneurons and was investigated through the use of current and voltage clamp recordings in conjunction with RNAi-induced protein knockdown. Findings indicate that passive properties of motoneurons cannot fully explain firing behavior and recruitment because 1b motoneurons exhibit shorter delays-to-spike but significantly lower input resistances than 1s motoneurons. If recruitment of motoneurons was governed by input resistance, the readily-recruited 1b motoneurons should exhibit significantly higher input resistances. Instead, the Shal channel that encodes a large portion of I_A in motoneuron somatodendritic regions is a critical determinant of delay-to-spike in larval *Drosophila* motoneurons. Depolarizing prepulses that inactivate I_A reduced delay-to-spike in all four motoneurons and had a relatively larger effect in 1s motoneurons (Fig. 4). RNAi knockdown of Shal expression significantly reduced delay-to-spike in both MN1-1b and MNISN-1s (Fig. 5). These results were confirmed with voltage clamp recordings that showed major I_A reduction in ShalRNAi-expressing motoneurons (Fig. 6). These results

do not indicate that other currents cannot contribute to motoneuron delay-to-spike but only that Shal is a major delay-to-spike determinant.

Finally, the third aim was to determine whether firing behaviors of identified motoneurons are relevant to crawling behavior and whether motoneuron intrinsic properties actively contribute to CPG output. This aim was addressed in a variety of experiments. Importantly, simultaneous recordings from MN1-1b and MNISN-1s projecting to the same body wall hemisegment indicated that the two cells receive coincident synaptic input but that MNISN-1s begins to fire after MN1-1b. Therefore, the firing behavior and intrinsic properties of motoneurons observed in current clamp recordings are behaviorally-relevant. Additionally, rhythmic synaptic input was visualized in recordings from all four motoneurons (Fig. 12) and EPSP size was increased in MNISN-1s after ShalRNAi expression, indicating that active currents may have an effect on EPSP amplitude (Fig. 16). This effect was not observed in MN1-1b.

4.2 Future directions

The larval *Drosophila* provides a powerful model for manipulation of ion channels and other neuronal properties in order to understand how they contribute to CPG and motoneuron function. A great deal of work remains to be done, though, before we can fully understand the larval *Drosophila* crawling CPG and the contribution of motoneurons to motor output.

Although the basic crawling behavior of the *Drosophila* larva has been well-described (Berrigan and Pepin 1995; Crisp et al. 2008; Hughes and Thomas 2007), a great deal remains unknown about muscle activation patterns during crawling. Characterization of the pattern of muscle contraction within a segment during crawling would provide a description of the crawling behavior by which motoneuron firing behaviors could be interpreted. Specifically, characterization of the dorsal and ventral muscle contraction pattern will be important for understanding if and how the firing behaviors of dorsally- and ventrally-projecting motoneurons contribute to intrasegmental offsets in muscle contractions. Additionally, the roles of the head, thorax, and abdomen for crawling can be inferred from existing data (Crisp et al. 2008), but detailed descriptions of their different roles would facilitate interpretation of segmental differences in motoneuron firing behaviors and intrinsic properties.

The neurons that compose the larval *Drosophila* crawling CPG are unknown. Identification of circuit components will be necessary in order to use this CPG for investigation of common principles of neural circuitry. Most relevant to this work, the synaptic inputs to motoneurons are unknown. Identification of presynaptic partners would greatly facilitate investigations of synaptic integration in motoneurons because identified synaptic inputs could then be reliably targeted for study. Further, the activity of presynaptic neurons could be modified using the GAL4-UAS system to alter ion channel and synaptic protein levels or more advanced channelrhodopsin proteins (Zhang

et al. 2007) in order to examine how specific inputs contribute to motoneuron recruitment.

Our findings indicate that recruitment and firing behavior of identified motoneurons are determined not only by passive properties but also by active currents, specifically the Shal current. Yet, the mechanisms through which active currents influence motoneuron output cannot be clearly understood until channel localization is known because of the effects channel localization can have on synaptic integration and motoneuron excitability (Hoffman et al. 1997; Burkhalter et al. 2006; Nusser 2009). It can be assumed that Shal channels are located in the somatodendritic region of the motoneurons because it is unlikely that our recordings include distal axonal regions of the cells due to space clamp issues. It is unknown, however, whether the putative dendritic expression of Shal follows a gradient, like in CA1 pyramidal neurons, clusters at synapses, like in cortical pyramidal cells, or is distributed in an as yet undescribed pattern. A Shal antibody would not yield much information regarding motoneuron localization of Shal because the ventral ganglion likely has widespread Shal expression in a variety of neuron types that would make it difficult to differentiate motoneuron-specific labeling. On the other hand, a GFP-tagged Shal construct could be expressed in specific motoneurons using the GAL4-UAS system in order to visualize Shal distribution in motoneurons.

Additional investigations of K^+ channels in larval motoneurons would be worthwhile because the role of different K^+ channel genes for larval motoneuron behavior is largely

unknown. Further, voltage clamp recordings comparing I_A in thoracic and abdominal MN1-1b may shed light on the mechanism through which abdominal and thoracic homologues maintain similar firing patterns in the face of significantly different input resistances. Theoretically, MN1-1b could compensate for its much lower input resistance with a lower I_A density. Voltage clamp recordings of I_A from MNSNb/d-1s and RP3 would indicate whether characteristics of I_A observed in MN1-1b and MNISN-1s can be generalized across1b and 1s motoneurons. Also, as addressed in *Chapter 3: Discussion*, whole-cell recordings from GFP-labeled and non-GFP labeled MNISN-1s cells in the same ShalRNAi animal would resolve whether the increased EPSP amplitude observed after Shal knockdown is an unexpected presynaptic effect or a motoneuron intrinsic effect that reflects a role for Shal in synaptic integration.

As described in *Chapter 1: Active motoneurons*, neuromodulators have effects on the intrinsic properties of neurons in a variety of organisms. Therefore, whole-cell recordings from *Drosophila* motoneurons could be utilized to investigate how neuromodulators, such as 5-HT, influence the intrinsic properties and active currents of motoneurons. Current clamp recordings would demonstrate the effects of neuromodulators on firing behavior but voltage clamp recordings would be necessary to determine whether the motoneuron is directly affected and, if so, which intrinsic properties are altered.

Finally, further development of the technique for simultaneous recordings from two motoneurons during fictive locomotion would be useful. Most importantly, the relative timing of synaptic input and the firing responses of dorsally- and ventrally-projecting motoneurons could be compared. Such recordings would indicate whether there is an offset in dorsal and ventral muscle contraction and whether such an offset is due to CPG input to motoneurons or motoneuron intrinsic properties. The role of Shal in motoneurons recruited by synaptic input could also be compared in GFP-labeled and non-GFP-labeled MNISN-1s from ShalRNAi animals. Currently, such investigations are limited by our inability to reliably evoke fictive crawling in filleted preparations. In other fictive preparations, ranging from mammals to insects, neuromodulator application initiates fictive locomotion patterns. It may be that an as yet unknown neuromodulator or neuromodulator cocktail serves an initiatory role in the larval *Drosophila* crawling CPG.

REFERENCES

Adelman JP, Shen KZ, Kavanaugh MP, Warren RA, Wu YN, Lagrutta A, Bond CT and North RA. Calcium-activated potassium channels expressed from cloned complementary DNAs. *Neuron* 9: 2: 209-216, 1992.

Alaburda A, Perrier JF and Hounsgaard J. An M-like outward current regulates the excitability of spinal motoneurones in the adult turtle. *J Physiol* 540: Pt 3: 875-881, 2002.

Albert JL and Lingle CJ. Activation of nicotinic acetylcholine receptors on cultured Drosophila and other insect neurones. *J Physiol* 463: 605-630, 1993.

Arber S, Han B, Mendelsohn M, Smith M, Jessell TM and Sockanathan S. Requirement for the homeobox gene Hb9 in the consolidation of motor neuron identity. *Neuron* 23: 4: 659-674, 1999.

Atkinson NS, Brenner R, Bohm RA, Yu JY and Wilbur JL. Behavioral and electrophysiological analysis of Ca-activated K-channel transgenes in Drosophila. *Ann N Y Acad Sci* 860: 296-305, 1998.

Atwood H. Parallel 'phasic' and 'tonic' motor systems of the crayfish abdomen. *J Exp Biol* 211: Pt 14: 2193-2195, 2008.

Atwood HL, Govind CK and Wu CF. Differential ultrastructure of synaptic terminals on ventral longitudinal abdominal muscles in Drosophila larvae. *J Neurobiol* 24: 8: 1008-1024, 1993.

Ausborn J, Stein W and Wolf H. Frequency control of motor patterning by negative sensory feedback. *J Neurosci* 27: 35: 9319-9328, 2007.

Baines RA and Bate M. Electrophysiological development of central neurons in the Drosophila embryo. *J Neurosci* 18: 12: 4673-4683, 1998.

Becker MN, Brenner R and Atkinson NS. Tissue-specific expression of a Drosophila calcium-activated potassium channel. *J Neurosci* 15: 9: 6250-6259, 1995.

Bergquist S, Dickman DK and Davis GW. A hierarchy of cell intrinsic and target-derived homeostatic signaling. *Neuron* 66: 220-234, 2010.

Berrigan D and Pepin DJ. How maggots move: allometry and kinematics of crawling in larval Diptera. *J Insect Physiol* 41: 4: 329-337, 1995.

Blitz DM, Beenhakker MP and Nusbaum MP. Different sensory systems share projection neurons but elicit distinct motor patterns. *J Neurosci* 24: 50: 11381-11390, 2004.

Bodmer R and Jan YN. Morphological differentiation of the embryonic peripheral neurons in Drosophila. *Roux's Arch Dev Biol* 196: 69-77, 1987.

Bohm RA, Wang B, Brenner R and Atkinson NS. Transcriptional control of Ca(2+)-activated K(+) channel expression: identification of a second, evolutionarily conserved, neuronal promoter. *J Exp Biol* 203: Pt 4: 693-704, 2000.

Brand AH and Perrimon N. Targeted gene expression as a means of altering cell fates and generating dominant phenotypes. *Development* 118: 2: 401-415, 1993.

Brenner R, Thomas TO, Becker MN and Atkinson NS. Tissue-specific expression of a Ca(2+)-activated K+ channel is controlled by multiple upstream regulatory elements. *J Neurosci* 16: 5: 1827-1835, 1996.

Brenner R, Yu JY, Srinivasan K, Brewer L, Larimer JL, Wilbur JL and Atkinson NS. Complementation of physiological and behavioral defects by a slowpoke Ca(2+) -activated K(+) channel transgene. *J Neurochem* 75: 3: 1310-1319, 2000.

Brewster R and Bodmer R. Origin and specification of type II sensory neurons in Drosophila. *Development* 121: 9: 2923-2936, 1995.

Briggman KL and Kristan WB. Multifunctional pattern-generating circuits. *Annu Rev Neurosci* 31: 271-294, 2008.

Briscoe J, Pierani A, Jessell TM and Ericson J. A homeodomain protein code specifies progenitor cell identity and neuronal fate in the ventral neural tube. *Cell* 101: 4: 435-445, 2000.

Broihier HT and Skeath JB. Drosophila homeodomain protein dHb9 directs neuronal fate via crossrepressive and cell-nonautonomous mechanisms. *Neuron* 35: 1: 39-50, 2002.

Budnik V, Koh YH, Guan B, Hartmann B, Hough C, Woods D and Gorczyca M. Regulation of synapse structure and function by the Drosophila tumor suppressor gene dlg. *Neuron* 17: 4: 627-640, 1996.

Burke RE, Dum RP, Fleshman JW, Glenn LL, Lev-Tov A, O'Donovan MJ and Pinter MJ. A HRP study of the relation between cell size and motor unit type in cat ankle extensor motoneurons. *J Comp Neurol* 209: 1: 17-28, 1982.

Burke RE, Levine DN, Tsairis P and Zajac FE,3rd. Physiological types and histochemical profiles in motor units of the cat gastrocnemius. *J Physiol* 234: 3: 723-748, 1973.

Burkhalter A, Gonchar Y, Mellor RL and Nerbonne JM. Differential expression of I(A) channel subunits Kv4.2 and Kv4.3 in mouse visual cortical neurons and synapses. *J Neurosci* 26: 47: 12274-12282, 2006.

Butler A, Wei AG, Baker K and Salkoff L. A family of putative potassium channel genes in Drosophila. *Science* 243: 4893: 943-947, 1989.

Cang J and Friesen WO. Model for intersegmental coordination of leech swimming: central and sensory mechanisms. *J Neurophysiol* 87: 6: 2760-2769, 2002.

Cang J, Yu X and Friesen WO. Sensory modification of leech swimming: interactions between ventral stretch receptors and swim-related neurons. *J Comp Physiol A* 187: 7: 569-579, 2001.

Chang Q and Balice-Gordon RJ. Gap junctional communication among developing and injured motor neurons. *Brain Res Brain Res Rev* 32: 1: 242-249, 2000.

Chang Q, Pereda A, Pinter MJ and Balice-Gordon RJ. Nerve injury induces gap junctional coupling among axotomized adult motor neurons. *J Neurosci* 20: 2: 674-684, 2000.

Choi JC, Park D and Griffith LC. Electrophysiological and morphological characterization of identified motor neurons in the Drosophila third instar larva central nervous system. *J Neurophysiol* 91: 5: 2353-2365, 2004.

Comer CM and Robertson RM. Identified nerve cells and insect behavior. *Prog Neurobiol* 63: 4: 409-439, 2001.

Crisp S, Evers JF, Fiala A and Bate M. The development of motor coordination in Drosophila embryos. *Development* 135: 22: 3707-3717, 2008.

Di Prisco GV, Pearlstein E, Le Ray D, Robitaille R and Dubuc R. A cellular mechanism for the transformation of a sensory input into a motor command. *J Neurosci* 20: 21: 8169-8176, 2000.

Diao F, Waro G and Tsunoda S. Fast inactivation of Shal (K(v)4) K+ channels is regulated by the novel interactor SKIP3 in Drosophila neurons. *Mol Cell Neurosci* 42: 1: 33-44, 2009.

Dickinson PS. Neuromodulation of central pattern generators in invertebrates and vertebrates. *Curr Opin Neurobiol* 16: 6: 604-614, 2006.

Dietzl G, Chen D, Schnorrer F, Su KC, Barinova Y, Fellner M, Gasser B, Kinsey K, Oppel S, Scheiblauer S, Couto A, Marra V, Keleman K and Dickson BJ. A genome-wide transgenic RNAi library for conditional gene inactivation in Drosophila. *Nature* 448: 7150: 151-156, 2007.

Dixit R, Vijayraghavan K and Bate M. Hox genes and the regulation of movement in Drosophila. *Dev Neurobiol* 68: 3: 309-316, 2008.

Eisenhart FJ, Cacciatore TW and Kristan WB,Jr. A central pattern generator underlies crawling in the medicinal leech. *J Comp Physiol A* 186: 7-8: 631-643, 2000.

Elbasiouny SM, Bennett DJ and Mushahwar VK. Simulation of dendritic CaV1.3 channels in cat lumbar motoneurons: spatial distribution. *J Neurophysiol* 94: 6: 3961-3974, 2005.

Elkins T, Ganetzky B and Wu CF. A Drosophila mutation that eliminates a calcium-dependent potassium current. *Proc Natl Acad Sci U S A* 83: 21: 8415-8419, 1986.

Enoka RM. Morphological features and activation patterns of motor units. *J Clin Neurophysiol* 12: 6: 538-559, 1995.

Faber ES and Sah P. Calcium-activated potassium channels: multiple contributions to neuronal function. *Neuroscientist* 9: 3: 181-194, 2003.

Fedirchuk B and Dai Y. Monoamines increase the excitability of spinal neurones in the neonatal rat by hyperpolarizing the threshold for action potential production. *J Physiol* 557: Pt 2: 355-361, 2004.

Fire A, Xu S, Montgomery MK, Kostas SA, Driver SE and Mello CC. Potent and specific genetic interference by double-stranded RNA in Caenorhabditis elegans. *Nature* 391: 6669: 806-811, 1998.

Fox LE, Soll DR and Wu CF. Coordination and modulation of locomotion pattern generators in Drosophila larvae: effects of altered biogenic amine levels by the tyramine beta hydroxlyase mutation. *J Neurosci* 26: 5: 1486-1498, 2006.

Friesen WO and Cang J. Sensory and central mechanisms control intersegmental coordination. *Curr Opin Neurobiol* 11: 6: 678-683, 2001.

Friesen WO, Poon M and Stent GS. Neuronal control of swimming in the medicinal leech. IV. Identification of a network of oscillatory interneurones. *J Exp Biol* 75: 25-43, 1978.

Fujioka M, Lear BC, Landgraf M, Yusibova GL, Zhou J, Riley KM, Patel NH and Jaynes JB. Even-skipped, acting as a repressor, regulates axonal projections in Drosophila. *Development* 130: 22: 5385-5400, 2003.

Gahtan E, Sankrithi N, Campos JB and O'Malley DM. Evidence for a widespread brain stem escape network in larval zebrafish. *J Neurophysiol* 87: 1: 608-614, 2002.

GanetzkyB and Wu CF. Drosophila mutants with opposing effects on nerve excitability: genetic and spatial interactions in repetitive firing. *J. Neurophysiol* 47: 3: 501-514, 1982.

Gasque G, Labarca P, Reynaud E and Darszon A. Shal and shaker differential contribution to the K+ currents in the Drosophila mushroom body neurons. *J Neurosci* 25: 9: 2348-2358, 2005.

Gebauer M, Isbrandt D, Sauter K, Callsen B, Nolting A, Pongs O and Bahring R. N-type inactivation features of Kv4.2 channel gating. *Biophys J* 86: 1: 210-223, 2004.

Gordon MD and Scott K. Motor control in a Drosophila taste circuit. *Neuron* 61: 3: 373-384, 2009.

Gosgnach S, Lanuza GM, Butt SJ, Saueressig H, Zhang Y, Velasquez T, Riethmacher D, Callaway EM, Kiehn O and Goulding M. V1 spinal neurons regulate the speed of vertebrate locomotor outputs. *Nature* 440: 7081: 215-219, 2006.

Goulding M and Pfaff SL. Development of circuits that generate simple rhythmic behaviors in vertebrates. *Curr Opin Neurobiol* 15: 1: 14-20, 2005.

Gouwens NW and Wilson RI. Signal propagation in Drosophila central neurons. *J Neurosci* 29: 19: 6239-6249, 2009.

Hannon GJ. RNA interference. *Nature* 418: 6894: 244-251, 2002.

Hardie J. Motor innervation of the supercontracting longitudinal ventrolateral muscles of the blowfly larva. *J Insect Physiol* 22: 5: 661-668, 1976.

Hartenstein V. The Muscle Pattern of Drosophila. In: *Muscle Development in Drosophila*, edited by Sink HSpringer New York, 2006, p. 8-27.

Hartwig CL, Worrell J, Levine RB, Ramaswami M and Sanyal S. Normal dendrite growth in Drosophila motor neurons requires the AP-1 transcription factor. *Dev Neurobiol* 68: 10: 1225-1242, 2008.

Haugland FN and Wu CF. A voltage clamp analysis of gene-dosage effects of the Shaker locus on larval muscle potassium currents in Drosophila. *J Neurosci* 10: 4: 1357-1371, 1990.

Hegde P, Gu GG, Chen D, Free SJ and Singh S. Mutational analysis of the Shab-encoded delayed rectifier K(+) channels in Drosophila. *J Biol Chem* 274: 31: 22109-22113, 1999.

Hellstrom J, Oliveira AL, Meister B and Cullheim S. Large cholinergic nerve terminals on subsets of motoneurons and their relation to muscarinic receptor type 2. *J Comp Neurol* 460: 4: 476-486, 2003.

Henneman E and Mendell LM. Functional organization of motoneuron pool and its inputs. In: *Handbook of Physiology: The Nervous System*, edited by Brooks VB. Bethesda: American Physiological Society, 1981, chapt. 1, p. 423-507.

Hill AA and Cattaert D. Recruitment in a heterogeneous population of motor neurons that innervates the depressor muscle of the crayfish walking leg muscle. *J Exp Biol* 211: Pt 4: 613-629, 2008.

Hill AA, Masino MA and Calabrese RL. Intersegmental coordination of rhythmic motor patterns. *J Neurophysiol* 90: 2: 531-538, 2003.

Hoang B and Chiba A. Single-cell analysis of Drosophila larval neuromuscular synapses. *Dev Biol* 229: 1: 55-70, 2001.

Hocker CG, Yu X and Friesen WO. Functionally heterogeneous segmental oscillators generate swimming in the medical leech. *J Comp Physiol A* 186: 9: 871-883, 2000.

Hodge JJ, Choi JC, O'Kane CJ and Griffith LC. Shaw potassium channel genes in Drosophila. *J Neurobiol* 63: 3: 235-254, 2005.

Hodge JJ and Stanewsky R. Function of the Shaw potassium channel within the Drosophila circadian clock. *PLoS One* 3: 5: e2274, 2008.

Hoffman DA, Magee JC, Colbert CM and Johnston D. K+ channel regulation of signal propagation in dendrites of hippocampal pyramidal neurons. *Nature* 387: 6636: 869-875, 1997.

Holderith NB, Shigemoto R and Nusser Z. Cell type-dependent expression of HCN1 in the main olfactory bulb. *Eur J Neurosci* 18: 2: 344-354, 2003.

Hounsgaard J, Hultborn H, Jespersen B and Kiehn O. Bistability of alpha-motoneurones in the decerebrate cat and in the acute spinal cat after intravenous 5-hydroxytryptophan. *J Physiol* 405: 345-367, 1988.

Hoyle G and Burrows M. Neural mechanisms underlying behavior in the locust Schistocerca gregaria. I. Physiology of identified motorneurons in the metathoracic ganglion. *J Neurobiol* 4: 1: 3-41, 1973.

Hughes CL and Thomas JB. A sensory feedback circuit coordinates muscle activity in Drosophila. *Mol Cell Neurosci* 35: 2: 383-396, 2007.

Hultborn H and Nielsen JB. Spinal control of locomotion--from cat to man. *Acta Physiol (Oxf)* 189: 2: 111-121, 2007.

Jan LY and Jan YN. Properties of the larval neuromuscular junction in Drosophila melanogaster. *J Physiol* 262: 1: 189-214, 1976.

Jerng HH, Pfaffinger PJ and Covarrubias M. Molecular physiology and modulation of somatodendritic A-type potassium channels. *Mol Cell Neurosci* 27: 4: 343-369, 2004.

Jessell TM. Neuronal specification in the spinal cord: inductive signals and transcriptional codes. *Nat Rev Genet* 1: 1: 20-29, 2000.

Johnson BR, Schneider LR, Nadim F and Harris-Warrick RM. Dopamine modulation of phasing of activity in a rhythmic motor network: contribution of synaptic and intrinsic modulatory actions. *J Neurophysiol* 94: 5: 3101-3111, 2005.

Katz PS and Frost WN. Intrinsic neuromodulation in the Tritonia swim CPG: serotonin mediates both neuromodulation and neurotransmission by the dorsal swim interneurons. *J Neurophysiol* 74: 6: 2281-2294, 1995.

Kennedy D and Takeda K. Reflex control of abdominal flexor muscles in the crayfish. I. The twitch system. *J Exp Biol* 43: 211-227, 1965a.

Kennedy D and Takeda K. Reflex control of abdominal flexor muscles in the crayfish. II. The tonic system. *J Exp Biol* 43: 229-246, 1965b.

Kiehn O, Kjaerulff O, Tresch MC and Harris-Warrick RM. Contributions of intrinsic motor neuron properties to the production of rhythmic motor output in the mammalian spinal cord. *Brain Res Bull* 53: 5: 649-659, 2000.

Kim MD, Wen Y and Jan YN. Patterning and organization of motor neuron dendrites in the Drosophila larva. *Dev Biol* 336: 2: 213-221, 2009.

Kitamoto T. Conditional disruption of synaptic transmission induces male-male courtship behavior in Drosophila. *Proc Natl Acad Sci U S A* 99: 20: 13232-13237, 2002.

Kjaerulff O and Kiehn O. 5-HT modulation of multiple inward rectifiers in motoneurons in intact preparations of the neonatal rat spinal cord. *J Neurophysiol* 85: 2: 580-593, 2001.

Ko EA, Han J, Jung ID and Park WS. Physiological roles of K+ channels in vascular smooth muscle cells. *J Smooth Muscle Res* 44: 2: 65-81, 2008.

Koh HY, Vilim FS, Jing J and Weiss KR. Two neuropeptides colocalized in a command-like neuron use distinct mechanisms to enhance its fast synaptic connection. *J Neurophysiol* 90: 3: 2074-2079, 2003.

Kohler M, Hirschberg B, Bond CT, Kinzie JM, Marrion NV, Maylie J and Adelman JP. Small-conductance, calcium-activated potassium channels from mammalian brain. *Science* 273: 5282: 1709-1714, 1996.

Koster JC, Permutt MA and Nichols CG. Diabetes and insulin secretion: the ATP-sensitive K+ channel (K ATP) connection. *Diabetes* 54: 11: 3065-3072, 2005.

Kraft R, Escobar MM, Narro ML, Kurtis JL, Efrat A, Barnard K and Restifo LL. Phenotypes of Drosophila brain neurons in primary culture reveal a role for fascin in neurite shape and trajectory. *J Neurosci* 26: 34: 8734-8747, 2006.

Kristan WB,Jr, Calabrese RL and Friesen WO. Neuronal control of leech behavior. *Prog Neurobiol* 76: 5: 279-327, 2005.

Kurdyak P, Atwood HL, Stewart BA and Wu CF. Differential physiology and morphology of motor axons to ventral longitudinal muscles in larval Drosophila. *J Comp Neurol* 350: 3: 463-472, 1994.

Lacin H, Zhu Y, Wilson BA and Skeath JB. Dbx Mediates Neuronal Specification and Differentiation through Cross-Repressive, Lineage-Specific Interactions with Eve and Hb9. *Development* 136: 19: 3257-3266, 2009.

Landgraf M, Bossing T, Technau GM and Bate M. The origin, location, and projections of the embryonic abdominal motorneurons of Drosophila. *J Neurosci* 17: 24: 9642-9655, 1997.

Landgraf M, Roy S, Prokop A, VijayRaghavan K and Bate M. even-skipped determines the dorsal growth of motor axons in Drosophila. *Neuron* 22: 1: 43-52, 1999.

Lee RH and Heckman CJ. Adjustable amplification of synaptic input in the dendrites of spinal motoneurons in vivo. *J Neurosci* 20: 17: 6734-6740, 2000.

Lee RH and Heckman CJ. Bistability in spinal motoneurons in vivo: systematic variations in rhythmic firing patterns. *J Neurophysiol* 80: 2: 572-582, 1998.

Lee YS, Nakahara K, Pham JW, Kim K, He Z, Sontheimer EJ and Carthew RW. Distinct roles for Drosophila Dicer-1 and Dicer-2 in the siRNA/miRNA silencing pathways. *Cell* 117: 1: 69-81, 2004.

Li X and Bennett DJ. Apamin-sensitive calcium-activated potassium currents (SK) are activated by persistent calcium currents in rat motoneurons. *J Neurophysiol* 97: 5: 3314-3330, 2007.

Lnenicka GA, Atwood HL and Marin L. Morphological transformation of synaptic terminals of a phasic motoneuron by long-term tonic stimulation. *J Neurosci* 6: 8: 2252-2258, 1986.

Lnenicka GA and Keshishian H. Identified motor terminals in Drosophila larvae show distinct differences in morphology and physiology. *J Neurobiol* 43: 2: 186-197, 2000.

Lorincz A, Notomi T, Tamas G, Shigemoto R and Nusser Z. Polarized and compartment-dependent distribution of HCN1 in pyramidal cell dendrites. *Nat Neurosci* 5: 11: 1185-1193, 2002.

Mahr A and Aberle H. The expression pattern of the Drosophila vesicular glutamate transporter: a marker protein for motoneurons and glutamatergic centers in the brain. *Gene Expr Patterns* 6: 3: 299-309, 2006.

Maimon G, Straw AD and Dickinson MH. Active flight increases the gain of visual motion processing in Drosophila. *Nat Neurosci* 13: 3: 393-399, 2010.

Marder E and Bucher D. Understanding circuit dynamics using the stomatogastric nervous system of lobsters and crabs. *Annu Rev Physiol* 69: 291-316, 2007.

Marder E and Bucher D. Central pattern generators and the control of rhythmic movements. *Curr Biol* 11: 23: R986-96, 2001.

Marder E and Goaillard JM. Variability, compensation and homeostasis in neuron and network function. *Nat Rev Neurosci* 7: 7: 563-574, 2006.

Marti E, Bumcrot DA, Takada R and McMahon AP. Requirement of 19K form of Sonic hedgehog for induction of distinct ventral cell types in CNS explants. *Nature* 375: 6529: 322-325, 1995.

Martinez-Padron M and Ferrus A. Presynaptic recordings from Drosophila: correlation of macroscopic and single-channel K+ currents. *J Neurosci* 17: 10: 3412-3424, 1997.

McClellan AD and Hagevik A. Coordination of spinal locomotor activity in the lamprey: long-distance coupling of spinal oscillators. *Exp Brain Res* 126: 1: 93-108, 1999.

McGuire SE, Le PT, Osborn AJ, Matsumoto K and Davis RL. Spatiotemporal rescue of memory dysfunction in Drosophila. *Science* 302: 5651: 1765-1768, 2003.

Mendell LM and Henneman E. Terminals of single Ia fibers: location, density, and distribution within a pool of 300 homonymous motoneurons. *J Neurophysiol* 34: 1: 171-187, 1971.

Milligan CJ, Edwards IJ and Deuchars J. HCN1 ion channel immunoreactivity in spinal cord and medulla oblongata. *Brain Res* 1081: 1: 79-91, 2006.

Muennich EA and Fyffe RE. Focal aggregation of voltage-gated, Kv2.1 subunit-containing, potassium channels at synaptic sites in rat spinal motoneurones. *J Physiol* 554: Pt 3: 673-685, 2004.

Nolazco GM, Nguyen P, Theisen H and McCaman R. Gene structure and developmental regulation of the small conductance calcium-activated potassium channel gene (dSK) in Drosophila. *A Dros Res Conf 42* 790A, 2001.

Notomi T and Shigemoto R. Immunohistochemical localization of Ih channel subunits, HCN1-4, in the rat brain. *J Comp Neurol* 471: 3: 241-276, 2004.

Nusser Z. Variability in the subcellular distribution of ion channels increases neuronal diversity. *Trends Neurosci* 32: 5: 267-274, 2009.

Odden JP, Holbrook S and Doe CQ. Drosophila HB9 is expressed in a subset of motoneurons and interneurons, where it regulates gene expression and axon pathfinding. *J Neurosci* 22: 21: 9143-9149, 2002.

O'Dowd DK and Aldrich RW. Voltage clamp analysis of sodium channels in wild-type and mutant Drosophila neurons. *J Neurosci* 8: 10: 3633-3643, 1988.

Parkis MA and Berger AJ. Clonidine reduces hyperpolarization-activated inward current (Ih) in rat hypoglossal motoneurons. *Brain Res* 769: 1: 108-118, 1997.

Parrish JZ, Emoto K, Kim MD and Jan YN. Mechanisms that regulate establishment, maintenance, and remodeling of dendritic fields. *Annu Rev Neurosci* 30: 399-423, 2007.

Pearson KG. Could enhanced reflex function contribute to improving locomotion after spinal cord repair? *J Physiol* 533: Pt 1: 75-81, 2001.

Pearson KG. Common principles of motor control in vertebrates and invertebrates. *Annu Rev Neurosci* 16: 265-297, 1993.

Peck JH, Gaier E, Stevens E, Repicky S and Harris-Warrick RM. Amine modulation of Ih in a small neural network. *J Neurophysiol* 96: 6: 2931-2940, 2006.

Peng IF and Wu CF. Differential contributions of Shaker and Shab K+ currents to neuronal firing patterns in Drosophila. *J Neurophysiol* 97: 1: 780-794, 2007a.

Peng IF and Wu CF. Drosophila cacophony channels: a major mediator of neuronal Ca2+ currents and a trigger for K+ channel homeostatic regulation. *J Neurosci* 27: 5: 1072-1081, 2007b.

Perrier JF, Alaburda A and Hounsgaard J. 5-HT1A receptors increase excitability of spinal motoneurons by inhibiting a TASK-1-like K+ current in the adult turtle. *J Physiol* 548: Pt 2: 485-492, 2003.

Powers RK and Binder MD. Input-output functions of mammalian motoneurons. *Rev Physiol Biochem Pharmacol* 143: 137-263, 2001.

Prinz AA, Bucher D and Marder E. Similar network activity from disparate circuit parameters. *Nat Neurosci* 7: 12: 1345-1352, 2004.

Puhl JG and Mesce KA. Keeping it together: mechanisms of intersegmental coordination for a flexible locomotor behavior. *J Neurosci* 30: 6: 2373-2383, 2010.

Puhl JG and Mesce KA. Dopamine activates the motor pattern for crawling in the medicinal leech. *J Neurosci* 28: 16: 4192-4200, 2008.

Pym EC, Southall TD, Mee CJ, Brand AH and Baines RA. The homeobox transcription factor Even-skipped regulates acquisition of electrical properties in Drosophila neurons. *Neural Dev* 1: 3, 2006.

Roelink H, Porter JA, Chiang C, Tanabe Y, Chang DT, Beachy PA and Jessell TM. Floor plate and motor neuron induction by different concentrations of the amino-terminal cleavage product of sonic hedgehog autoproteolysis. *Cell* 81: 3: 445-455, 1995.

Rogero O, Hammerle B and Tejedor FJ. Diverse expression and distribution of Shaker potassium channels during the development of the Drosophila nervous system. *J Neurosci* 17: 13: 5108-5118, 1997.

Rohrbough J and Broadie K. Electrophysiological analysis of synaptic transmission in central neurons of Drosophila larvae. *J Neurophysiol* 88: 2: 847-860, 2002.

Rossignol S, Dubuc R and Gossard JP. Dynamic sensorimotor interactions in locomotion. *Physiol Rev* 86: 1: 89-154, 2006.

Ryglewski S and Duch C. Shaker and Shal mediate transient calcium-independent potassium current in a Drosophila flight motoneuron. *J Neurophysiol* 102: 6: 3673-3688, 2009.

Saito M and Wu CF. Expression of ion channels and mutational effects in giant Drosophila neurons differentiated from cell division-arrested embryonic neuroblasts. *J Neurosci* 11: 7: 2135-2150, 1991.

Salkoff LB and Wyman RJ. Ion currents in Drosophila flight muscles. *J Physiol* 337: 687-709, 1983.

Saraswati S, Fox LE, Soll DR and Wu CF. Tyramine and octopamine have opposite effects on the locomotion of Drosophila larvae. *J Neurobiol* 58: 4: 425-441, 2004.

Schmid A, Chiba A and Doe CQ. Clonal analysis of Drosophila embryonic neuroblasts: neural cell types, axon projections and muscle targets. *Development* 126: 21: 4653-4689, 1999.

Schrader S and Merritt DJ. Dorsal longitudinal stretch receptor of Drosophila melanogaster larva - fine structure and maturation. *Arthropod Struct Dev* 36: 2: 157-169, 2007.

Schulz DJ, Goaillard JM and Marder E. Variable channel expression in identified single and electrically coupled neurons in different animals. *Nat Neurosci* 9: 3: 356-362, 2006.

Schwarz TL, Papazian DM, Carretto RC, Jan YN and Jan LY. Immunological characterization of K+ channel components from the Shaker locus and differential distribution of splicing variants in Drosophila. *Neuron* 4: 1: 119-127, 1990.

Schwindt P and Crill W. Role of a persistent inward current in motoneuron bursting during spinal seizures. *J Neurophysiol* 43: 5: 1296-1318, 1980.

Schwindt P and Crill WE. A persistent negative resistance in cat lumbar motoneurons. *Brain Res* 120: 1: 173-178, 1977.

Sharifullina E, Ostroumov K and Nistri A. Metabotropic glutamate receptor activity induces a novel oscillatory pattern in neonatal rat hypoglossal motoneurones. *J Physiol* 563: Pt 1: 139-159, 2005.

Sheng M, Tsaur ML, Jan YN and Jan LY. Subcellular segregation of two A-type K+ channel proteins in rat central neurons. *Neuron* 9: 2: 271-284, 1992.

Shmukler BE, Bond CT, Wilhelm S, Bruening-Wright A, Maylie J, Adelman JP and Alper SL. Structure and complex transcription pattern of the mouse SK1 K(Ca) channel gene, KCNN1. *Biochim Biophys Acta* 1518: 1-2: 36-46, 2001.

Sicaeros B, Campusano JM and O'Dowd DK. Primary neuronal cultures from the brains of late stage Drosophila pupae. *J Vis Exp* (4): 4: 200, 2007.

Simon M, Perrier JF and Hounsgaard J. Subcellular distribution of L-type Ca2+ channels responsible for plateau potentials in motoneurons from the lumbar spinal cord of the turtle. *Eur J Neurosci* 18: 2: 258-266, 2003.

Singh A and Singh S. Unmasking of a novel potassium current in Drosophila by a mutation and drugs. *J Neurosci* 19: 16: 6838-6843, 1999.

Sink H and Whitington PM. Location and connectivity of abdominal motoneurons in the embryo and larva of Drosophila melanogaster. *J Neurobiol* 22: 3: 298-311, 1991.

Straub VA and Benjamin PR. Extrinsic modulation and motor pattern generation in a feeding network: a cellular study. *J Neurosci* 21: 5: 1767-1778, 2001.

Suster ML and Bate M. Embryonic assembly of a central pattern generator without sensory input. *Nature* 416: 6877: 174-178, 2002.

Suster ML, Martin JR, Sung C and Robinow S. Targeted expression of tetanus toxin reveals sets of neurons involved in larval locomotion in Drosophila. *J Neurobiol* 55: 2: 233-246, 2003.

Suster ML, Seugnet L, Bate M and Sokolowski MB. Refining GAL4-driven transgene expression in Drosophila with a GAL80 enhancer-trap. *Genesis* 39: 4: 240-245, 2004.

Svensson E, Grillner S and Parker D. Gating and braking of short- and long-term modulatory effects by interactions between colocalized neuromodulators. *J Neurosci* 21: 16: 5984-5992, 2001.

Svensson E, Wikstrom MA, Hill RH and Grillner S. Endogenous and exogenous dopamine presynaptically inhibits glutamatergic reticulospinal transmission via an action of D2-receptors on N-type Ca2+ channels. *Eur J Neurosci* 17: 3: 447-454, 2003.

Takahashi T and Berger AJ. Direct excitation of rat spinal motoneurones by serotonin. *J Physiol* 423: 63-76, 1990.

Tamarkin DA and Levine RB. Synaptic interactions between a muscle-associated proprioceptor and body wall muscle motor neurons in larval and Adult manduca sexta. *J Neurophysiol* 76: 3: 1597-1610, 1996.

Tartas M, Morin F, Barriere G, Goillandeau M, Lacaille JC, Cazalets JR and Bertrand SS. Noradrenergic modulation of intrinsic and synaptic properties of lumbar motoneurons in the neonatal rat spinal cord. *Front Neural Circuits* 4: 4, 2010.

Thor S and Thomas JB. The Drosophila islet gene governs axon pathfinding and neurotransmitter identity. *Neuron* 18: 3: 397-409, 1997.

Tsalik EL and Hobert O. Functional mapping of neurons that control locomotory behavior in Caenorhabditis elegans. *J Neurobiol* 56: 2: 178-197, 2003.

Tsunoda S and Salkoff L. Genetic analysis of Drosophila neurons: Shal, Shaw, and Shab encode most embryonic potassium currents. *J Neurosci* 15: 3 Pt 1: 1741-1754, 1995.

Ueda A and Wu CF. Distinct frequency-dependent regulation of nerve terminal excitability and synaptic transmission by IA and IK potassium channels revealed by Drosophila Shaker and Shab mutations. *J Neurosci* 26: 23: 6238-6248, 2006.

Vahasoyrinki M, Niven JE, Hardie RC, Weckstrom M and Juusola M. Robustness of neural coding in Drosophila photoreceptors in the absence of slow delayed rectifier K+ channels. *J Neurosci* 26: 10: 2652-2660, 2006.

Van Roessel P, Hayward NM, Barros CS and Brand AH. Two-color GFP imaging demonstrates cell-autonomy of GAL4-driven RNA interference in Drosophila. *Genesis* 34: 1-2: 170-173, 2002.

Wallen P and Williams TL. Fictive locomotion in the lamprey spinal cord in vitro compared with swimming in the intact and spinal animal. *J Physiol* 347: 225-239, 1984.

Wang Z. Roles of K+ channels in regulating tumour cell proliferation and apoptosis. *Pflugers Arch* 448: 3: 274-286, 2004.

Warmke J, Drysdale R and Ganetzky B. A distinct potassium channel polypeptide encoded by the Drosophila eag locus. *Science* 252: 5012: 1560-1562, 1991.

Williams TL. Phase coupling by synaptic spread in chains of coupled neuronal oscillators. *Science* 258: 5082: 662-665, 1992.

Wilson JM, Hartley R, Maxwell DJ, Todd AJ, Lieberam I, Kaltschmidt JA, Yoshida Y, Jessell TM and Brownstone RM. Conditional rhythmicity of ventral spinal interneurons defined by expression of the Hb9 homeodomain protein. *J Neurosci* 25: 24: 5710-5719, 2005.

Wilson RI, Turner GC and Laurent G. Transformation of olfactory representations in the Drosophila antennal lobe. *Science* 303: 5656: 366-370, 2004.

Worrell JW and Levine RB. Characterization of voltage-dependent Ca2+ currents in identified Drosophila motoneurons in situ. *J Neurophysiol* 100: 2: 868-878, 2008.

Wu CF and Ganetzky B. Properties of Potassium Channels Altered by Mutations of Two Genes in Drosophila. *Biophys J* 45: 1: 77-78, 1984.

Wu CF, Sakai K, Saito M and Hotta Y. Giant Drosophila neurons differentiated from cytokinesis-arrested embryonic neuroblasts. *J Neurobiol* 21: 3: 499-507, 1990.

Wu CF, Suzuki N and Poo MM. Dissociated neurons from normal and mutant Drosophila larval central nervous system in cell culture. *J Neurosci* 3: 9: 1888-1899, 1983.

Wulff H, Castle NA and Pardo LA. Voltage-gated potassium channels as therapeutic targets. *Nat Rev Drug Discov* 8: 12: 982-1001, 2009.

Yu JY, Upadhyaya AB and Atkinson NS. Tissue-specific alternative splicing of BK channel transcripts in Drosophila. *Genes Brain Behav* 5: 4: 329-339, 2006.

Yu X, Nguyen B and Friesen WO. Sensory feedback can coordinate the swimming activity of the leech. *J Neurosci* 19: 11: 4634-4643, 1999.

Zhang M, Sukiasyan N, Moller M, Bezprozvanny I, Zhang H, Wienecke J and Hultborn H. Localization of L-type calcium channel Ca(V)1.3 in cat lumbar spinal cord--with emphasis on motoneurons. *Neurosci Lett* 407: 1: 42-47, 2006.

Zhang W, Ge W and Wang Z. A toolbox for light control of Drosophila behaviors through Channelrhodopsin 2-mediated photoactivation of targeted neurons. *Eur J Neurosci* 26: 9: 2405-2416, 2007.